National Library of Canada
Acquisitions and Bibliographic Services Branch
395 Wellington Street
Ottawa, Ontario
K1A 0N4

Bibliothèque nationale du Canada
Direction des acquisitions et des services bibliographiques
395, rue Wellington
Ottawa (Ontario)
K1A 0N4

Your file Votre référence

Our file Notre référence

NOTICE

The quality of this microform is heavily dependent upon the quality of the original thesis submitted for microfilming. Every effort has been made to ensure the highest quality of reproduction possible.

If pages are missing, contact the university which granted the degree.

Some pages may have indistinct print especially if the original pages were typed with a poor typewriter ribbon or if the university sent us an inferior photocopy.

AVIS

La qualité de cette microforme dépend grandement de la qualité de la thèse soumise au microfilmage. Nous avons tout fait pour assurer une qualité supérieure de reproduction.

S'il manque des pages, veuillez communiquer avec l'université qui a conféré le grade.

La qualité d'impression de certaines pages peut laisser à désirer, surtout si les pages originales ont été dactylographiées à l'aide d'un ruban usé ou si l'université nous a fait parvenir une photocopie de qualité inférieure.

Canada

Monitoring and Control of HVDC Transmission Systems Using Neural Networks

Nahi Kandil

A Thesis
in
The Department
of
Electrical and Computer Engineering

Presented in Partial Fulfillment of the Requirements
for the Degree of Master of Applied Science at
Concordia University
Montreal, Quebec, Canada

April 1993

ISBN 0-315-97619-5

Canada

ABSTRACT

Monitoring and Control of HVDC Transmission Systems Using Neural Networks

Nahi Kandil

In this thesis, Neural Networks (NNs) have been used in a novel application in the monitoring and control of High Voltage Direct Current (HVDC) Transmission systems.

In the first part, the possibility of using a NN to identify faults that may have occurred in an ac-dc system is explored. Based on the ability of these networks to distinguish reliably between different types of faults, appropriate control measures can be taken to improve the dynamic performance of the ac-dc power system. Depending on the inputs used, three different Counter Propagation Network (CPN) architectures are studied. Comparison between these architectures and their performances is made.

In the second part, NNs are used as a current regulator for the rectifier terminal of an HVDC system. Traditionally, a PI regulator is used for this purpose to provide a fast and robust controller. However, such regulators are optimal only over a limited range of operation and have no self-learning capability. In contrast, NNs are adaptive, can learn from previous experience, and they do not need prior knowledge of the system dynamics. In this thesis, three NN regulators are investigated. Comparisons between the PI and NN regulators have been made to demonstrate the capabilities of these NN regulators.

CONTENTS

Page

Page

FIGURES

Figure Page

Chapter 4 (continue)

Chapter 5

Figure Page

Chapter 5 (continue)

TABLES

CHAPTER 1

INTRODUCTION

This thesis deals with a new application of Neural Networks in the monitoring and control of High Voltage Direct Current (HVDC) Transmission systems.

Neural Networks (NNs) are various architectures of highly interconnected, simple processing elements that offer an alternative to conventional computing approaches. NNs are naturally massively parallel, so they are able to make decisions at high-speed and are fault tolerant. They do not sequentially execute instructions nor do they contain memory for storing operations, instructions, or data. Instead, they respond in parallel to a set of inputs, and they are more concerned with transformations than algorithms and procedures. Their real strength is derived from their ability to self-adapt and learn. There have been significant demonstrations of NN capabilities in vision, speech, signal processing, robotics, control, and power systems.

In power systems, there have been many NN applications. In [34], a NN was used to associate patterns of a prefault voltage angles and immediate postfault accelerating power within the critical clearing time for a faulted line. In [35], a NN was used to recognize current waveforms associated with incipient high impedance faults on distribution feeders. In [36], a two-stage NN was proposed for ideal real-time control of multi-tap capacitors installed on a distribution system with a non-conforming load profile. In [37], a NN was used to monitor and identify harmonic sources. In [38], a digital controller was adaptively modified to improve the small signal response of a current controller. In [39], NN was used to model synchronous machine dynamics; i.e. to learn synchronous machine behavior and to predict time response of synchronous generator for new initial conditions. In [40], a NN was used for harmonic source monitoring and identification. In [41], the Kohonen's self-organizing map was used for the classification of power system states. In [30], NNs were used as a power system stabilizer. In [43], unsupervised and supervised learning paradigms were used to discover what combinations of direct system measurements are significant in determining the critical clearing time (CCT). Finally, in [44], a NN was used for digital current regulation of inverter drives.

In controls, NNs have also had some applications. In [11], NNs were used as a robot controller. In [25], it was demonstrated that NNs can be used effectively for the identification and control of nonlinear dynamical systems. In [26], NNs were used to control a given plant. Several learning architectures were proposed for training the neural controller to provide the appropriate inputs to the plant so that a desired response is obtained. In [27], NNs were used as a feedback controller. In [28], the laboratory implementation of a NN controller for high performance dc drives was described. In [29], an Adaptive Model-Based NN Controller (AMBNNC) using multilayer perceptron artificial neural networks to enhance the high speed trajectory tracking accuracy of robotic manipulators was presented. In [31], a Self-Adaptive Neural Controller (SANC) was used to explore the potential use of the modeling capacity of neural networks for control applications. The two important computational features of NNs are (1) associative storage and retrieval of knowledge and (2) uniform rate of convergence of network dynamics, independent of network dimension. In [32], it was indicated how to use these features for adaptive control. In [33], the usefulness of the feedforward NN as a controller was examined. The case of controlling two-dimensional linear systems was considered.

This thesis can be divided into two parts. The first part deals with the identification of faults in HVDC systems using NNs. The second part deals with the control of dc current using NNs for a typical HVDC system.

In Chapter 2, HVDC transmission systems are briefly discussed. The advantages and disadvantages of HVDC systems as compared to ac transmission systems are explained. Then the theory and control of a 6-pulse bridge converter is briefly analyzed.

Chapter 3 describes the structure and mode of operation of artificial NNs. In addition, two important configurations of NNs (the BackPropagation and CounterPropagation networks) are introduced. The characteristics of these two networks, their theory, advantages, and limitations are discussed.

In Chapter 4, the possibility of using a NN to identify faults that may have occurred in an ac-dc system is explored. Based on the ability of these networks to distinguish reliably between different types of faults, appropriate control measures can be taken to improve the dynamic performance of the ac-dc power system. The inputs to the NN are the three phase voltages V_a, V_b, V_c, and the dc voltage V_{dc}. Sensing of the three phase node voltages could

be achieved either as rms voltages, with or without phase angles, or as instantaneous values of phase voltages. Based on a combination of these possibilities, three different CPN architectures are studied depending on the inputs used.

In Chapter 5, NNs are used as a current regulator for the rectifier terminal of an HVDC system. In a typical two-terminal HVDC transmission system, the rectifier is in constant current control whilst the inverter is in constant voltage control. Both ends of the system have traditionally relied on PI controller to provide fast, robust controllers. However PI controllers suffer from some disadvantages. The controller parameters are optimal only over a limited range of operation. Also, prior knowledge of the system dynamics is required to optimize these parameters. In addition, this type of controller has no self-learning capability.

In contrast, NNs are adaptive, can learn from previous experience, and they do not need prior knowledge of the system dynamics. After reviewing the control characteristics for the rectifier, three approaches are studied to replace the PI controller at the rectifier by a NN. In the first approach, the NN based current regulator is trained on-line using the error between the dc current and its order. In the second approach, the PI controller is used to train, off-line, the NN giving a fast regulator but not an adaptive

one. The third approach is a combination of these two NN based regulators i.e. having both adaptive and fast controller.

Finally in Chapter 6, the conclusions from this work are presented. Suggestions for further work are also provided.

CHAPTER 2

HVDC TRANSMISSION SYSTEMS

In this chapter, High Voltage Direct Current (HVDC) transmission systems are introduced. Their advantages over AC transmission systems are shown. The mode of operation of a 6-pulse bridge converter, with overlap less than 60^{o}, is analyzed. Then, the control of dc transmission is discussed. The equivalent circuit, basic means, and actual characteristics of the dc transmission control are explained.

A representative single-circuit of a simple dc link is shown in Figure 2.1. The line itself usually has two conductors, although some lines can have only one, the return path being in the earth or seawater or both. At both ends of the lines are converters, the components of which are transformers and groups of valves. The converter at the sending end is called a rectifier, and that at the receiving end an inverter. Either converter, however, can function as

a rectifier or inverter, permitting power to be transmitted in either direction. In addition to their use in transmitting power for a long distance, dc links are used as a back-to-back tie (Figure 2.2) to interconnect two different ac systems. The reason of doing so, and the advantages of HVDC transmission systems are discussed next.

Figure 2.1 A simple HVDC transmission system.

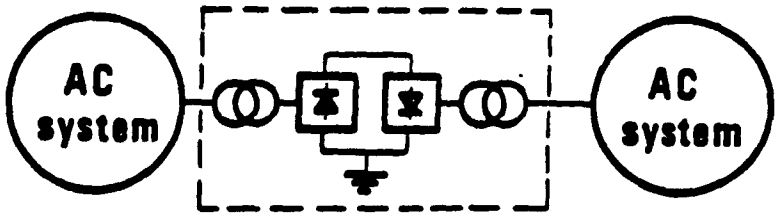

Figure 2.2 HVDC back-to-back station

2.1 Advantages of the DC (over AC) Transmission Systems

In spite of the practically universal use of the ac transmission, dc transmission systems have some advantages for long distances:

1- Greater power per conductor: Taking $\cos\phi = 0.945$, it can be shown that the transmitted dc power per conductor is 1.5 times the transmitted ac power per conductor, $P_{dc} = 1.5\ P_{ac}$.

2- Distance not limited to stability: The problem of stability constitutes the most serious limitation of a long distance ac transmission system. The stability of ac system means its ability to operate with all synchronous machines in synchronism. If a long ac line is loaded to a certain value, known as its steady-state stability limit, the synchronous machines at the sending end accelerate and go out of synchronism with those at the receiving end, then the system will fail to transmit the required power and the voltage will be raised.

A dc transmission link by itself has no stability problem. Two separate ac systems interconnected only by a dc line do not operate in synchronism, even if their nominal frequencies are equal, and they can operate at different

frequencies, for example, one at 50 Hz and other at 60 Hz. Each of the separate ac systems may have its own internal stability problems.

3- Power Factor and Reactive Compensation: On long HV AC lines, the production and consumption of reactive power by the line constitutes a serious problem since most lines cannot operate at their natural load, for the loads vary with time. If the load is greater than the natural load, net reactive power is consumed by the line and must be supplied from one or both ends. If the load on the line is less than the natural load, net reactive power is produced by the line and is delivered to one or both ends. Thus, to maintain constant equal voltages at both ends, reactive power must be absorbed at light load and supplied at heavy load, and this reactive power increases with distance.

A dc line itself requires no reactive power, and the voltage drop on the line itself is merely the resistive drop. However, the converters at both ends of the line draw reactive power from the ac system.

In addition to those above, dc transmission system has other advantages, like, it is simpler to construct, ground return can be used, and each conductor can be operated as an independent circuit. Also in the dc transmission line there

is no charging current, no skin effect, and dc cables can be worked at a higher voltage gradient. Moreover, it has less corona loss and radio interference and lower short-circuit current.

However, dc transmission has also some disadvantages since the converters are expensive and they require much reactive power. Also they generate harmonics, so filters are needed. Direct current circuit breakers do not have the natural advantage which the ac current has (natural zero crossing of the current). Therefore they have to force the current to zero. Figure 2.1 shows an over all economic comparison between ac and dc overhead transmission lines. It shows that dc transmission becomes cheaper for long distances.

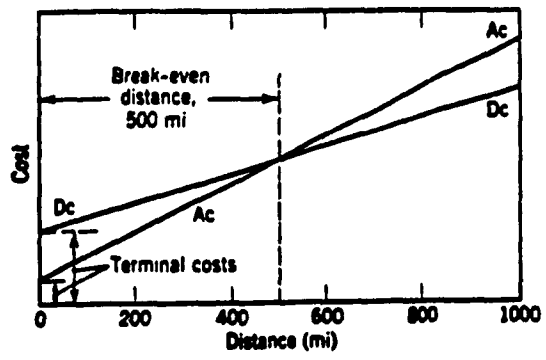

Fig.2.3 Comparative costs of ac and dc overhead lines [3]

2.2 The Bridge Converter

Figure 2.2 shows a 6-pulse bridge circuit. The instantaneous line-to-neutral voltages are

$$e_a = E_m \cos(\omega t + 60^\circ)$$

$$e_b = E_m \cos(\omega t - 60^\circ)$$

$$e_c = E_m \cos(\omega t - 180^\circ)$$

and the line-to-line voltages are

$$e_{ac} = e_a - e_c = \sqrt{3}\, E_m \cos(\omega t + 30^\circ)$$

$$e_{ba} = e_b - e_a = \sqrt{3}\, E_m \cos(\omega t - 90^\circ)$$

$$e_{cb} = e_c - e_b = \sqrt{3}\, E_m \cos(\omega t + 150^\circ)$$

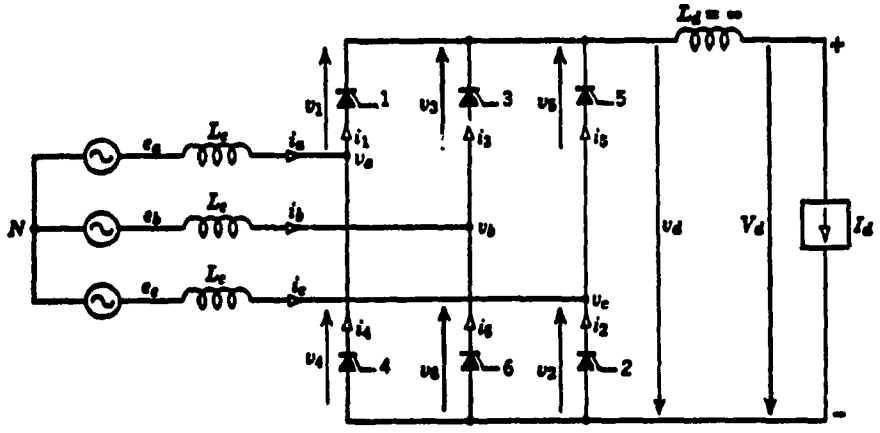

Fig.2.4 Bridge converter, the valves are numbered according to their firing order [3].

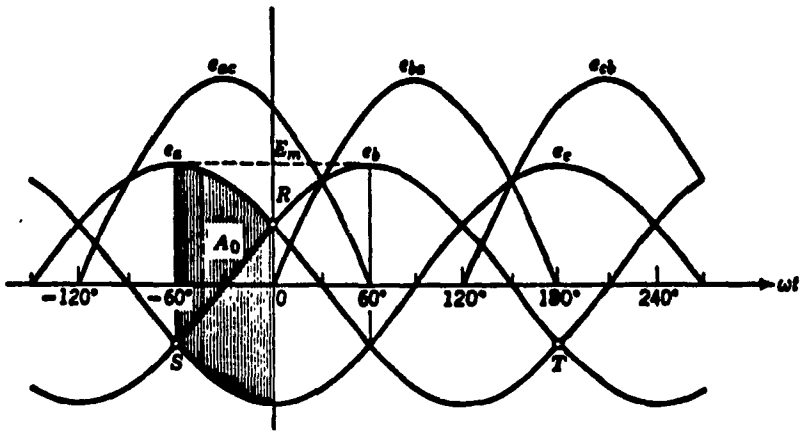

Figure 2.5 Instantaneous voltage waves of ac source [3]

Bridge Analysis

Bridge analysis With Grid Control and Overlap Less than 60 degrees is considered below:

Due to the inductance of the ac part of the system, the current can vary only at a finite time called the commutation time or the overlap time, u/ω, where u is the overlap angle. Typical full load values of u are between 20 and 25 degrees. During commutation three valves conduct simultaneously, but between commutations only two valves conduct. Since a new commutation begins every 60° and lasts for angle u, the interval when two valves conduct is 60°- u.

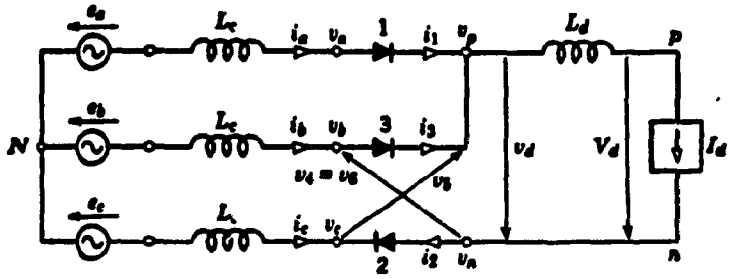

Figure 2.6 Bridge converter with valves 1, 2, 3 conducting [3].

Figure 2.6 shows the effective circuit while valves 1,2, and 3 are conducting. During this interval direct current is transferred from valve 1 to valve 3. The interval begins at $\omega t = \alpha$ and ends at $\omega t = \alpha + u$. The extinction angle is $\delta = \alpha + u$. from the loop N31N in Figure 2.6 we can write

$$e_b - e_a = L_c \frac{di_3}{dt} - L_c \frac{di_1}{dt} \qquad (2.2.1)$$

but $$e_b - e_a = \sqrt{3}\, E_m \cos(\omega t - 90^\circ)$$

$$= \sqrt{3}\, E_m \sin \omega t \qquad (2.2.2)$$

since $$i_1 = I_d - i_3 \qquad (2.2.3)$$

then $$\frac{di_1}{dt} = 0 - \frac{di_3}{dt} \qquad (2.2.4)$$

from above equations, we can get

$$\sqrt{3}\, E_m \sin \omega t = 2\, L_c \frac{di_3}{dt} \qquad (2.2.5)$$

By integrating both sides and knowing that at the beginning of the interval($\omega t = \alpha$), $i_1 = i_d$ and $i_3 = 0$,

$$\frac{\sqrt{3}\, E_m}{2\, L_c}\int_{\alpha/\omega}^{t} \sin \omega t \, dt = \int_0^{i_3} di_3 \qquad (2.2.6)$$

then

$$i_3 = I_d - i_1 = \frac{\sqrt{3}\, E_m}{2\, \omega\, L_c}(\cos \alpha - \cos \omega t) \qquad (2.2.7)$$

using

$$\frac{\sqrt{3}\, E_m}{2\, \omega\, L_c} = I_{s2} \qquad (2.2.8)$$

then

$$i_3 = I_{2s}(\cos \alpha - \cos \omega t) \qquad (2.2.9)$$

at $\omega t = \delta = \alpha + u$, $i_1 = o$ and $i_3 = I_d$ this leads to

$$I_d = I_{s2}(\cos \alpha - \cos \delta) \qquad (2.2.10)$$

This gives the direct current in terms of the ignition and extinction angles α and δ.

During commutation, the line-to-line voltage of the short circuit phase is zero, and the two line-to-ground voltages are equal

$$v_a = v_b = \frac{e_a + e_b}{2} = \frac{E_m}{2} \cos \omega t = -\frac{e_c}{2} \qquad (2.2.11)$$

Due to the overlap, there is a voltage drop ΔV_d represented by the area A in Figure 2.7. Then the effect of the overlap is to subtract an area A from the area A_0 every sixth of a cycle.

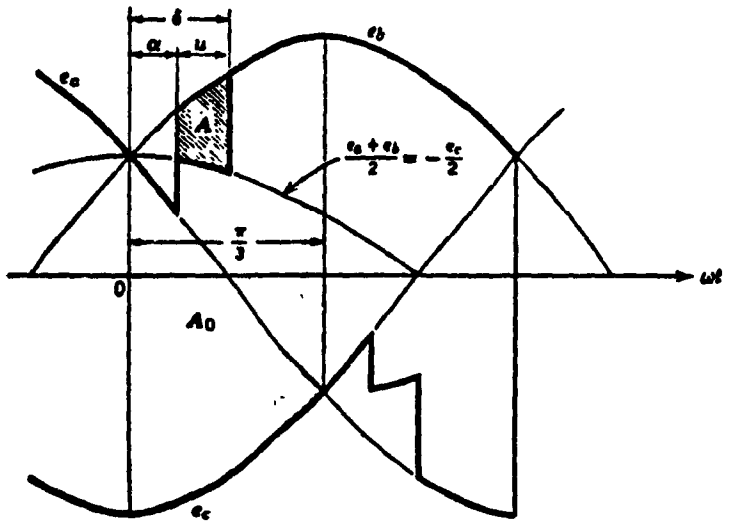

Figure 2.7 Voltage drop caused by the overlap [3]

It has been already shown that $A_o = V_{do}\,\pi/3$. Similarly,

$$A = \int_{\alpha}^{\delta}\left(e_b - \frac{e_a + e_b}{2}\right) d\theta = \int_{\alpha}^{\delta}\frac{e_b - e_a}{2}\, d\theta \qquad (2.2.12)$$

$$= \frac{\sqrt{3}\,E_a}{2}\int_{\alpha}^{\delta}\sin\theta\, d\theta = \frac{\sqrt{3}\,E_a}{2}\,(\cos\alpha - \cos\delta) \qquad (2.2.13)$$

That gives ΔV_d

$$\Delta V_d = \frac{V_{do}}{2}(\cos\alpha - \cos\delta) \qquad (2.2.14)$$

then V_d will be

$$V_d = V_{do}\cos\alpha - \Delta V_d = \frac{V_{do}(\cos\alpha + \cos\delta)}{2} \qquad (2.2.15)$$

from the above equations, it can be found that

$$V_d = V_{do}\cos\alpha - R_c\, I_d \qquad (2.2.16)$$

where R_c is the equivalent commutating resistance

$$R_c = \frac{3}{\pi}\,\omega\, L_c = \frac{3}{\pi}\,X_c = 6\ f\ L_c \text{ ohms} \qquad (2.2.17)$$

Figure 2.6 shows the equivalent circuit of the bridge rectifier. The direct voltage and direct current are average values without ripple.

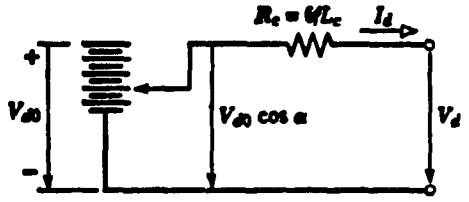

Figure 2.8 Equivalent circuit of bridge rectifier [3]

For the inverter, the equations are similar. It can be shown that with no overlap, rectification occurs for $0 < \alpha < 90^\circ$ and inversion occurs for $90^\circ < \alpha < 180^\circ$. Since in a practical case there is always overlap, the value of α at which the inversion begins depends on the overlap. In rectifier theory, the ignition angle α was defined as the angle by which ignition is delayed from the instant ($\omega t = 0$ for valve 3) at which the commutating voltage (e_{ba} for valve 3) is zero and increasing. Also the extinction angle δ is measured by the delay from the same instant($\omega t=0$ for valve 1). For the inverter, the ignition angle β and the extinction angle γ are defined by their advance with respect to the instant($\omega t = 180^\circ$ for ignition of valve 3 and extinction of valve 1) when the commutation voltage is zero

and decreasing. Then the general equations of the rectifier can be changed to inverter equations by changing the sign of V_d and putting $\cos \alpha = - \cos \beta$ and $\cos \delta = - \cos \gamma$, then the inverter current and voltage will be

$$I_d = I_{s2}(\cos \gamma - \cos \beta) \qquad (2.2.18)$$

$$V_d = \frac{V_{do}(\cos \gamma + \cos \beta)}{2} \qquad (2.2.19)$$

Since inverters usually operate at constant extinction advance angle γ, then by eliminating $\cos \beta$ from the above equations we get

$$V_d = V_{do} \cos \gamma - R_c I_d \qquad (2.2.20)$$

Figure 2.9 shows the equivalent circuit of the inverter.

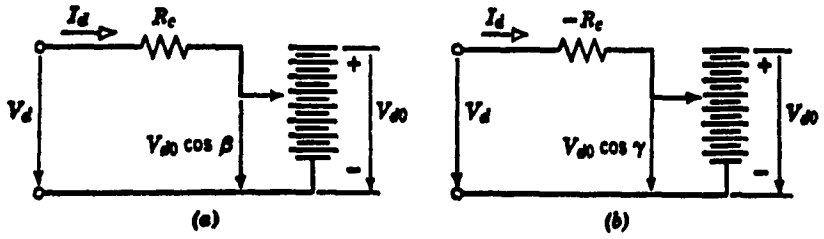

a) β - version b) γ - version

Figure 2.9 Equivalent circuits of inverter [3]

2.3 Control of the DC Transmission

Control in the HVDC system is needed to:

- limit the maximum current to avoid damaging valves and other devices,
- limit the fluctuation of current caused by the fluctuation of the ac voltage,
- keep the power factor as high as possible,
- prevent a commutation failure in the inverter,
- prevent an arcback at the rectifier valves,
- provide a sufficient anode voltage before ignition occurs,
- keep the voltage at the sending end as constant as possible in order to minimize the losses for a given power, and finally to
- control the power delivered or, sometimes, the frequency at one end.

The Equivalent Circuit and Basic Means of Control: Figure 2.8 shows the equivalent circuit of the dc transmission in the steady state. From this circuit, the dc current I_d is given by

$$I_d = \frac{V_{do1} \cos \alpha - V_{do2} \cos (\beta \text{ or } \gamma)}{R_{c1} + R_l + R_{c2}} \qquad (2.3.1)$$

If the inverter is operated with constant ignition angle β, then in equation (2.3.1) cos β and $+R_{c2}$ are used. But if the inverter is operated with a constant extinction angle γ, then cos γ and $-R_{c2}$ should be used. The voltage drop due to overlap is represented by the resistances R_{c1} and R_{c2}.

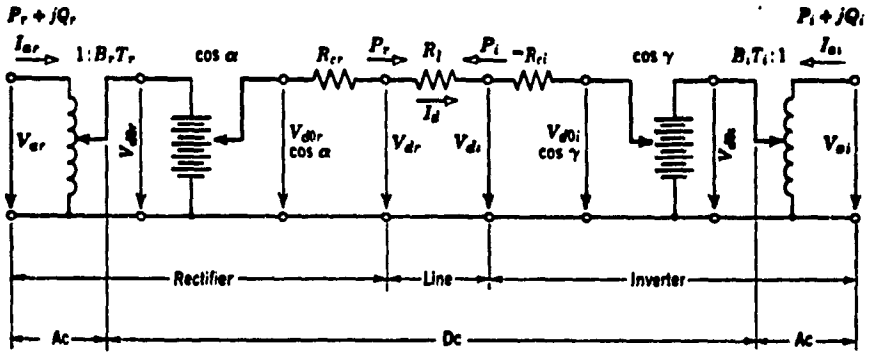

Figure 2.10 Equivalent circuit of dc transmission in the steady state [3].

The internal voltages V_{do1} cos α and V_{do2} cos β can be controlled by either of two different methods: grid control or control of the ac voltage. For example on the rectifier side, grid control (i.e. delaying the ignition α) reduces the internal voltage from the ideal no-load voltage V_{do1} by the factor cos α. The ideal no-load voltage V_{do1} is directly proportional to the ac voltage which is usually controlled by tap changing on the converter transformers. Grid control is faster and is used for rapid actions.

Actual Control Characteristics: The characteristics of rectifier and inverter are plotted in rectangular coordinates of direct current I_d and direct voltage V_d at some common point, for example, at the sending end of the dc line. Let the rectifier be controlled with a constant-current regulator, then the rectifier characteristic is a vertical line (AB in Figure 2.11).

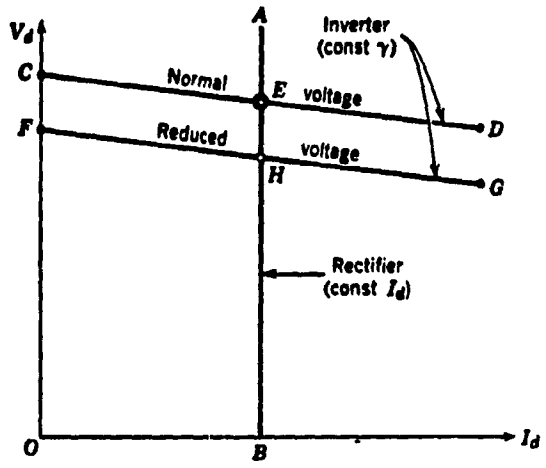

Figure 2.11 Characteristics of control of dc transmission [3]

If the inverter is controlled with a constant extinction angle (CEA) regulator, then its characteristic is given by

$$V_d = V_{do2} \cos \gamma + (R_1 - R_{c2}) I_d$$

The commutation resistance R_{c2} is greater than the line resistance. Then this line (CD in Figure 2.11) has a small

negative slope. Since at the common point there can be only one voltage and one current, their values must be given by the coordinates of the intersection of the rectifier and inverter characteristics (E). AB can be shifted by adjusting the current order and CD is shifted by the tap changer on the transformer at the inverter station. If the measured current is less then the current order, the regulator advances the firing time (decreases the delay angle α), thus raising the rectifier internal voltage in proportion to cos α and thus raising I_d. If the opposite is true, it increases α and then decreases cos α and I_d.

But rapid changes of voltages at either end or both ends may occur because of short circuits in the ac system or a collapse of the voltage at one valve group. Consider first a reduction of inverter voltage. The inverter characteristic is shifted downward (from CD to FG in Figure 2.11). The new operating point is H. The voltage is reduced but the current is still constant, the power is reduced in proportion to the voltage. Now, if the ac voltage is decreased at the rectifier side, the dc voltage would decrease proportionally. The current regulator, trying to maintain constant current, raises the direct rectifier voltage either to its initial value or until $\alpha = 0$ (or 5°). If the voltage dip is more then a few percent, the minimum α limit is reached first. Then the rectifier characteristic really

consists of two line segments: one of constant minimum ignition angle α_0 and one of constant current, as shown in Figure 2.12 by ABH. The inverter characteristic is assumed to be CD, as before. Now a big dip at the rectifier voltage shifts the rectifier characteristic down to A′B′H, which does not intersect the inverter characteristic, therefore the current and the power drop to zero. In order to avoid such great change of current and power, the inverter is also controlled by a current regulator, but which is set at a lower current then the rectifier's one. The inverter characteristic is now DFG consisting of two segments, one of constant extinction angle as before and one of constant current. The difference between the current order of the rectifier and that of the inverter is called the current margin, ΔI_d. It is typically about (10% - 15%) of the current order.

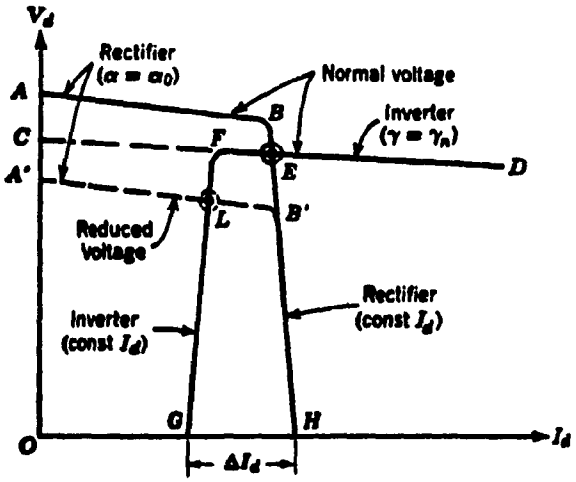

Figure 2.12 Actual characteristic of control scheme [3]

CHAPTER 3

NEURAL NETWORKS

This chapter provides a brief background on artificial Neural Networks (NNs). Since an artificial NN is a computer model that matches the functionality of the brain, some brief knowledge of the human brain structure is provided. Then, artificial NNs are introduced. Their architecture, theory, and mode of operation are described. In addition, two important configurations of NNs (BackPropagation, and CounterPropagation networks) are discussed.

3.1 The Human Brain Structure

The human brain consists of tens of billions of densely inter-connected neurons. The neuron is the fundamental cellular unit of the nervous system. Its nucleus is a simple processing unit which receives and combines signals from many other neurons through input paths called dendrites. If the combined signal is strong enough, it activates the

firing of the neuron which produces an output signal; the path of the output signal is called the axon. This later splits up and connects to dendrites of other neurons through a junction called synapse. The amount of the signal transferred depends on the synaptic strength of the junction. This synaptic strength is what is modified when the brain learns, so the synapse can be considered the basic memory unit of the brain. Figure 3.1 shows the structure of a pair of typical biological neurons.

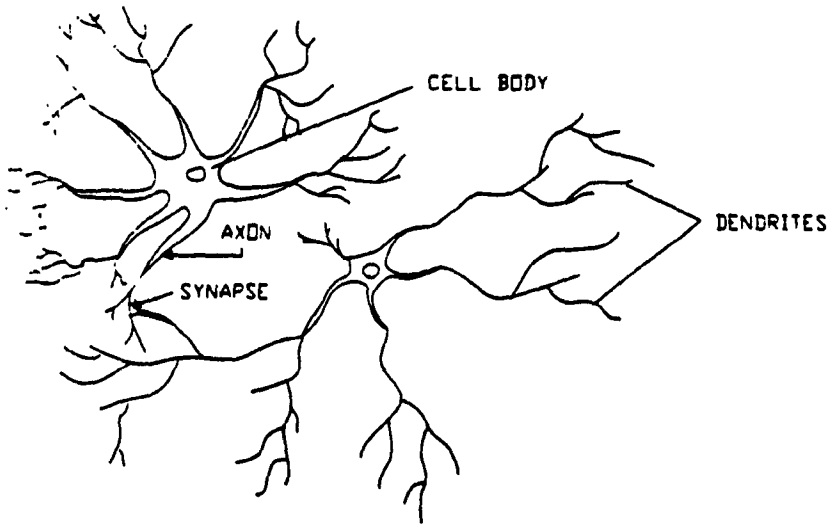

Figure 3.1 Biological neuron [7]

3.2 The Artificial Neural Network Structure

An artificial neural network is a computer model that matches the functionality of the brain in a very simplified

manner. The artificial neuron (the processing element) was designed to mimic the first-order characteristics of the biological neuron. A set of inputs are applied, each representing the output of another neuron. Each input is multiplied by a corresponding weight, simulation of the synaptic strength, and all of the weighted inputs are then summed and modified by a transfer function. This transfer function can be a threshold function which passes information only if the combined input reaches a certain level, or it can be a continuous function of the combined input. If this combined input reaches the activation level of the processing element, then it is generally passed to the output path of this processing element. This output path can be connected to input paths of other processing elements.

Suppose that there are n inputs to the processing element J. These inputs are weighted and summed forming the combined input I

$$I = \sum_{i=1}^{n} W_{ji} X_i \qquad (3.2.1)$$

where X_1, X_2, ..., X_n are the inputs to this processing element, and W_{ji} is the weight connecting the i^{th} input to this neuron.

Then the combined input is modified by the transfer function F giving the output Y_j of this processing element

$$Y_j = F(I) \qquad (3.2.2)$$

This output can be an input to other processing elements. Figure 3.2 illustrates the above description.

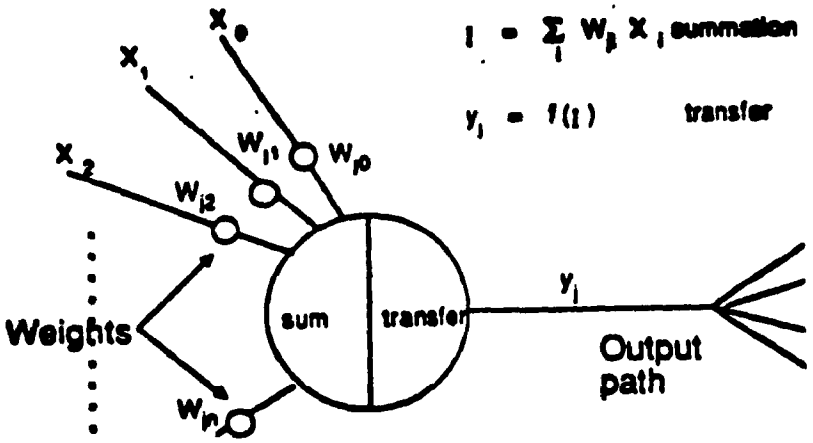

Figure 3.2 An artificial neuron (processing element) [5]

A neural network consists of many processing elements joined together in the above manner. Elements are usually organized into a sequence of layers with full or random connections between successive layers. Full connection means that every element in a layer is connected to every element in the next layer. If the connection is made randomly to only some of the elements in the next layer, then it is a random connection. The layer where the data is represented to the

network is called the input layer. The one which has an output as the output of the network is called the output layer. Layers between these two are called hidden layers. Figure 3.3 shows an example of a simple network architecture.

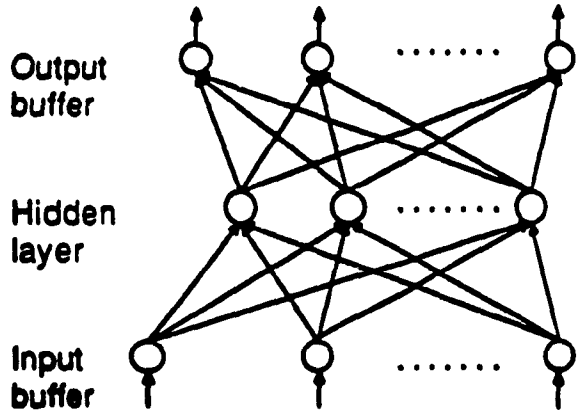

Figure 3.3 A simple neural network architecture.

Neural Network Operation

Two main phases are in the operation of a neural network, learning and recalling.

Learning is the process of adapting the connection weights in response to stimuli being presented in the input and the

output buffer (supervised learning), but if no desired output is shown, then the learning is unsupervised.

Supervised Learning: It requires the pairing of each input vector with a target vector representing the desired output; these two are called the training pair. An input vector is applied, the output of the network is calculated and compared to the corresponding target vector, and the difference (error) is fed back to the network and weights are changed according to an algorithm that tends to minimize the error. The process is repeated until the error for the entire learning is small enough.

Unsupervised Learning: Supervised learning has been questioned as being the process in the brain. If this was the brain's mechanism, where did the desired output patterns come from and how could the brain accomplish the self-organization in early development? Developed by Kohonen [7] (1984), unsupervised training requires no target vector for the outputs. The training set consists of input vectors, and the training algorithm modifies network weights to produce output vectors that are consistent. An application of a vector that is sufficiently similar to one of the training vectors will lead to the same output. It extracts the statistical proprieties of the training set and divides similar vectors into classes. Applying a vector from a given

class to the input will produce a specific output vector, but we cannot determine before the training which specific pattern will be produced.

Recalling refers to how the network globally processes a stimulus presented at its input buffer and creates a response at the output buffer. In feedforward network, information is passed from the input through hidden layers to the output layer in a straightforward manner using the summation and the transfer function characteristics of the particular network. If there are feedback connections, information will go around the network, across layers or within layers, and then it is passed to the output layer. In the recalling phase, weights are not modified. It is just that the network will do what it was trained to do.

3.3 Neural Network Configurations

In the 1960's, perceptrons created a great deal of interest and optimism. Rosenblatt (1962) proved a remarkable theorem about perceptron learning. Widrow (1960-1963) made some convincing demonstrations of perceptron-like systems. But Minsky (1969) proved that there are many restrictions on what a single-layer perceptron can learn. Because there was no techniques known at that time for training multilayer

networks, neural network research went into near eclipse. These days, the discovery of training methods for multilayer networks has recreated a lot of interest and research effort in this area. Now, the progress in this field is moving rapidly, and there are many different NN configurations (the Perceptron, BackProPagation, CounterPropagation, Hopfield nets, BAM, ART, ... etc). However, in this study, two important networks are used, the CounterPropagation as a vector classifier (i.e. for fault identification) and BackPropagation (i.e. for the dc current control). Therefore, the characteristics of these two networks, their theory, advantages, and limitations are discussed here.

BackPropagation NN

Since single-layer networks proved severely limited in what they could learn, the entire field went into virtual eclipse until the discovery of training methods for multilayer networks. Backpropagation is a systematic method for training multilayer artificial neural networks. It has a strong mathematical foundation, and it has dramatically expanded the range of problems to which neural networks can be applied. The system architecture for such a network is illustrated schematically in Figure 3.4. The network input to a node in layer j is

$$Net_j = \sum W_{ji}\ O_i \qquad (3.3.1)$$

The output of node j is

$$O_j = F(Net_j) \qquad (3.3.2)$$

where F is the activation function.

For the nodes in the Hidden layer, layer k, the input

$$Net_k = \sum W_{kj}\ O_j \qquad (3.3.3)$$

and the corresponding outputs

$$O_k = F(Net_k) \qquad (3.3.4)$$

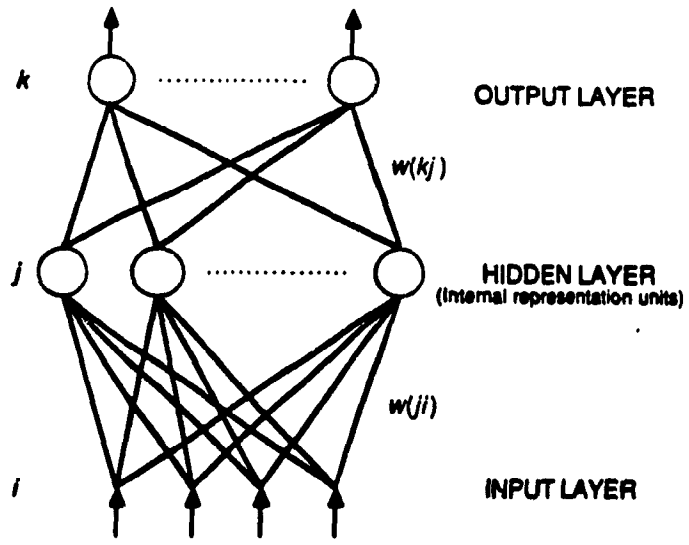

Figure 3.4 A schematic depiction of BackPropagation NN

In the learning phase, we present the pattern X as input and ask the network to adjust its weights in all the connecting links such that the desired outputs T at the Output layer, Layer k, are obtained. In general the outputs (O_k) will not be the same as the target or desired values (T_k). For each pattern, the square of the error is

$$E = \frac{1}{2} \sum (T_k - O_k)^2 \qquad (3.3.5)$$

Training the network is actually minimizing the error E. That is finding a set of weights which will satisfy all the (input output) pairs presented to the network. According to the Steepest Descent method, which is next reviewed, we achieve convergence toward improved values for the weights by taking incremental changes ΔW_{kj} proportional to $-\partial E/\partial W_{kj}$; that is

$$\Delta W_{kj} = -\eta \frac{\partial E}{\partial W_{kj}} \qquad (3.3.6)$$

where η is a constant called the learning rate (step size)

The partial derivative $\partial E/\partial W_{kj}$ can be evaluated using the chain rule

$$\frac{\partial E}{\partial W_{kj}} = \frac{\partial E}{\partial Net_k} \frac{\partial Net_k}{\partial W_{kj}} \qquad (3.3.7)$$

Using expression (3.3.1), we obtain

$$\frac{\partial Net_k}{\partial W_{kj}} = \frac{\partial}{\partial W_{kj}} \sum W_{kj}\, O_j = O_j \qquad (3.3.8)$$

Defining δ_k to be

$$\delta_k = - \frac{\partial E}{\partial Net_k} \qquad (3.3.9)$$

gives

$$\Delta W_{kj} = \eta\, \delta_k\, O_j \qquad (3.3.10)$$

To compute δ_k, we use the chain rule to express the partial derivative in terms of two factors, one expressing the rate of change of error with respect to the output O_k, and the other expressing the rate of change of the output of the node k with respect to the input to that same node. That is

$$\delta_k = - \frac{\partial E}{\partial Net_k} = - \frac{\partial E}{\partial O_k} \frac{\partial O_k}{\partial Net_k} \qquad (3.3.11)$$

But from eq. (3.3.5)

$$\frac{\partial E}{\partial O_k} = - (T_k - O_k) \qquad (3.3.12)$$

and from eq. (3.3.4)

$$\frac{\partial O_k}{\partial Net_k} = F'(Net_k) \qquad (3.3.13)$$

this gives δ_k for any output layer node k to be

$$\delta_k = (T_k - O_k)\ F'(Net_k) \qquad (3.3.14)$$

giving

$$\Delta W_{kj} = \eta\ (T_k - O_k)\ F'(Net_k)\ O_j = \eta\ \delta_k\ O_j \qquad (3.3.15)$$

For the Hidden layer, circumstances are different since the weights here do not affect output nodes directly. But we still can write

$$\begin{aligned}
\Delta W_{ji} &= -\eta \frac{\partial E}{\partial W_{ji}} \\
&= -\eta \frac{\partial E}{\partial Net_j} \frac{\partial Net_j}{\partial W_{ji}} \\
&= -\eta \frac{\partial E}{\partial Net_j} O_i \\
&= \eta \left(-\frac{\partial E}{\partial O_j} \frac{\partial O_j}{\partial Net_j}\right) O_i \\
&= \eta \left(-\frac{\partial E}{\partial O_j}\right) F'(Net_j)\ O_i \\
&= \eta\ \delta_j\ O_i \qquad (3.3.16)
\end{aligned}$$

However the factor $\partial E/\partial O_j$ cannot be evaluated directly. Instead, we write it in terms of quantities that are known or can be evaluated. Specifically, we write

$$- \frac{\partial E}{\partial O_j} = - \sum_k \frac{\partial E}{\partial Net_k} \frac{\partial Net_k}{\partial O_j}$$

$$= \sum_k \left(- \frac{\partial E}{\partial Net_k} \right) W_{kj}$$

$$= \sum_k \delta_k W_{kj} \qquad (3.3.17)$$

we see that, in this case

$$\delta_j = F'(Net_j) \sum_k \delta_k W_{kj} \qquad (3.3.18)$$

that is, the deltas at an internal node can be evaluated in terms of deltas at an upper layer. Thus, starting at the highest (the output layer) we can evaluate δ_k using eq. (3.3.14), and we can then propagate the error backward to the lower layers.

As it can be seen, with BackPropagation algorithm it became possible to adjust the weights of the hidden layers in a multi-layer neural network. However, the question of choosing the value of η has not been solved yet. A constant low value results in slow learning while a constant large η

corresponds to rapid learning but might also result in oscillations. This is not a new or unusual problem; it is common to all steepest-descent methods of locating minima of functions.

The CounterPropagation Networks

Counterpropagation is a combination of two well known algorithms: the self-organizing map of Kohonen and the Grossberg outstar. It is not general as backpropagation but it can reduce the training time by one hundredfold. The training process associates input vectors with corresponding output vectors. Once it is trained, application of an input vector produces the desired output vector. The generalization capability of the network allows it to produce a correct output even when it is given an input vector that is partially incomplete or partially incorrect. Figure 3.5 shows a uni-flow counterpropagation network. It constructs a mapping from a set of input vector X to a set of output Y. This acts as a hetro-associative nearest-neighbor classifier.

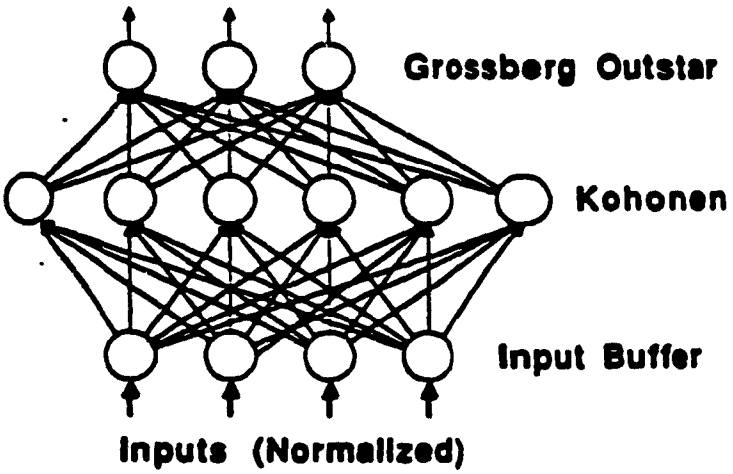

Figure 3.5 Uni-flow counterpropagation network [5]

The input layer acts as a buffer and perform no computation. The network operation requires that every input vector have the same length, the input vectors are to be normalized.

$$X \cdot X = 1$$

This can be done by dividing each component of an input vector by that vector's length.

$$x_i = \frac{x_i}{(x_1^2 + x_2^2 + x_3^2 + \ \ldots \ + x_n^2)^{1/2}}$$

where x_1, x_2, ... x_n are the components of the input vector X

This converts an input vector into a unit vector pointing in the same direction, a vector of unit length in n-dimensional space. Figure 3.6.a shows a vector V which has two

components x and y. Figure 3.6 b shows some two-dimensional unit vectors terminate at points on a unit circle. This is the situation when there is only two inputs to the network, but with three inputs, vectors would be represented as arrows terminating on the surface of a unit sphere.

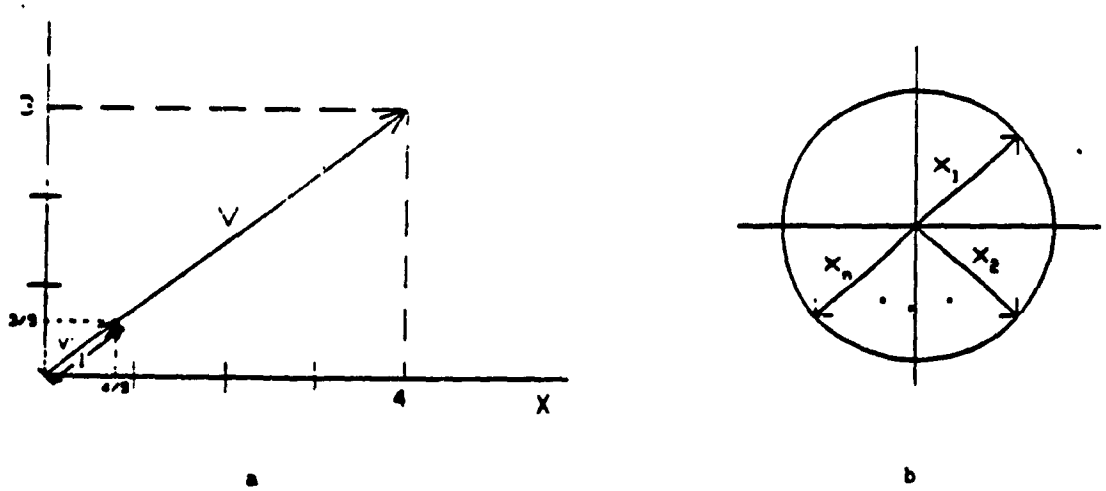

a b

Figure 3.6 a) Unit input vector [7]

b) Two-dimensional unit vectors on the unit circle

The Kohonen layer classifies the input vectors into groups that are similar. Its weights are adjusted so that similar input vectors activate the same neuron. This layer acts as a nearest neighbor classifier. Here, the processing elements compete. The one with the highest output wins. The Kohonen training is a self-organizing algorithm that operates in the unsupervised mode. It is difficult to predict which specific

Kohonen neuron will be activated for a given input vector. The following equation is used in the training algorithm.

$$W_{new} = W_{old} + A(X - W_{old}) \qquad (3.3.19)$$

where W_{new} is the new value of a weight connecting an input component x to winning neuron, W_{old} is the previous value of this weight, and A is a training rate coefficient that may vary during the training process $0 < A < 1$

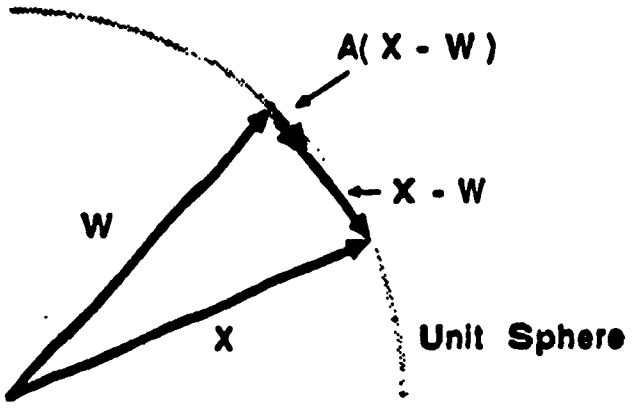

Figure 3.7 Kohonen learning in vector form [5]

As shown in Figure 3.7, the effect of training is to rotate the weight vector toward the input vector without materially changing its length. The output I of the processing element (before competition) is:

$$I = W \cdot X \qquad (3.3.20)$$

This inner product is just:

$$I = \| W \| * \| X \| * \cos (t) \qquad (3.3.21)$$

Since the length of both W and X is one, then the above equation can be written as

$$I = \cos(t) \qquad (3.3.22)$$

The Kohonen layer measures the cosine of the angle between the input vector X and the weight vector W. The processing element with the closest weight vector (smallest angle t) has the highest output and wins. Actually what happens is that the processing elements in the competitive layer adjust their weight vectors to divide input space in approximate correspondence to the frequency with which the inputs occur.

The output layer uses a Grossberg outstar. This is simply a processing element which learns to produce a certain output when a particular input is applied. The output of the Grossberg layer in a vector form is:

$$Y = I V \qquad (3.3.23)$$

where

Y is the Grossberg-layer output vector

I is the Kohonen-layer output vector

V is the Grossberg layer weight matrix

Since the Kohonen layer produces only a single output (through competition), only one element of the I vector is nonzero and the calculation is simple. In fact, the only action of each neuron in the Grossberg layer is to output the value of the weight that connects it to the single nonzero Kohonen neuron.

CHAPTER 4

FAULT IDENTIFICATION IN AN HVDC SYSTEM USING NEURAL NETWORKS

HVDC systems and neural networks (NNs) were introduced in chapters 2 and 3 respectively. In this chapter an application of NNs to identify faults in HVDC systems is discussed. A Counter-Propagation NN (CPN) is used to identify the type of a fault when it occurs in any part of the ac/dc system. This is done by three different approaches. A comparison between these approaches is made.

4.1 HVDC System Model

The HVDC system, modeled using the EMTDC package (see appendix A) is based on one pole of the two-pole 1000 MW Chateauguay (Hydro-Quebec) back to back tie. Although the actual tie is a 12-pulse system, the model simulated here is an equivalent 6-pulse system to save on computational time.

The ac filters used are, therefore, appropriately modified to account for the 5^{th} and 7^{th} harmonics generated by the converters. Data for the model is available in Appendix B. The system modeled (Figure 4.1) is divided into three subsystems:

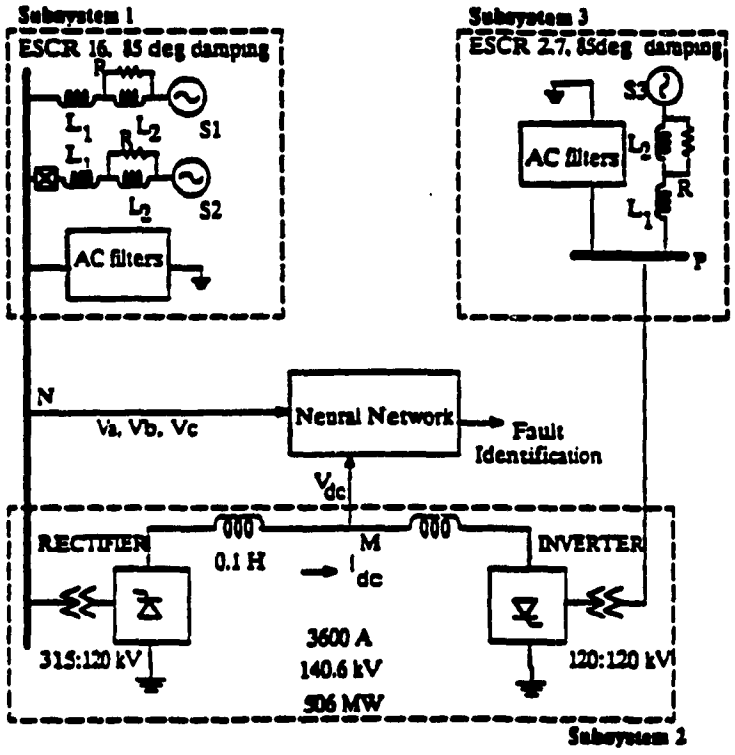

Figure 4.1 Back to back HVDC system modeled

Sub-system 1 : This is the sending or rectifier end ac system. This system consists of two constant voltage and frequency sources S1 and S2 behind equivalent impedances

(comprised of 2L-R networks) to represent simplified systems. AC filters for the 5^{th}, 7^{th}, 11^{th}, and 13^{th} harmonics are provided. The reactive power demand of the converter is supplied by a shunt capacitor bank. The system parameters are selected to represent a strong (almost infinite) ac system with an Effective Short Circuit Ratio (SCR) of 16. The neural network is connected to the 315 kV busbar N (to sense the three phase voltages V_a, V_b, and V_c).

Sub-system 2 : The rectifier is connected to the inverter via two 0.1 H smoothing reactors. There is no dc line in the case of a back-to-back tie. The neural network is attached to node M for sensing of the dc voltage, V_{dc}; the nominal value of V_{dc} is 140.6 kV. The dc current I_d of the tie is 3600 A, giving a nominal dc power transmission capability of 506 MW.

Sub-system 3 : This is the receiving or inverter end ac system. This system consists of one constant voltage, constant frequency source S3 behind equivalent impedances to represent a simplified system with an ESCR of 2.7. AC filters for the 5^{th}, 7^{th}, 11^{th}, and 13^{th} harmonics are provided. The remaining reactive power demand of the converter is supplied by a shunt capacitor bank. The ac busbar P rating is 120 kV.

4.2 Fault Identification

A counter-propagation neural network was described in chapter 3, section 3. Since it is a good classifier, this network is used here for fault identification in an ac-dc transmission system. Different parameters which can be used to describe the system state are:

- voltage measurements at busbar,
- current measurements in line,
- phase angle between voltage and current
- network topology parameters (i.e. breaker status)

Other derivatives of these fundamental primary parameters may also be utilized i.e. active or reactive power, node self-admittances etc. In the context of the present study, and for reasons of simplicity, only the node voltages at a busbar are used. For the ac-dc system studied here, six types of faults are to be classified by the neural network:

Class (0)	There is no fault	NF
Class (1)	Single line to ground fault	SLG
Class (2)	Double line to ground fault	DLG
Class (3)	Three phase to ground fault	3PH
Class (4)	Line to line fault	LL
Class (5)	DC fault	DCF

The NN output is to be divided into the above six categories. At any time t, there is only one winner i.e. only one output is going to be a logical one and all the other five outputs are going to be logical zeros. The inputs to the neural network are:

- V_{dc}, dc voltage at the node M (Figure 4.1), and
- V_a, V_b, and V_c, 3-phase voltages at rectifier bus N

Sensing of the three phase node voltages could be achieved either as rms voltages, with or without phase angles, or as instantaneous values of phase voltages. Based on a combination of these possibilities, three different CPN architectures are studied depending in the inputs used.

METHOD_1: (RMS Values Of Phase Voltages)

In this method, the (per unit) rms values of the three phase voltages as well as the dc voltage are used as inputs to the NN. Figure 4.2 shows this network where V_a, V_b, and V_c are the rms values of the three phase voltages at the rectifier bus (node N). V_{dc} is the dc voltage at the rectifier side (node M at the dc system). This network consists of four layers, the input layer, the normalizing

layer, Kohonen layer, and the output (Grossberg) layer. The input layer acts as a buffer and performs no computation. The network operation requires that every input vector have the same length, so the second layer is to normalize the input vectors, as explained in chapter 3. The Kohonen layer classifies the input vectors into groups that are similar. Its weights are adjusted so that similar input vectors activate the same neuron. This layer acts as a nearest neighbor classifier. The processing elements compete, and the one with the highest output wins. So, only one neuron fires at a time in the Kohonen layer. Then the action of each neuron in the Grossberg (output) layer is to output the value of the weight that connects it to the single nonzero Kohonen neuron. Training of CounterPropagation neural network is explained in chapter 3, section 3.

This CPN is trained to classify the input vectors into the six classes mentioned above. The training set is shown in Table 4.1. The training is done off-line and the global error converges rapidly to zero.

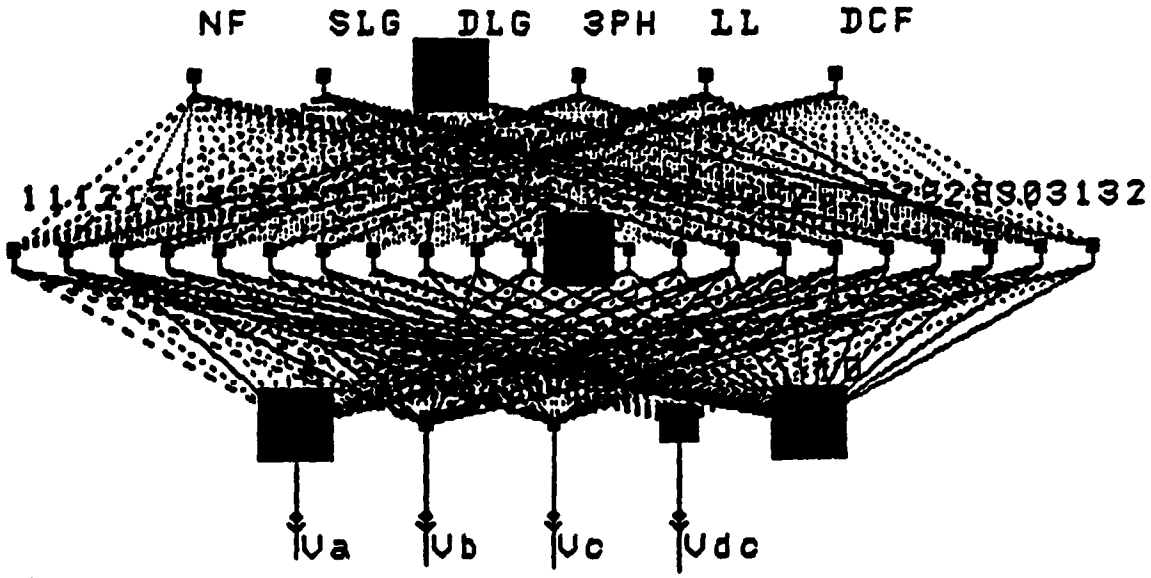

Figure 4.2 CPN for fault identification (METHOD 1)

Inputs to the NN are the rms values of the three phase voltages (V_a,V_b,V_c) and the dc voltage, V_{dc}

Table 4.1 The training set for METHOD 1: inputs to NN are rms values of 3-phase voltages and dc voltage.

class	phase A	phase B	phase C	dc voltage	type of fault
0	1.0	1.0	1.0	1.0	!No fault
1	0.0	1.0	1.0	1.0	!Single line
1	0.0	1.0	1.0	0.0	!Single line
1	1.0	0.0	1.0	1.0	!Single line
1	1.0	0.0	1.0	0.0	!Single line
1	1.0	1.0	0.0	1.0	!Single line
1	1.0	1.0	0.0	0.0	!Single line
2	0.0	0.0	1.0	1.0	!Double line
2	0.0	0.0	1.0	0.0	!Double line
2	0.0	1.0	0.0	1.0	!Double line
2	0.0	1.0	0.0	0.0	!Double line
2	1.0	0.0	0.0	1.0	!Double line
2	1.0	0.0	0.0	0.0	!Double line
3	0.0	0.0	0.0	1.0	!Three phase
3	0.0	0.0	0.0	0.0	!Three phase
4	0.5	1.0	0.5	1.0	!Line to line
4	0.5	1.0	0.5	0.0	!Line to line
4	0.5	0.5	1.0	1.0	!Line to line
4	0.5	0.5	1.0	0.0	!Line to line
4	1.0	0.5	0.5	1.0	!Line to line
4	1.0	0.5	0.5	0.0	!Line to line
5	1.0	1.0	1.0	0.0	!DC fault

All fault cases described in the training set were tried. Results of this method are shown in Figures 4.3-1 ... 4.3-6. In these figures, the following traces are shown:

- The three phase voltages at rectifier bus (in pu)
- The rms values of these voltages (in pu)
- the dc voltage and dc current (in pu)
- neural network outputs (in boolean i.e. logical 1 or 0)

These results show that the simple network is able to identify both the duration and type of the fault. However, there is a delay of 1-2 cycles in its response time and some apparent tendency for false alarms during the transitional periods, in particular during the recovery period. This time delay is inherent to the algorithm utilized to compute the rms value of the phase voltage. However, closer analysis of the neural network output value revealed that the transitional false alarms are not an actual problem due to the following reason:

In an ac system, fault currents are interrupted at current zeros to avoid damage to equipment such as circuit breakers. So the switching occurs at different times for the three phases. For example, in the case of clearing of a three phase fault, one phase switches before the others leaving a

double line to ground fault. When the next phase switches, it leaves a single phase fault until the last phase is cleared. Hence, during the transitional stages indication of three phase fault will progress to a double line fault (DLGF) to a single line fault (SLGF) to a no fault (NF) until the fault is finally cleared. And, therefore, the output of the neural network is valid.

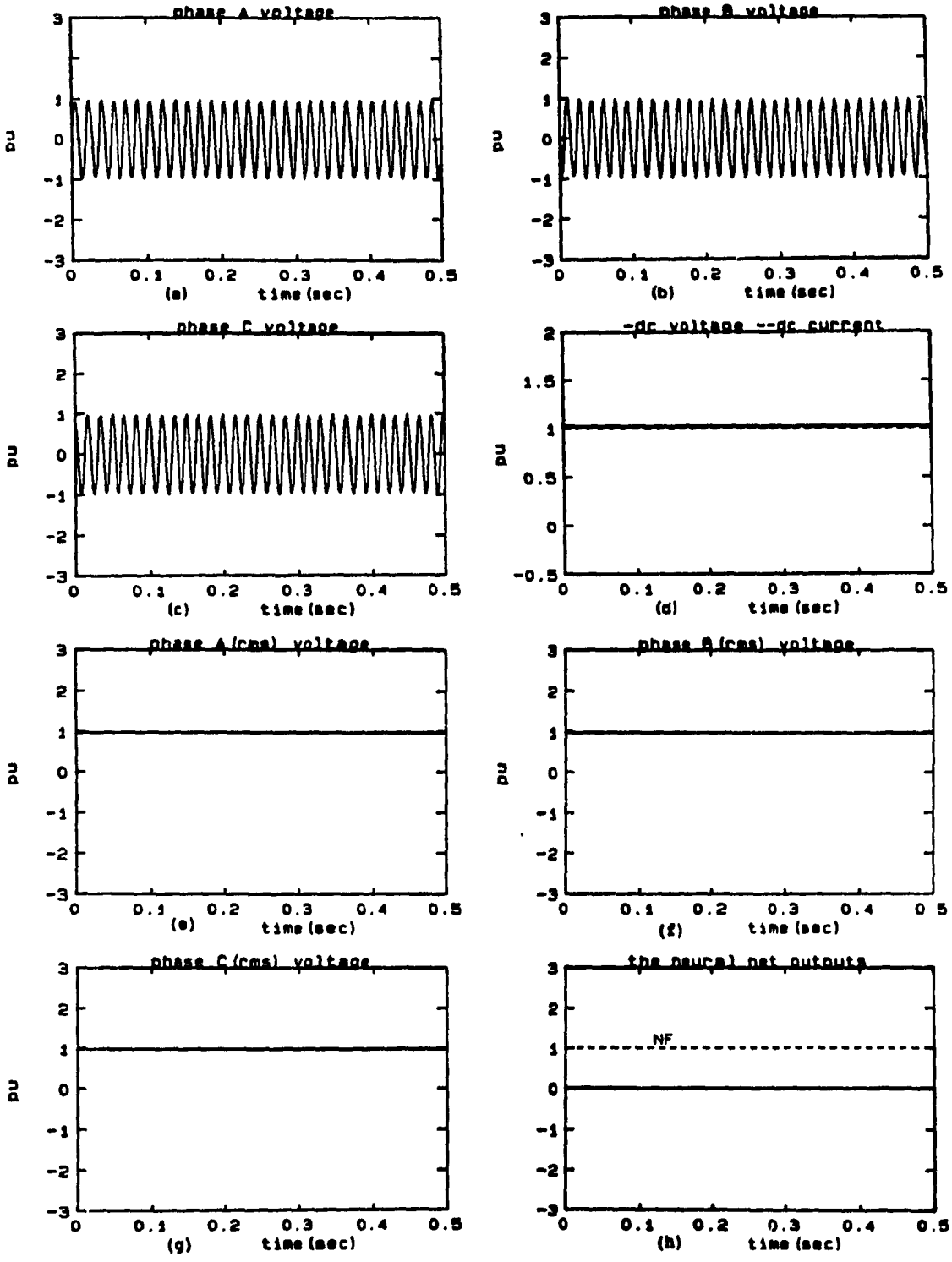

Figure 4.3-1 No fault is applied (METHOD 1).

a,b,c - The three phase voltages at the rectifier bus
d - The dc voltage and current at rectifier side
e,f,g - The rms values of the three phase voltages
h - The neural network outputs

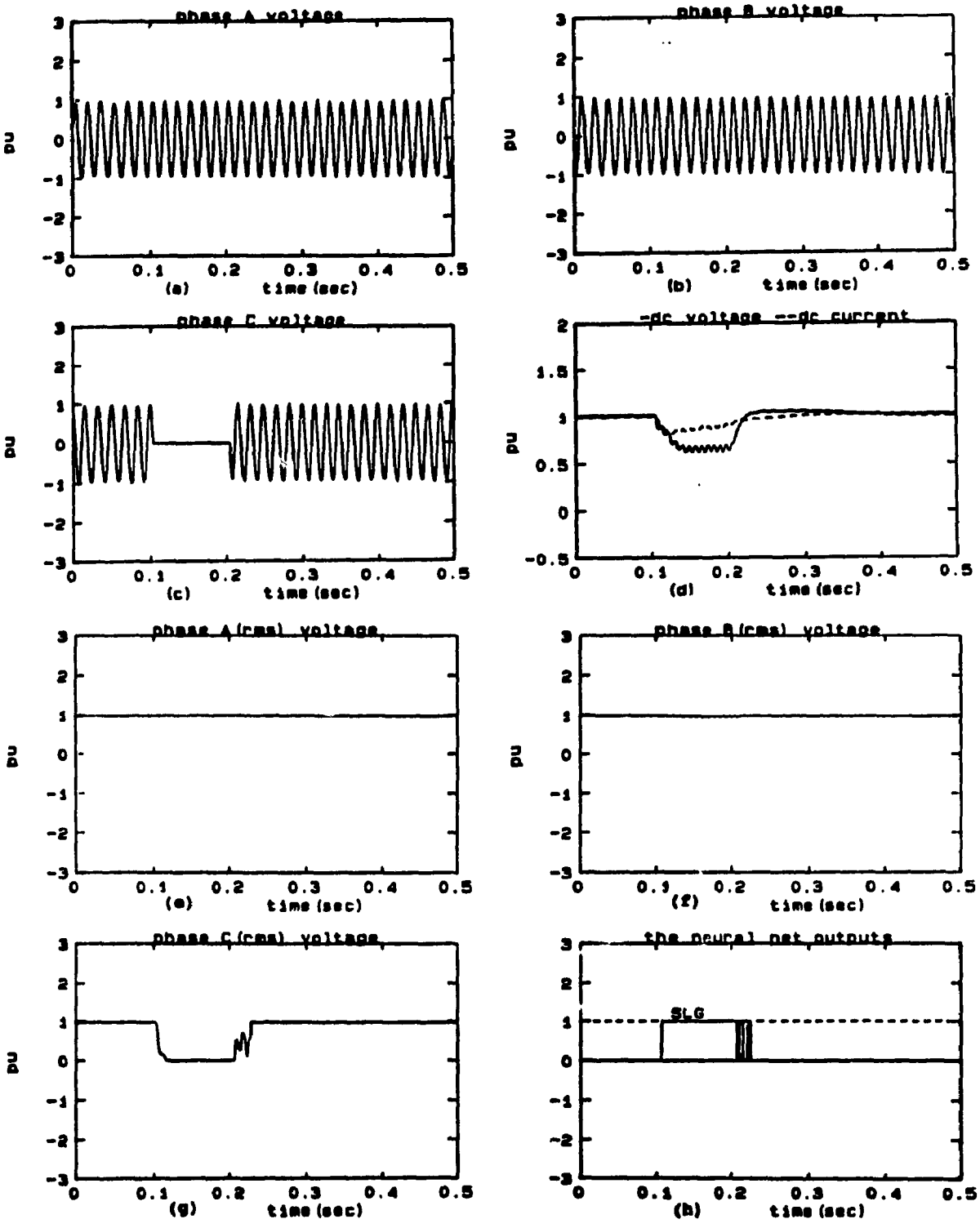

Figure 4.3-2 Single line to ground fault (METHOD 1).

a,b,c - The three phase voltages at the rectifier bus
d - The dc voltage and current at rectifier side
e,f,g - The rms values of the three phase voltages
h - The neural network outputs

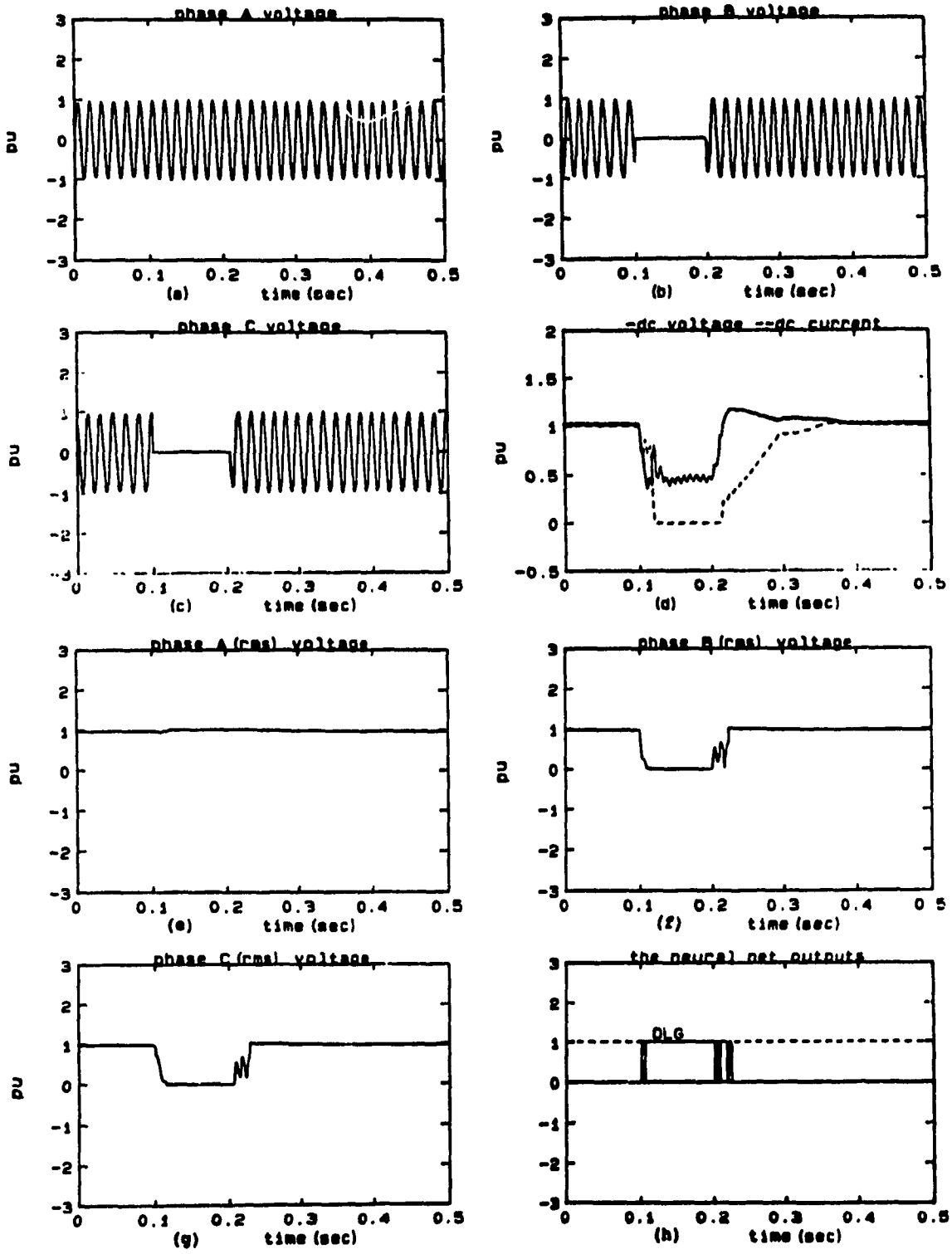

Figure 4.3-3 Double line to ground fault (METHOD 1).

a,b,c - The three phase voltages at the rectifier bus
d - The dc voltage and current at rectifier side
e,f,g - The rms values of the three phase voltages
h - The neural network outputs

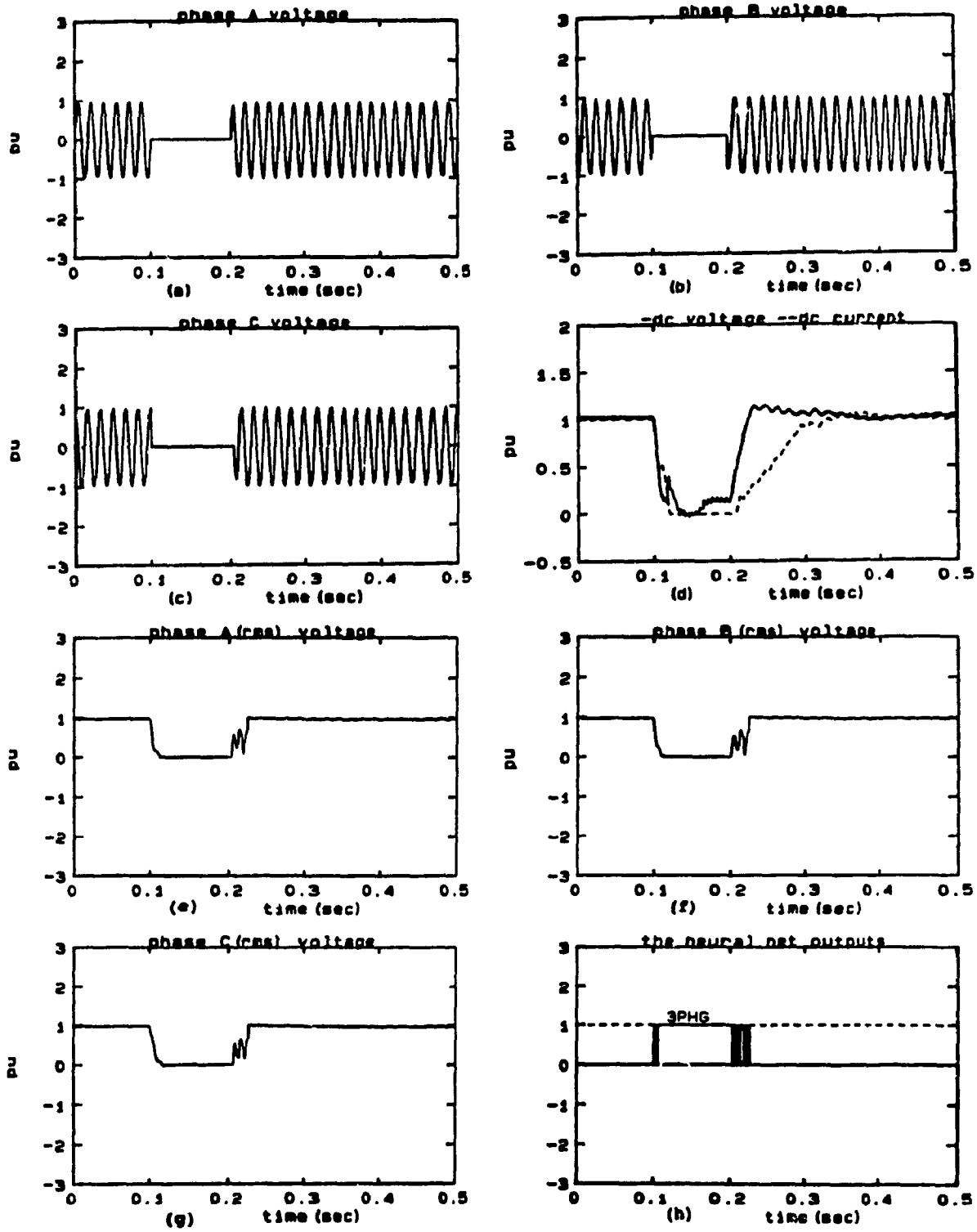

Figure 4.3-4 Three phase to ground fault (METHOD 1).

a,b,c - The three phase voltages at the rectifier bus
d - The dc voltage and current at rectifier side
e,f,g - The rms values of the three phase voltages
h - The neural network outputs

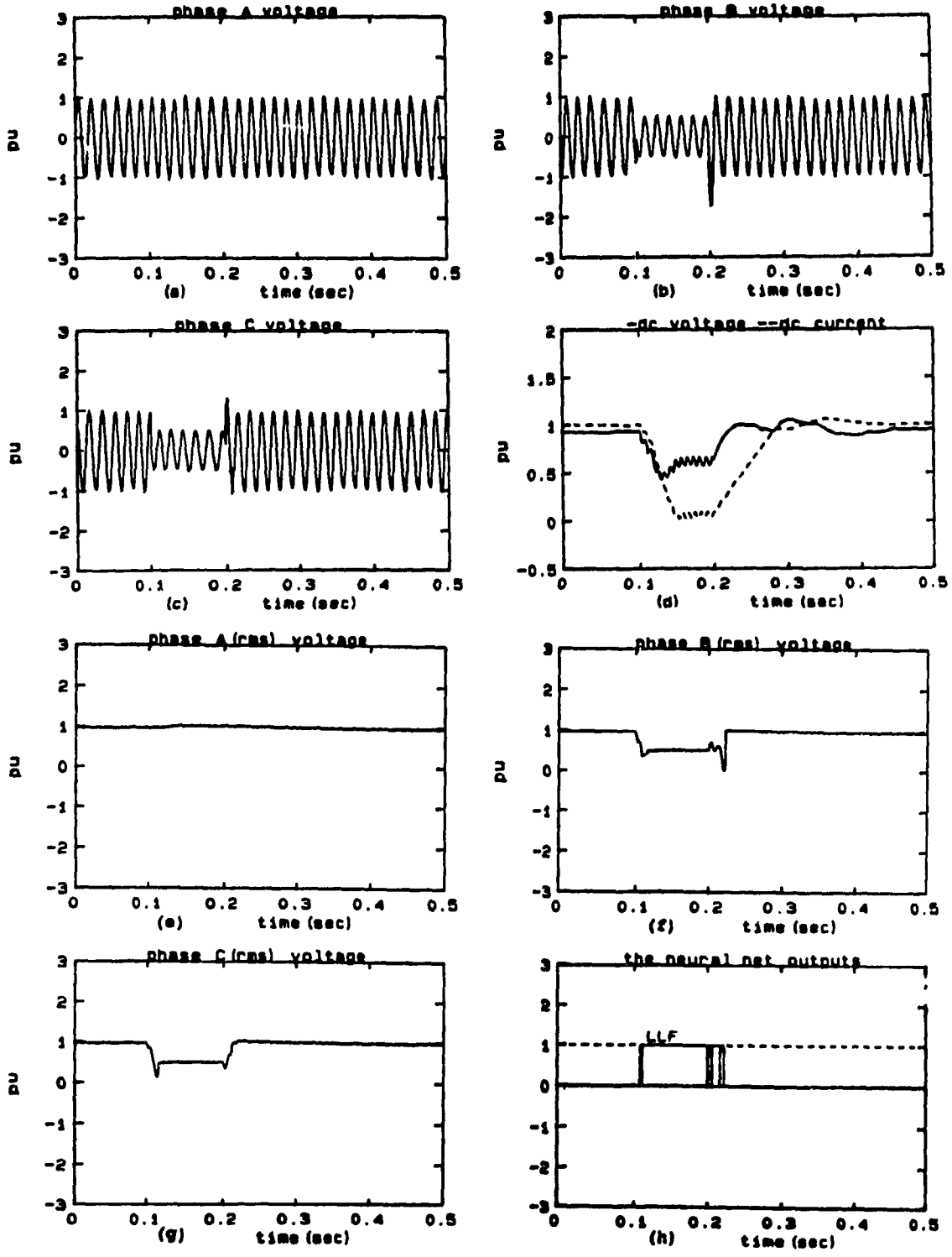

Figure 4.3-5 Line to line fault (METHOD 1).

a,b,c - The three phase voltages at the rectifier bus
d - The dc voltage and current at rectifier side
e,f,g - The rms values of the three phase voltages
h - The neural network outputs

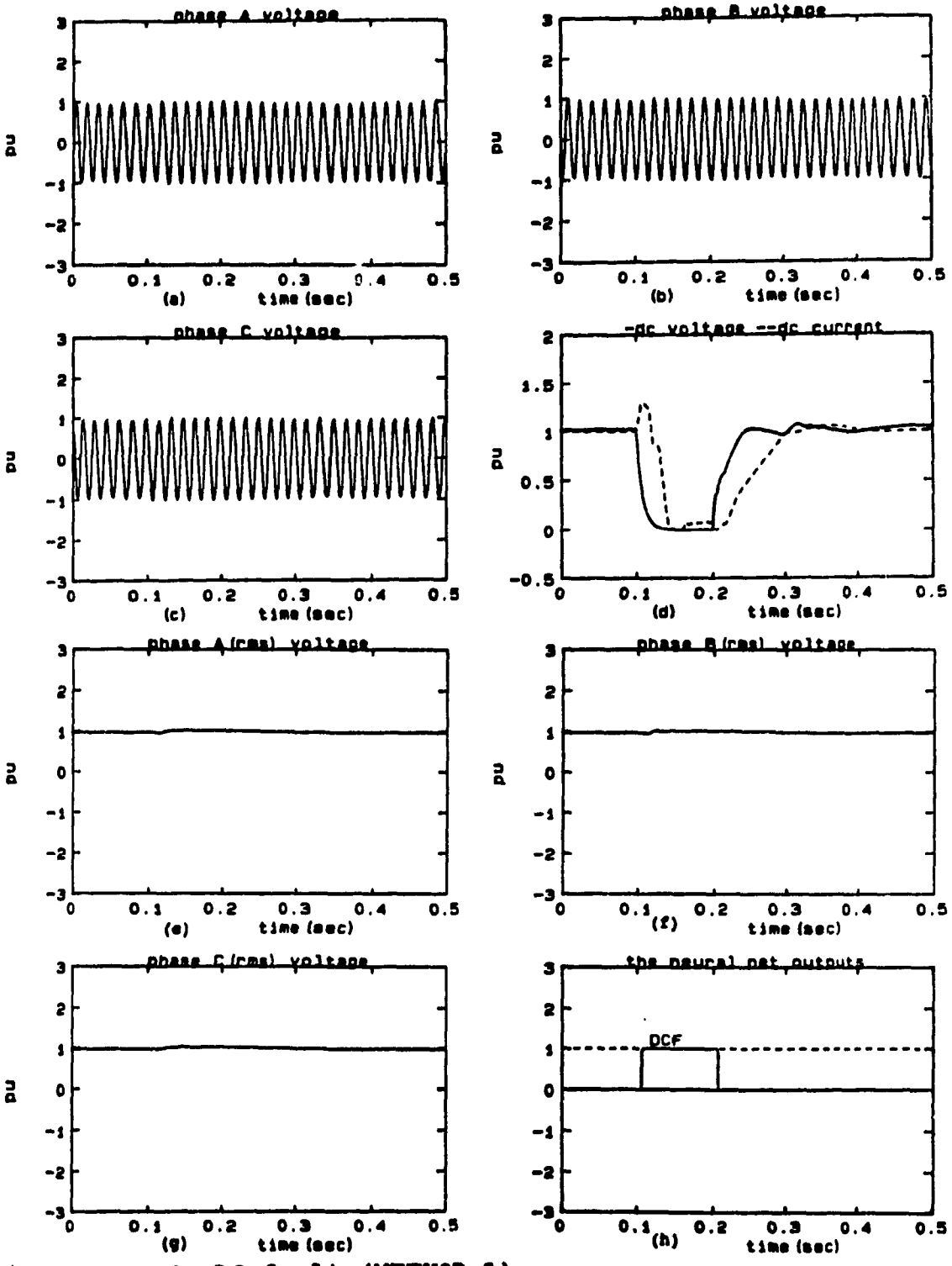

Figure 4.3-6 DC fault (METHOD 1).

a,b,c - The three phase voltages at the rectifier bus
d - The dc voltage and current at rectifier side
e,f,g - The rms values of the three phase voltages
h - The neural network outputs

During full evaluation of this method with all possible types of faults, it became apparent that there could be some confusion between detection of (a) a line to line fault and (b) a remote (i.e. high impedance) double line to ground fault. A comparison between these two types of fault with Method 1 is made in Figure 4.4, where phases B and C are the faulted phases. For LLF case (Figure 4.4a), the NN is able to correctly identify the fault type. However, for a DLGF (Figure 4.4b), the NN is erroneously indicating a LLF. Note also the phase shift between the phase voltages during the fault period.

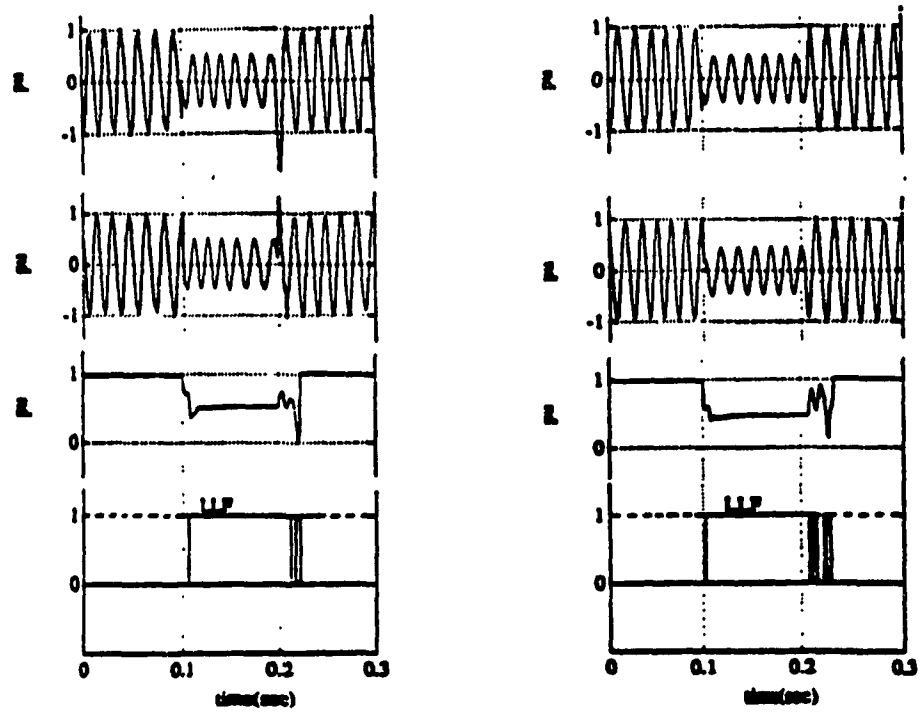

(a) Case of LLF (b) Case of remote DLGf

Figure 4.4 Cases of LLF and remote DLGF with Method 1.

Hence, to distinguish between these two types of faults, additional information is necessary. Analysis showed that for the case of a line to line fault (LLF), the bus voltage magnitude drops to about 0.5 pu and the angle between these phases is reduced to zero degrees. Also, the third unfaulted phase (not shown) is at 180 degrees phase shift from the two faulted phases. The NN is trained to detect a line to line fault (LLF) when the magnitude on any two phases drops to 0.5 pu. This condition is fulfilled in the case of a remote double to ground fault also. Any confusion between detecting either of these two types of faults is therefore unsatisfactory (Figure 4.4). Additional information is deemed necessary to clearly distinguish between these two types of faults; it is possible that this information could be the inherent phase shift between the three phases, and this is the approach of Method 2 below.

METHOD 2: (RMS Values Of 3 Phase Voltages Plus Phase Angles)

In this method, additional information i.e. phase angles between the three phases are provided, to enable the NN to make a decision. The concept of using the phase shift of $\pm$ 120 degrees (plus or minus some tolerance) between the three phases is novel and can be used to distinguish between line

to line faults and remote line to ground faults. Hence one additional NN per phase (Figure 4.5) is needed to detect these faults. These phase detector networks are fed with the following inputs per phase (i.e for phase A):

- rms phase voltage, i.e. V_a, in pu,
- angle between phases A and B, i.e. Ph A-B, in pu,
- angle between phases A and C, i.e. Ph A-C, in pu.

At its output, one processing element is attached in an additional layer. This element is connected with fixed weights such that the output from the Phase Detector Network is:

- 1, when there is No Fault NF,
- -1, when there is a Line to Line Fault LL,
- 0, when there is a Line to Ground Fault LG.

These outputs, of the three phase detectors, are then connected to the main network (Figure 4.5). A subroutine in EMTDC is developed to detect the phase angles between the three phases. This subroutine is based on measuring the time elapsed following a phase voltage zero-crossing. These times are then converted to per unit values for the neural network.

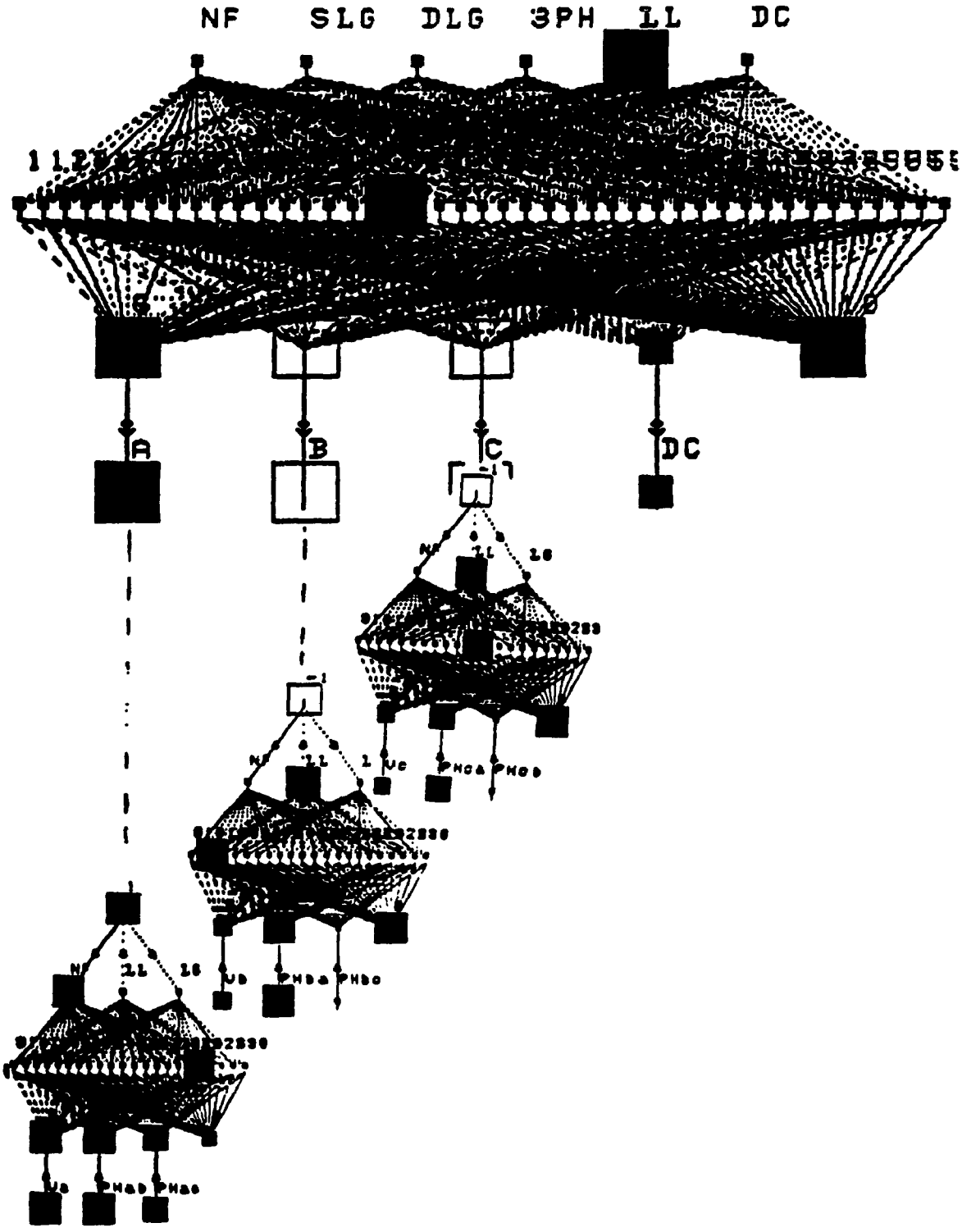

Figure 4.5 CPN for fault identification (METHOD 2). Inputs to the NN ar t e rms values of the three phase voltages (V_a, V_b, V_c), The phase angles between these phases (PH_{ab}, PH_{ac}, PH_{bc}), and the dc voltage

Training of these CPN networks (main and phase detectors) is done off-line. The training set for the phase A Detector Network is shown in Table 4.4. Similar training sets are used for phases B and C. Some tolerance (0.2) are built into the inputs to give to the network more generalization capability i.e. a value of 0.8 pu or more is interpreted as 1 pu, and a value of 0.2 pu or less is interpreted as 0.0 pu. The training set of the main network is shown in table 4.3. The outputs of the three Phase Detectors Networks are used as inputs to the main network.

Table 4.2 Training set for Phase A Detector Network.

class	voltage A (rms)	PHab	PHac	type of fault
0	0.8	0.8	0.8	!No fault
0	0.8	0.8	0.2	!No fault
0	0.8	0.2	0.8	!No fault
0	0.8	0.2	0.2	!No fault
1	0.5	0.8	0.2	!Lint to line
1	0.5	0.2	0.8	!Line to line
1	0.5	0.2	0.2	!Line to line
2	0.5	0.8	0.8	!Line to ground
2	0.2	0.8	0.8	!Line to ground
2	0.2	0.8	0.2	!Line to ground
2	0.2	0.2	0.8	!Line to ground
2	0.2	0.2	0.2	!Line to ground

Table 4.3 Training set for main network for Method 2.

class	phase A	phase B	phase C	dc voltage	type of fault
0	1.0	1.0	1.0	1.0	!No fault
0	-1.0	1.0	1.0	1.0	!No fault
0	-1.0	1.0	1.0	0.0	!No fault
0	-1.0	0.0	1.0	1.0	!No fault
0	-1.0	0.0	1.0	0.0	!No fault
0	-1.0	1.0	0.0	1.0	!No fault
0	-1.0	1.0	0.0	0.0	!No fault
0	1.0	-1.0	1.0	1.0	!No fault
0	1.0	-1.0	1.0	0.0	!No fault
0	1.0	-1.0	0.0	1.0	!No fault
0	1.0	-1.0	0.0	0.0	!No fault
0	0.0	-1.0	1.0	1.0	!No fault
0	0.0	-1.0	1.0	0.0	!No fault
0	0.0	1.0	-1.0	1.0	!No fault
0	0.0	1.0	-1.0	0.0	!No fault
0	1.0	0.0	-1.0	1.0	!No fault
0	1.0	0.0	-1.0	0.0	!No fault
0	1.0	1.0	-1.0	1.0	!No fault
0	1.0	1.0	-1.0	0.0	!No fault
1	0.0	1.0	1.0	1.0	!Single line
1	0.0	1.0	1.0	0.0	!Single line
1	1.0	0.0	1.0	1.0	!Single line
1	1.0	0.0	1.0	0.0	!Single line
1	1.0	1.0	0.0	1.0	!Single line
1	1.0	1.0	0.0	0.0	!Single line
2	0.0	0.0	1.0	1.0	!Double line
2	0.0	0.0	1.0	0.0	!Double line
2	0.0	1.0	0.0	1.0	!Double line
2	0.0	1.0	0.0	0.0	!double line
2	1.0	0.0	0.0	1.0	!Double line
2	1.0	0.0	0.0	0.0	!Double line
3	0.0	0.0	0.0	1.0	!Three phase
3	0.0	0.0	0.0	0.0	!Three phase
4	-1.0	1.0	-1.0	1.0	!Line to line
4	-1.0	1.0	-1.0	0.0	!Line to line
4	-1.0	-1.0	1.0	1.0	!Line to line
4	-1.0	-1.0	1.0	0.0	!Line to line
4	1.0	-1.0	-1.0	1.0	!Line to line
4	1.0	-1.0	-1.0	0.0	!line to line
5	1.0	1.0	1.0	0.0	!DC fault

All six types of faults are verified with this method and good indications are obtained from the NN. These results are shown in Figures 4.7-1 ... 4.7-6. In addition, a comparison between the outputs is available in Figure 4.6 for a LLF and a remote DLGF; the fault being applied between phases B and C. Figure 4.6 depicts the three phase rms voltage inputs including the phase angles between phases A-B, B-C, and A-C and the output of the network using Method 2. With this method, it is possible to discriminate between LLF and DLGF. This is not the case with Method 1. (The corresponding result of Figure 4.6b should also be compared to those of Figure 4.4b, since these results are for identical faults).

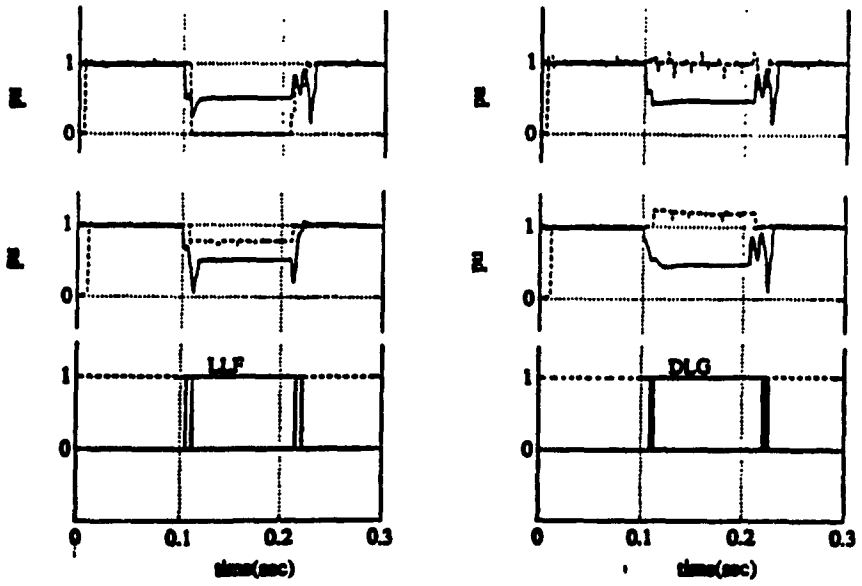

(a) Case of LLF (b) Case of remote DLGf

Figure 4.6 Cases of LLF and remote DLGF with Method 2.

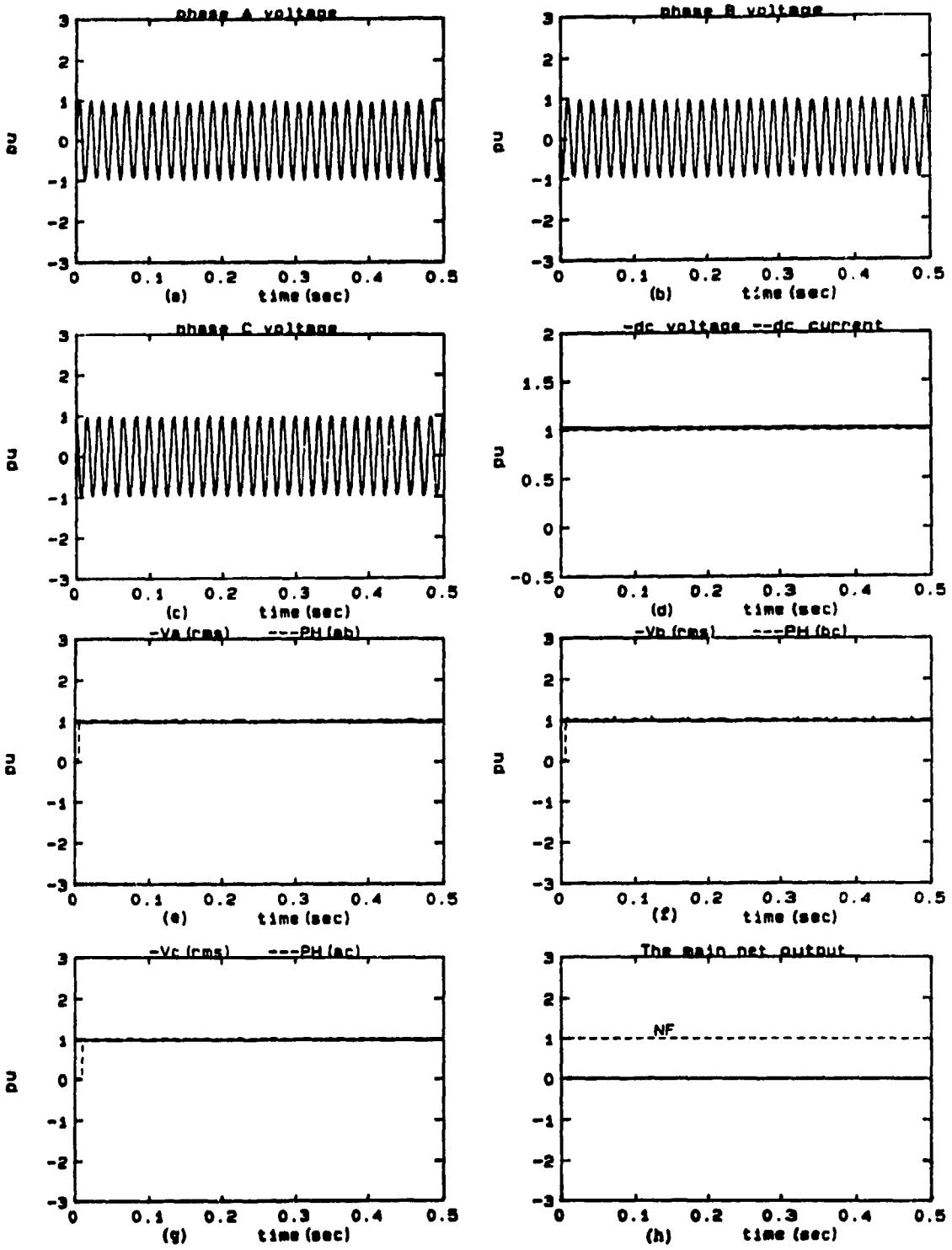

Figure 4.7-1 No fault is applied (METHOD 2).

a,b,c - The three phase voltages at the rectifier bus
d - The dc voltage and current at rectifier side
e,f,g - The rms values of the three phase voltages
- The phase angles between the phase voltages
h - The main neural network outputs

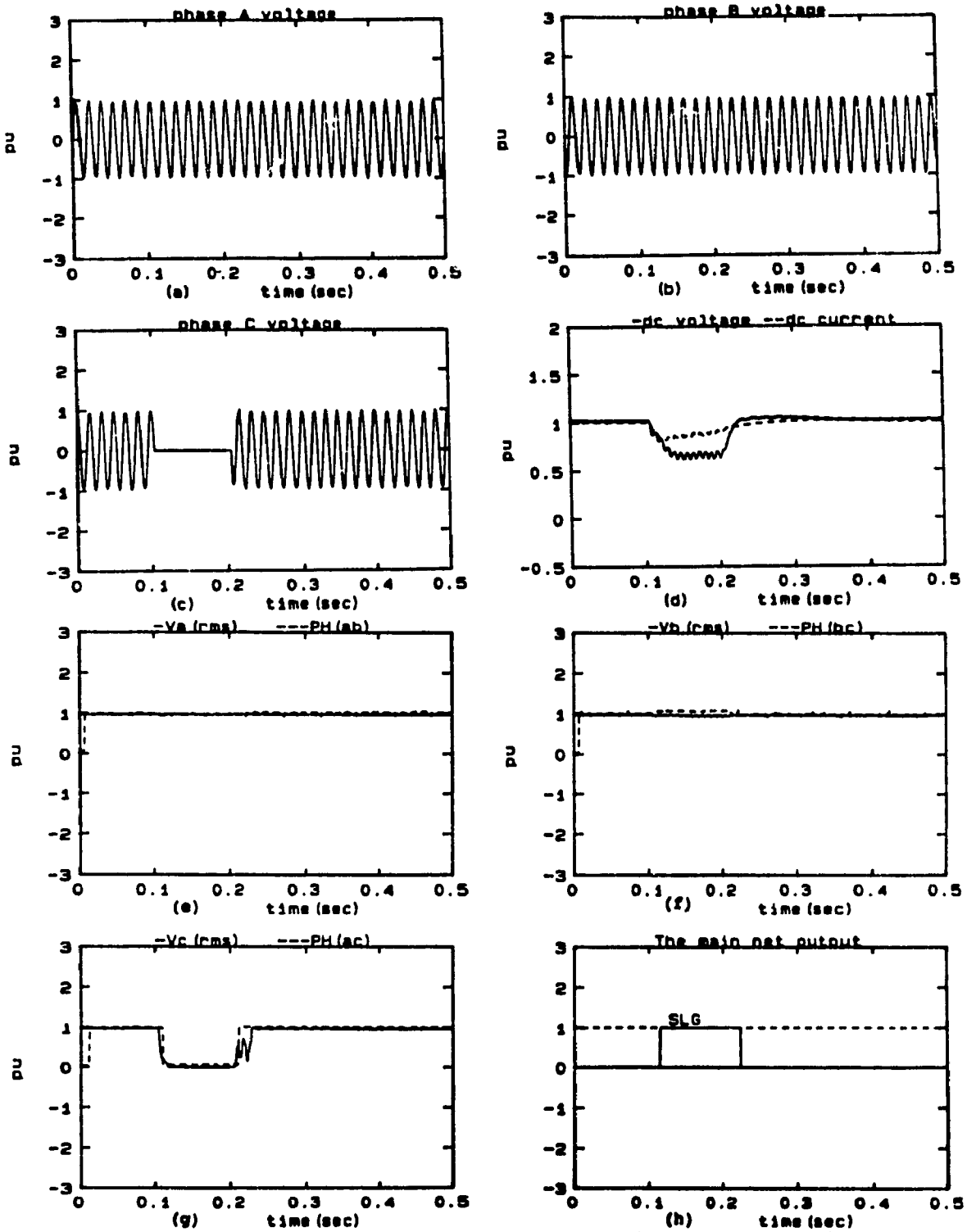

Figure 4.7-2 Single line to ground fault (METHOD 2).

a,b,c - The three phase voltages at the rectifier bus
d - The dc voltage and current at rectifier side
e,f,g - The rms values of the three phase voltages
- The phase angles between the phase voltages
h - The main neural network outputs

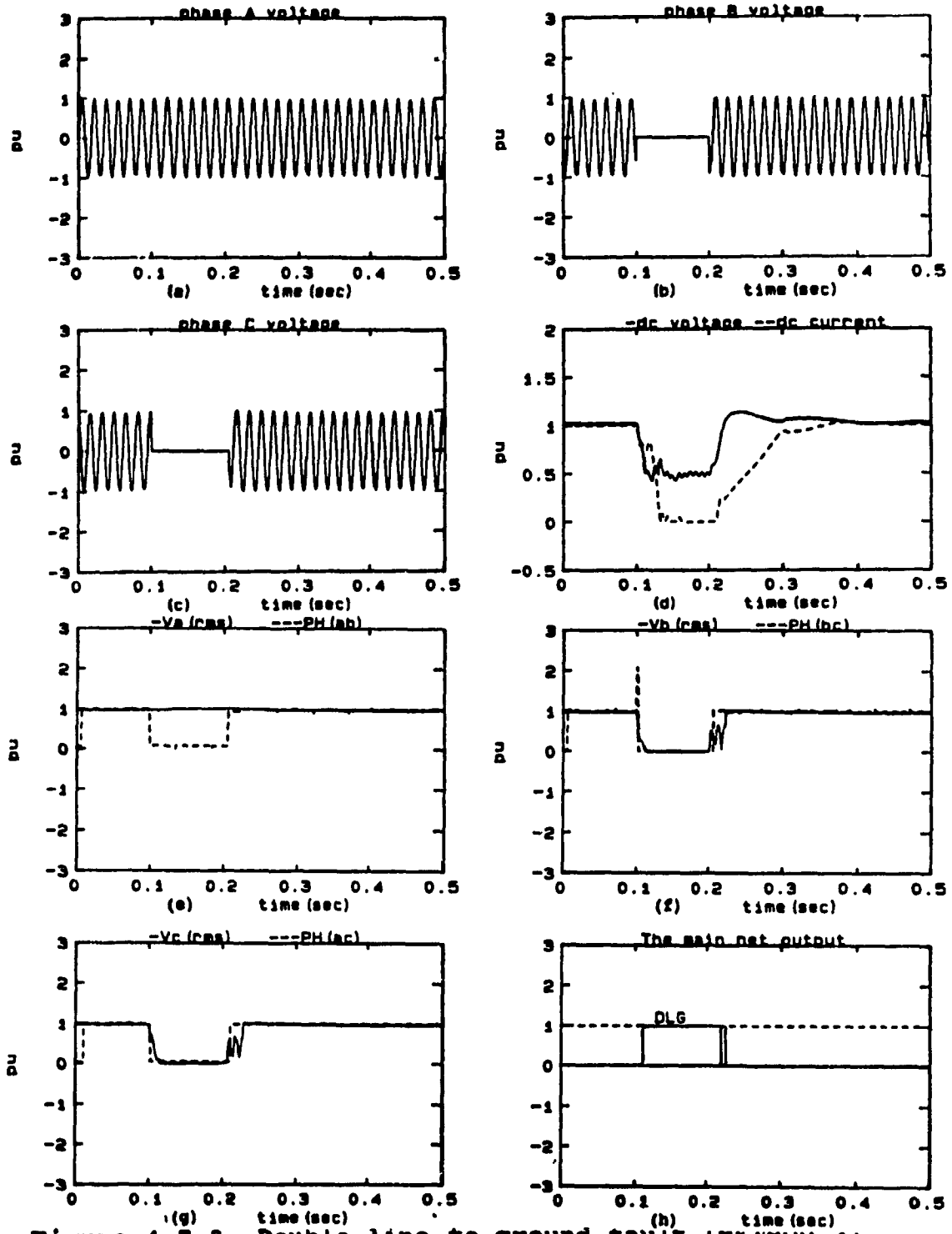

Figure 4.7-3 Double line to ground fault (METHOD 2).

a,b,c - The three phase voltages at the rectifier bus
d - The dc voltage and current at rectifier side
e,f,g - The rms values of the three phase voltages
- The phase angles between the phase voltages
h - The main neural network outputs

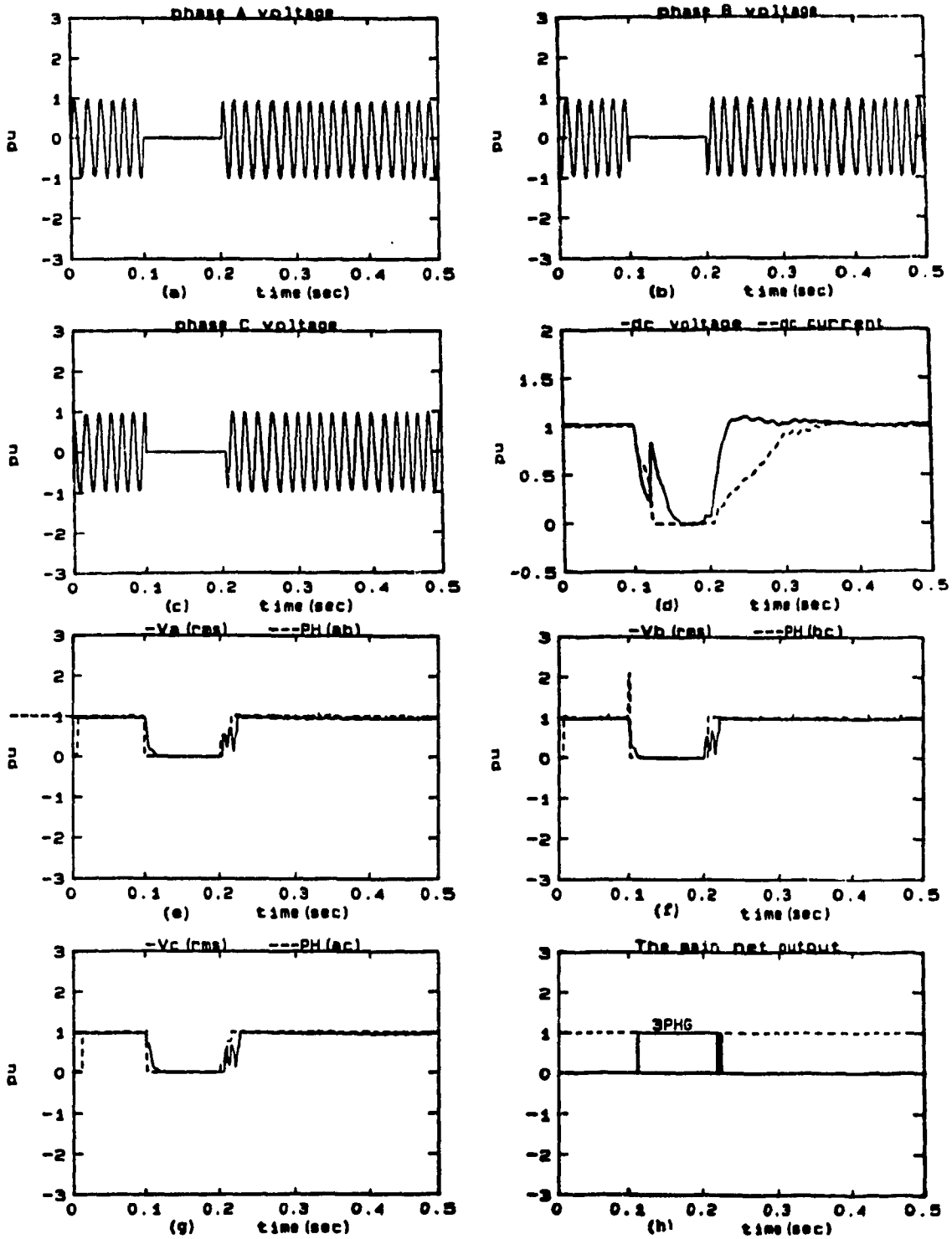

Figure 4.7-4 Three phase to ground fault (METHOD 2).

a,b,c - The three phase voltages at the rectifier bus
d - The dc voltage and current at rectifier side
e,f,g - The rms values of the three phase voltages
- The phase angles between the phase voltages
h - The main neural network outputs

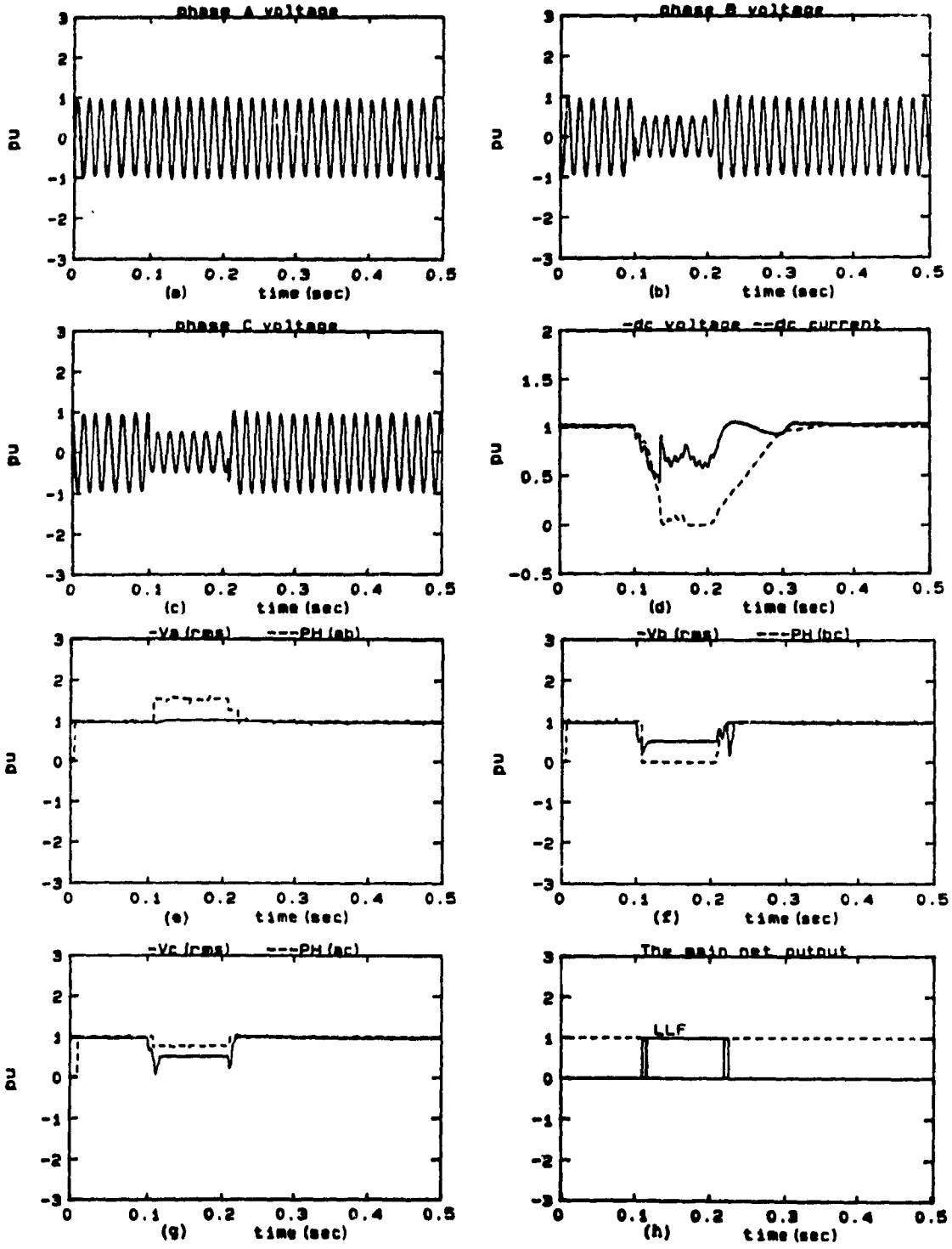

Figure 4.7-5 Line to line fault (METHOD 2).

a,b,c - The three phase voltages at the rectifier bus
d - The dc voltage and current at rectifier side
e,f,g - The rms values of the three phase voltages
- The phase angles between the phase voltages
h - The main neural network outputs

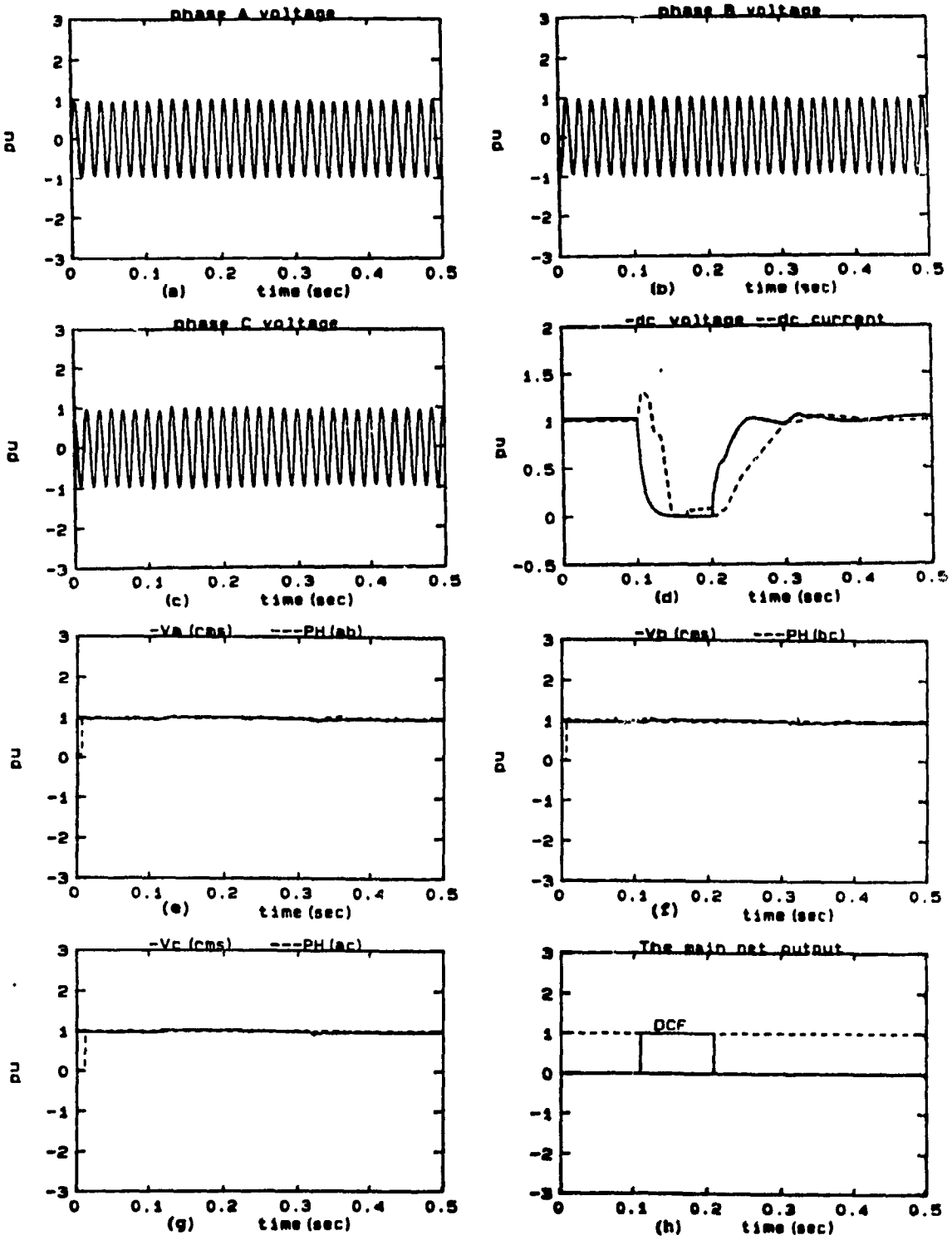

Figure 4.7-6 DC fault (METHOD 2).

a,b,c - The three phase voltages at the rectifier bus
d - The dc voltage and current at rectifier side
e,f,g - The rms values of the three phase voltages
- The phase angles between the phase voltages
- The main neural network outputs

METHOD 3: (Instantaneous Values Of Phase Voltages)

In this method (Figure 4.8) the sampled instantaneous values of the three phase voltages are used as inputs along with the dc voltage. Similar to Method 2, a separate Phase Detector Network for each phase is required. Samples of the instantaneous voltages are taken at time t, t-k, t-2k, and t-3k second intervals, with k=0.001 seconds.

At the output of each Phase Detector Network, one processing element is attached in an additional layer. This element is connected with fixed weights such that the output from the Phase Detector Network is : 1, when there is No Fault NF; -1, when there is a Line to Line Fault LLF; 0, when there is a Line to Ground Fault LGF. These outputs for the three Phase Detectors are then connected to the main NN which is the a main network similar to the one used in Method 2 and has the same training set (Table 4.3).

The training set for a Phase Detector for each of the three phases is given in table 4.4. The inputs to the network are sampled values of the instantaneous phase voltage. The training time was longer in this case due to 71 neurons being used in the Kohonen layer for this approach. Results of this method are shown in Figures 4.9-1 ... 4.9-6.

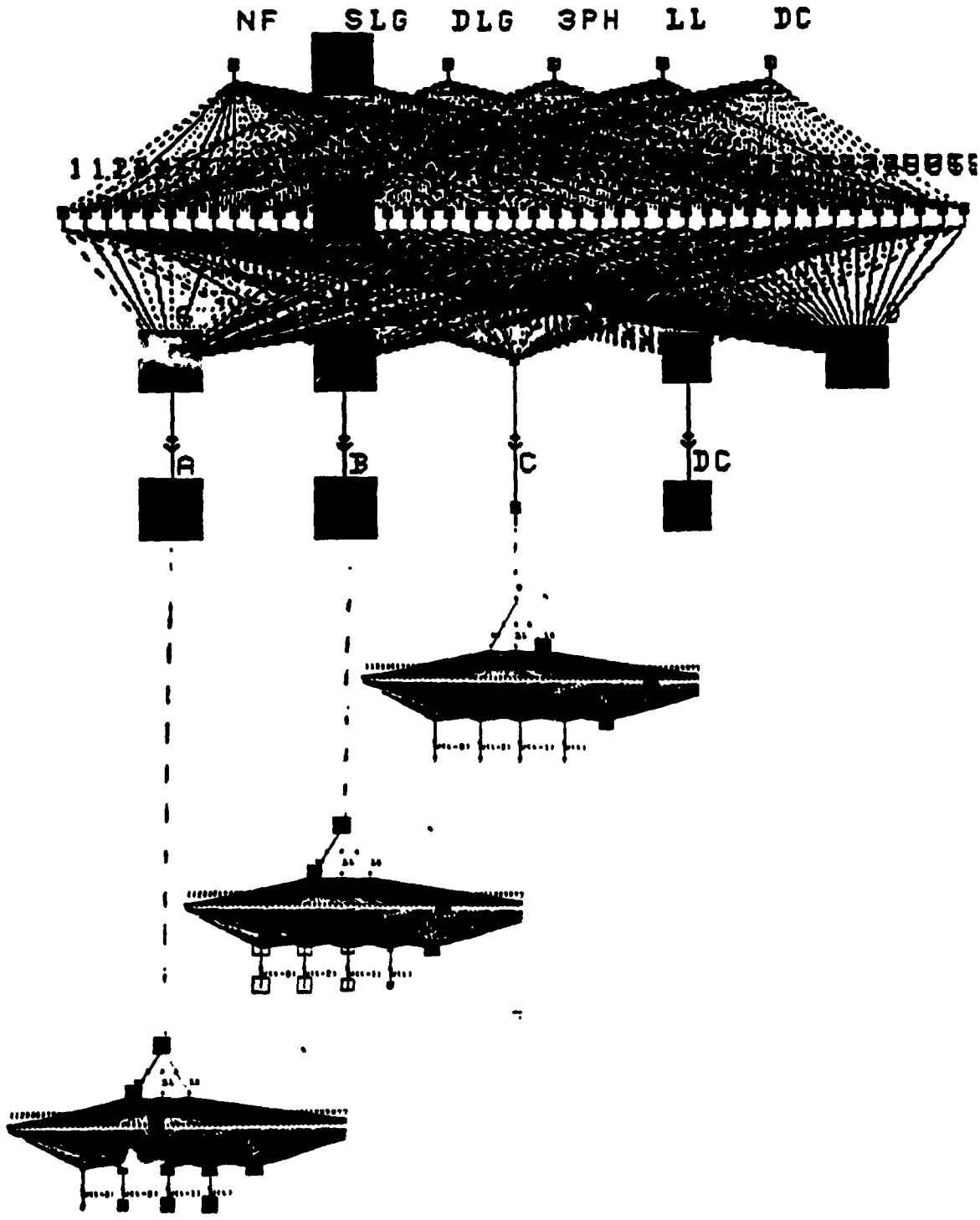

Figure 4.8 CPN for fault identification (METHOD 3). Inputs to the NN are the sine waves of the three phase voltages and the dc voltage.

Table 4.4 Training set using instantaneous values of phase voltages used for Method 3.

class	Va(t)	Va(t-1)	Va(t-2)	Va(t-3)	type of fault
0	0.0000	0.3679	0.6843	0.9046	!No Fault
0	0.1873	0.5356	0.8087	0.9684	
0	0.3679	0.6843	0.9046	0.9980	
0	0.5356	0.8087	0.9684	0.9922	
0	0.6843	0.9046	0.9980	0.9514	
0	0.8087	0.9684	0.9922	0.8768	
0	0.9046	0.9980	0.9514	0.7712	
0	0.9684	0.9922	0.8768	0.6384	
0	0.9980	0.9514	0.7712	0.4829	
0	0.9922	0.8768	0.6384	0.3104	
0	0.9514	0.7712	0.4829	0.1268	
0	0.8768	0.6384	0.3104	-0.0612	
0	0.7712	0.4829	0.1268	-0.2470	
0	0.6384	0.3104	-0.0612	-0.4241	
0	0.4829	0.1268	-0.2470	-0.5862	
0	0.3104	-0.0612	-0.4241	-0.7276	
0	0.1268	-0.2470	-0.5862	-0.8432	
0	-0.0612	-0.4241	-0.7276	-0.9290	
0	-0.2470	-0.5862	-0.8432	-0.9819	
0	-0.4241	-0.7276	-0.9290	-1.0000	
0	-0.5862	-0.8432	-0.9819	-0.9827	
0	-0.7276	-0.9290	-1.0000	-0.9307	
0	-0.8432	-0.9819	-0.9827	-0.8458	
0	-0.9290	-1.0000	-0.9307	-0.7309	
0	-0.9819	-0.9827	-0.8458	-0.5901	
0	-1.0000	-0.9307	-0.7309	-0.4285	
0	-0.9827	-0.8458	-0.5901	-0.2516	
0	-0.9307	-0.7309	-0.4285	-0.0659	
0	-0.8458	-0.5901	-0.2516	0.1221	
0	-0.7309	-0.4285	-0.0659	0.3058	
0	-0.5901	-0.2516	0.1221	0.4787	
0	-0.4285	-0.0659	0.3058	0.6347	
0	-0.2516	0.1221	0.4787	0.7682	
1	0.0000	0.1656	0.3079	0.4071	!Line to line fault
1	0.0843	0.2410	0.3639	0.4358	
1	0.1656	0.3079	0.4071	0.4491	
1	0.2410	0.3639	0.4358	0.4465	
1	0.3079	0.4071	0.4491	0.4281	
1	0.3639	0.4358	0.4465	0.3946	
1	0.4071	0.4491	0.4281	0.3471	
1	0.4358	0.4465	0.3946	0.2873	
1	0.4491	0.4281	0.3471	0.2173	
1	0.4465	0.3946	0.2873	0.1397	
1	0.4281	0.3471	0.2173	0.0571	
1	0.3946	0.2873	0.1397	-0.0275	
1	0.3471	0.2173	0.0571	-0.1112	
1	0.2873	0.1397	-0.0275	-0.1909	
1	0.2173	0.0571	-0.1112	-0.2638	
1	0.1397	-0.0275	-0.1909	-0.3274	
1	0.0571	-0.1112	-0.2638	-0.3794	
1	-0.0275	-0.1909	-0.3274	-0.4180	
1	-0.1112	-0.2638	-0.3794	-0.4418	
1	-0.1909	-0.3274	-0.4180	-0.4500	
1	-0.2638	-0.3794	-0.4418	-0.4422	
1	-0.3274	-0.4180	-0.4500	-0.4188	
1	-0.3794	-0.4418	-0.4422	-0.3806	
1	-0.4180	-0.4500	-0.4188	-0.3289	
1	-0.4418	-0.4422	-0.3806	-0.2655	
1	-0.4500	-0.4188	-0.3289	-0.1928	
1	-0.4422	-0.3806	-0.2655	-0.1132	
1	-0.4188	-0.3289	-0.1928	-0.0297	
1	-0.3806	-0.2655	-0.1132	0.0549	
1	-0.3289	-0.1928	-0.0297	0.1376	
1	-0.2655	-0.1132	0.0549	0.2154	
1	-0.1928	-0.0297	0.1376	0.2856	
1	-0.1132	0.0549	0.2154	0.3457	
1	-0.0297	0.1376	0.2856	0.3935	
1	0.0549	0.2154	0.3457	0.4274	
2	0.0010	0.0010	0.0010	0.0010	!Line to ground fault

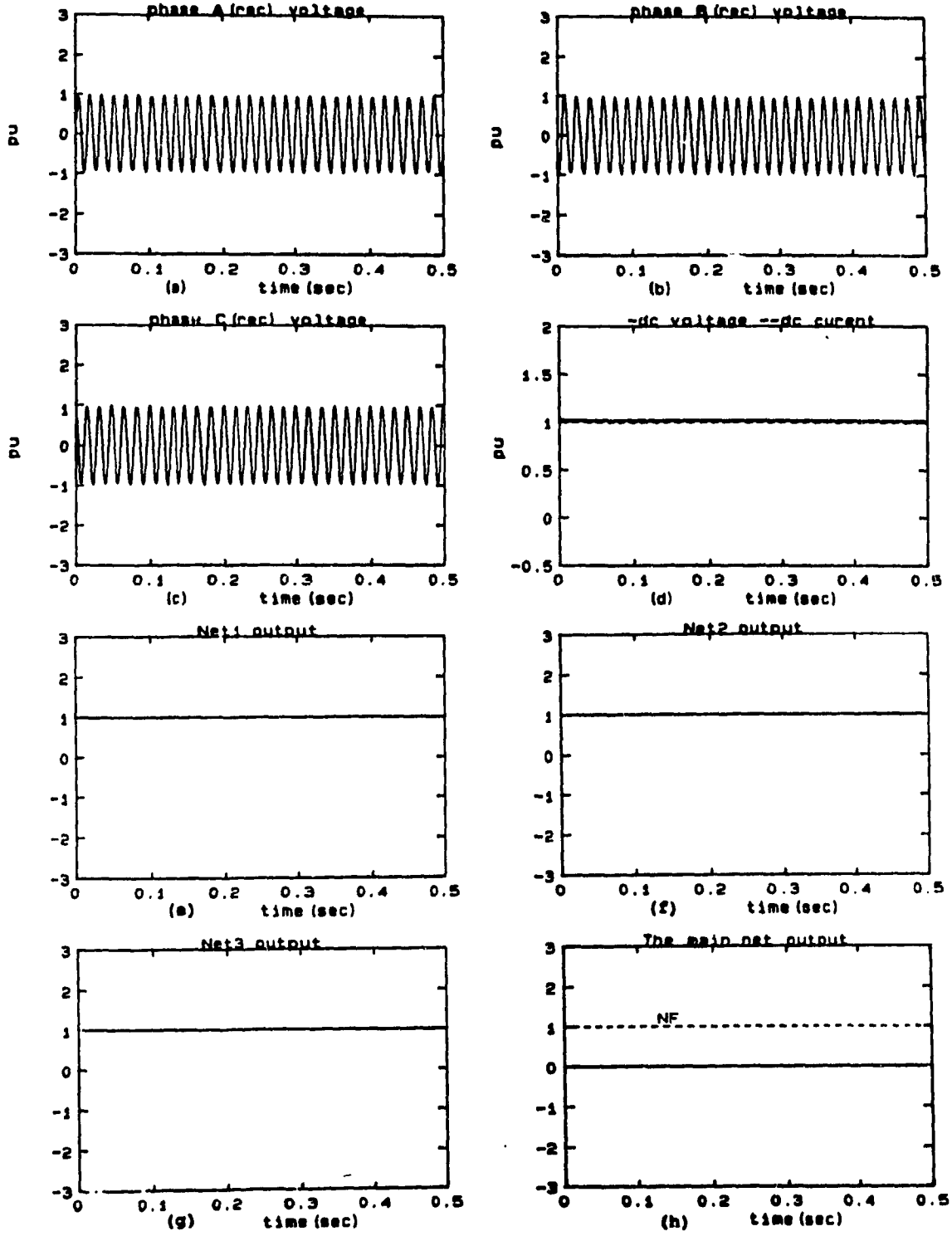

Figure 4.9-1 No fault is applied (METHOD 3).

a,b,c - The three phase voltages at the rectifier bus
d - The dc voltage and current at rectifier side
e,f,g - The outputs of the three Phase Detectors
h - The main neural network outputs

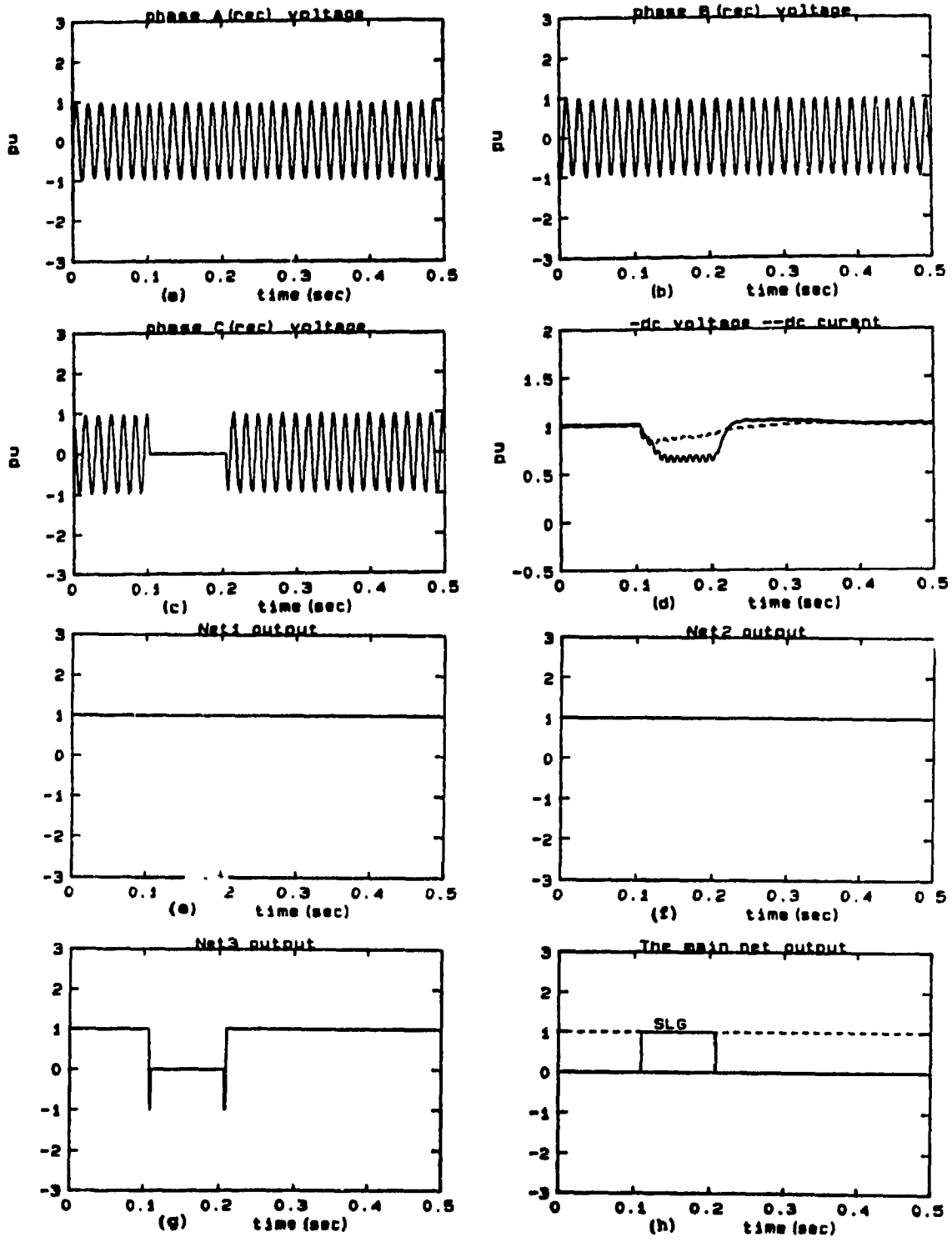

Figure 4.9-2 Single line to ground fault (METHOD 3).

a,b,c - The three phase voltages at the rectifier bus
d - The dc voltage and current at rectifier side
e,f,g - The outputs of the three Phase Detectors
h - The main neural network outputs

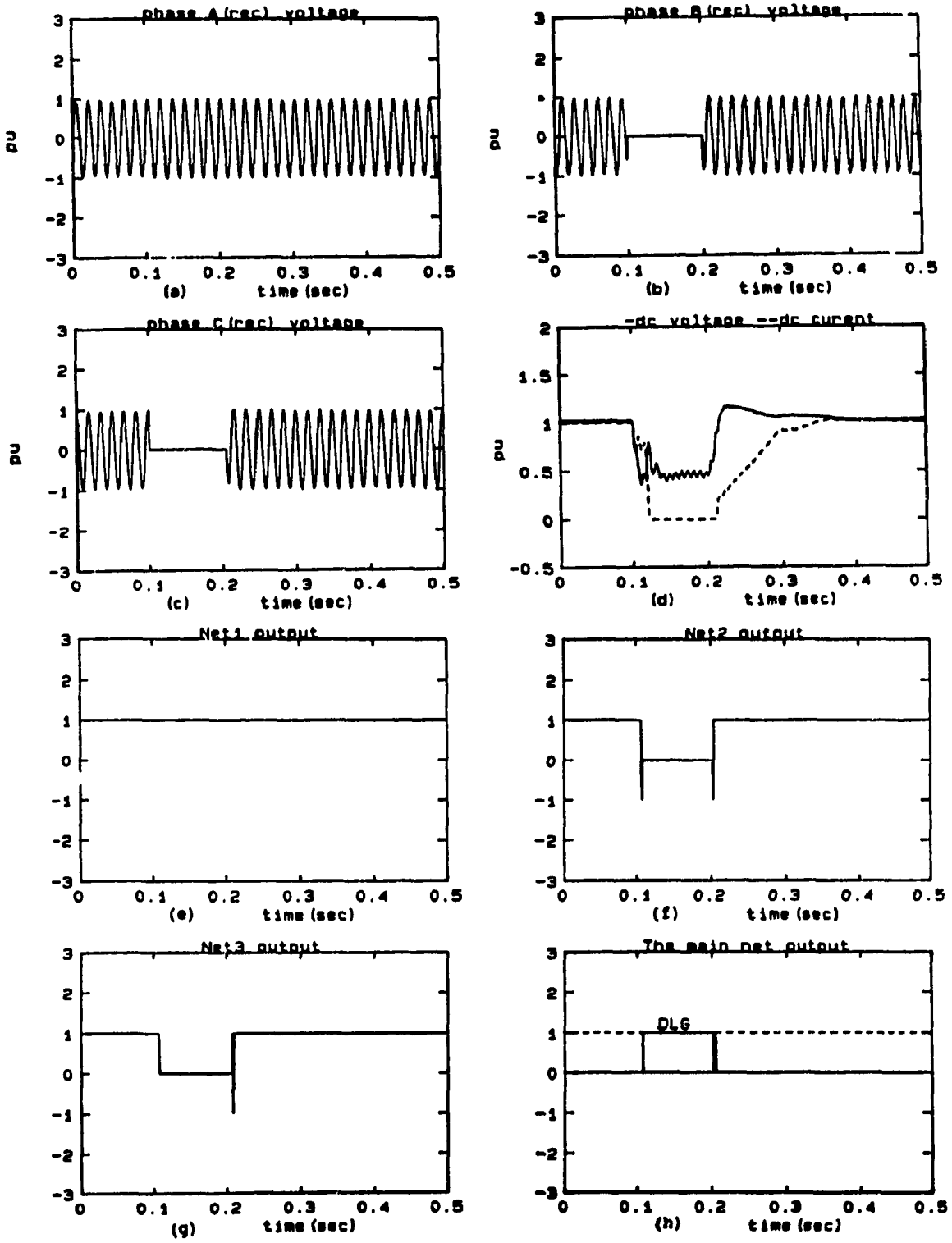

Figure 4.9-3 Double line to ground fault (METHOD 3).

a,b,c - The three phase voltages at the rectifier bus
d - The dc voltage and current at rectifier side
e,f,g - The outputs of the three Phase Detectors
h - The main neural network outputs

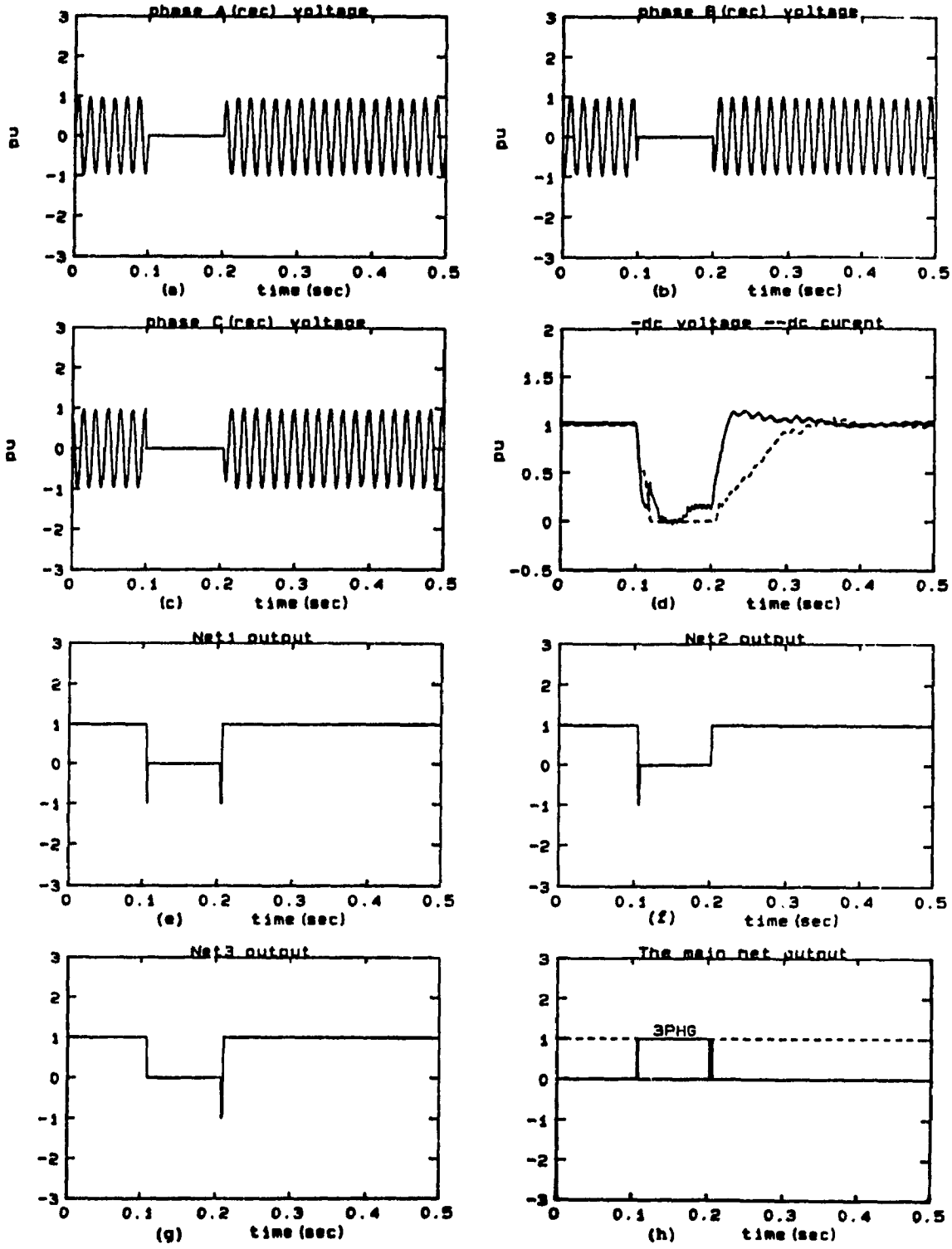

Figure 4.9-4 Three phase to ground fault (METHOD 3).

a,b,c - The three phase voltages at the rectifier bus
d - The dc voltage and current at rectifier side
e,f,g - The outputs of the three Phase Detectors
h - The main neural network outputs

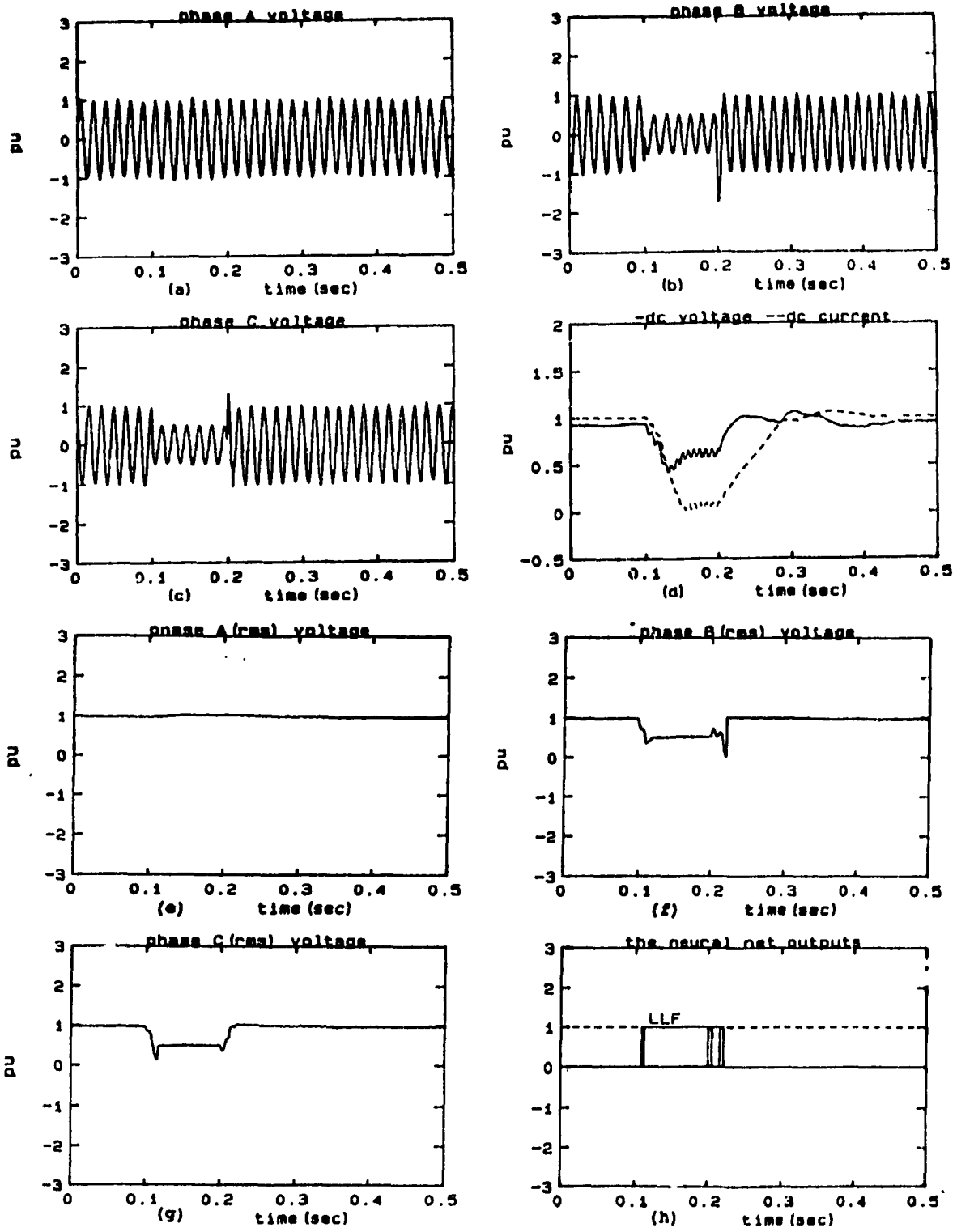

Figure 4.9-5 Line to line fault (**METHOD** 3).

a,b,c - The three phase voltages at the rectifier bus
d - The dc voltage and current at rectifier side
e,f,g - The outputs of the three Phase Detectors
h - The main neural network outputs

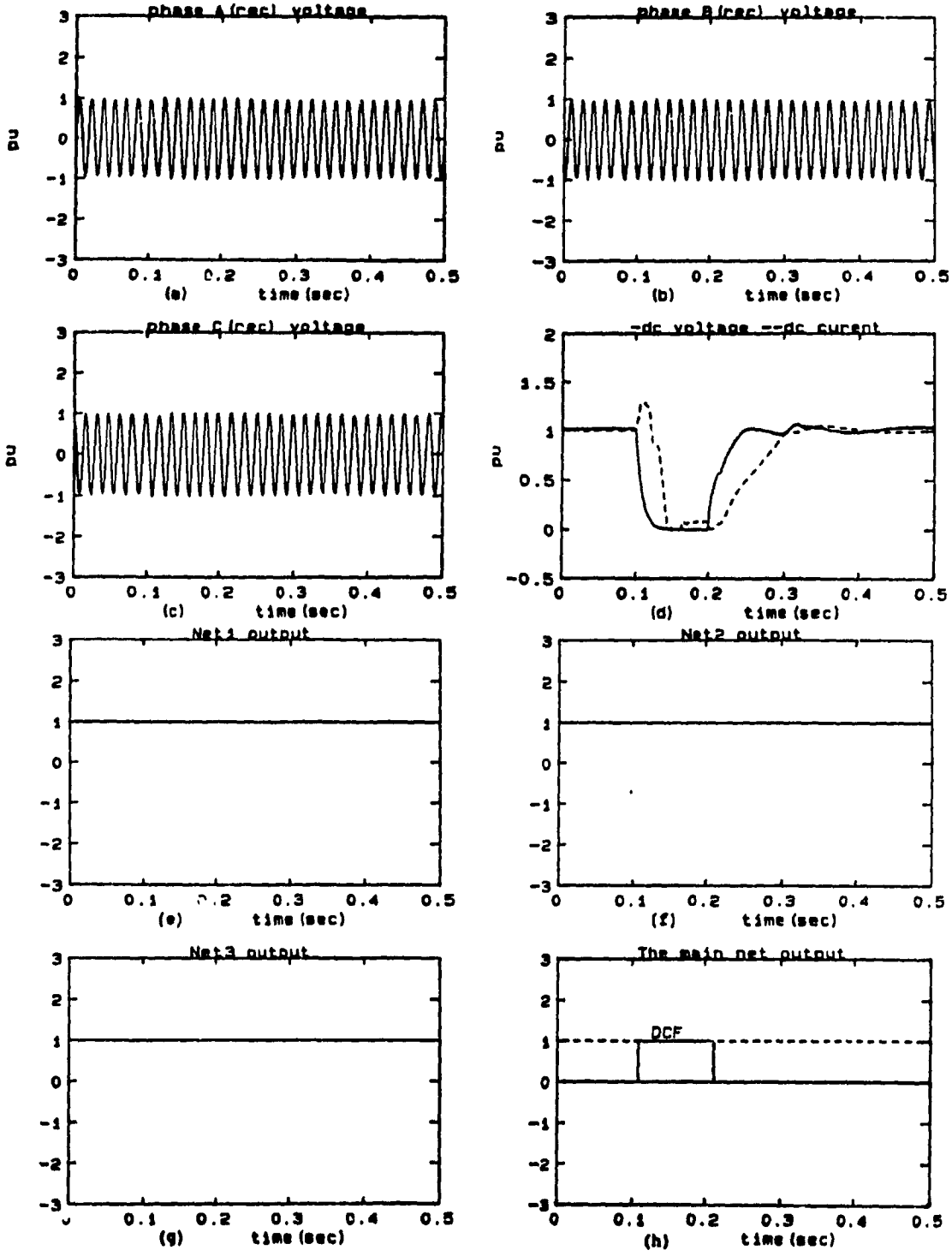

Figure 4.9-6 DC fault (METHOD 3).

a,b,c - The three phase voltages at the rectifier bus
d - The dc voltage and current at rectifier side
e,f,g - The outputs of the three Phase Detectors
h - The main neural network outputs

Generalization Capability

The generalization capability of the NN produces the correct output even when the input is partially incomplete or partially incorrect. In the case of solid bus faults near to the sensing location, this is unlikely to cause any confusion in detection of the type of fault. However, such types of faults are rarer than the more frequent remote high impedance faults which occur on the transmission lines. In the case of these remote faults, the rectifier ac voltage may not drop to zero. Although the NN has not been trained for these types faults, it still can detect them i.e. identify faults it had not seen due to its generalization capability.

A remote (high impedance) three phase to ground fault is applied at the sending end ac-system (subs. # 1). Figure 4.10 shows the three phase voltages, dc voltage and current, rms values, and the NN outputs. The voltages at the rectifier bus do not drop to zero in this fault, but the NN is still able to determine that a fault has occurred in the system and to identify its type. This network was not trained for this type of fault, but it has the generalization capability to produce a correct output even if it had not seen this exact input.

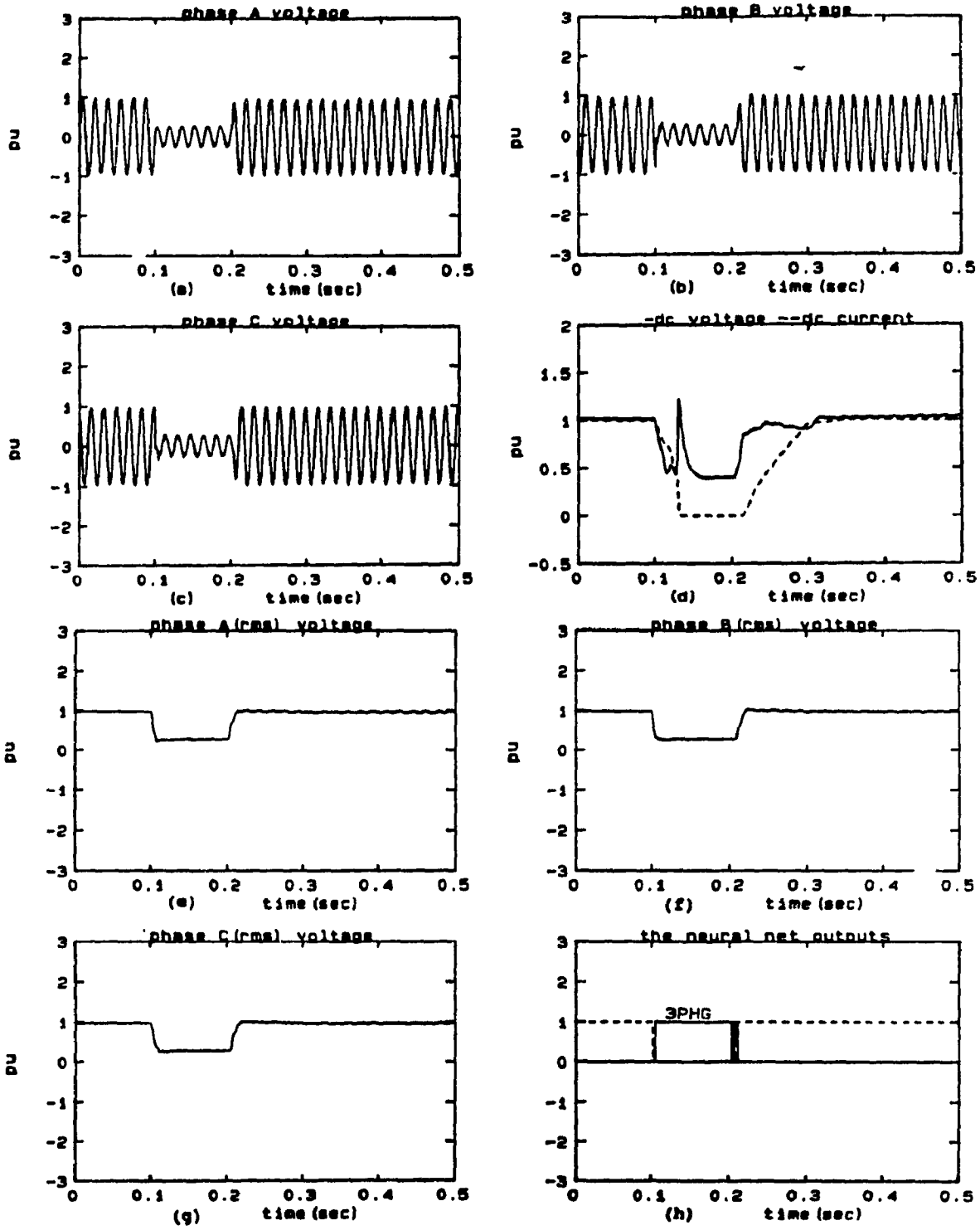

Figure 4.10 A remote three phase to ground fault.

a,b,c - The three phase voltages at the rectifier bus
d - The dc voltage and current at rectifier side
e,f,g - The rms values of the three phase voltages
h - The neural network outputs

4.4 Comparison

All neural networks used in these three methods are Counter Propagation Networks, with the same number of layers (4 layers: the input layer, the normalizing layer, the Kohonen layer, and the output layer). For the input, normalizing, and the output layers, the same number of neurons is used in the three methods. But for the Kohonen layer, the number of neurons is different for the three methods because of the difference in the training sets. In the second and third methods, more than one network is needed to simplify the training. The following sections presents the characteristics of the three methods and makes a comparison between them.

Method 1:

In this method, the NN has four inputs: the dc voltage at the rectifier side and the rms values of the three phase ac voltages at the rectifier bus. Using the three phase rms values as inputs gave the network some simplicity in its construction and its learning ability, but at the same time, it led to some difficulties in getting the desired results.

Advantages: Only one network is used in this method (Figure 4.2). It has 4 inputs, and 22 neurons in the Kohonen layer. Table 4.1 shows the training set for this network. Since it is a small set, training is easy and the construction of the network is simple. Also, because the three phase rms voltages are used here, harmonics and (transient spikes) can be filtered out, so false alarms did not occur. So, in this method, the NN is smaller, simpler, easier, and faster to train. It is therefore more economical, but unfortunately, it has the following disadvantages too.

Disadvantages: Since the detection circuit takes one period to compute the rms value, a time delay is introduced in the output of the NN. In addition, this network is unable to distinguish between line to line fault and a remote double line to ground fault. The reason being that only one piece of information (i.e. the rms value) is available to the network. This rms value drops to 0.5 pu in both types of faults, and the NN is unable to distinguish between these two types unless some additional information is available to make this distinction.

Method 2:

In this method, additional information is given to the network. Besides the dc voltage and the three phase rms values of the ac voltages, the phase angles between these ac voltages are used as input to the NN. This gave the network some advantages, but at the same time, increased its complexity.

Advantages: As shown in Figure 4.5, a small network is used for each phase of the ac system. These networks read the rms values of the ac voltages and the phase angles between them. When line to line fault occurs in the ac system, these two lines become in-phase; i.e. the phase angle between these two phases become zero. Using this information, the NN is now able to identify a line to line fault and to distinguish between this type of fault and a remote double line to ground fault. Also the training sets here are still simple and small, but more than one network are needed to avoid the complexity of the network and its training procedure.

Disadvantages: There is still a time delay because of the computation of the rms values. The oscillation in the rms value at the transient time, when the fault is cleared, still causes some false alarms from the NN at that time. In

addition, four networks are needed for this method to avoid the complexity of the training procedure as a result of adding more inputs.

Method 3:

Here, the instantaneous values of the ac voltages are used in addition to the dc voltage as inputs to the neural network. The objective of using the continuous values of the sine waves is to eliminate the delay (the time needed to compute the rms values), and then, if possible, to avoid these false alarms when the fault is cleared.

Advantages: The advantage of this method is that the time delay and the false alarms at the fault clearing time are reduced as shown in the results of this method. The main network, Figure 4.8, is the same as used in the second method. Its training is not difficult, but the networks at the ac phases are big and its training took more time (see table 3).

Disadvantages: Training a Counter-Propagation neural network on the sine waves needs more time and many more neurons in the Kohonen layer. In this method, 70 neurons are used in the Kohonen layer. So the disadvantage of this method is the

complexity of the network used here. Again, we are not able to make the distinction between line to line fault and a remote double line to ground fault because the three networks on the three ac phases do not share information between each other. Some more work and some more improvement is needed here to make that possible.

The outputs from the main neural network (Figure 4.11) for Methods 1, 2, and 3 for the case of three phase fault are compared. The advantage of using Method 3 instead of either Methods 1 or 2 is a reduction in the time response to determine the type of fault from 1-2 cycles to about 0.5 cycles. However, the use of Method 3 requires an additional overhead for a large number of neurons in the Kohonen layer which increases complexity and training time (table 4.5). The secondary problem of being able to distinguish between a line to line fault and a remote double line to ground fault can be resolved only if the phase angle information (Method 2) is used. This also entails the use of separate Phase Detector Networks which increases complexity and training time. If, however, it is not desired to make such a distinction, then Method 1 is both simple and practical; the slower response time delay may be acceptable for most HVDC system applications.

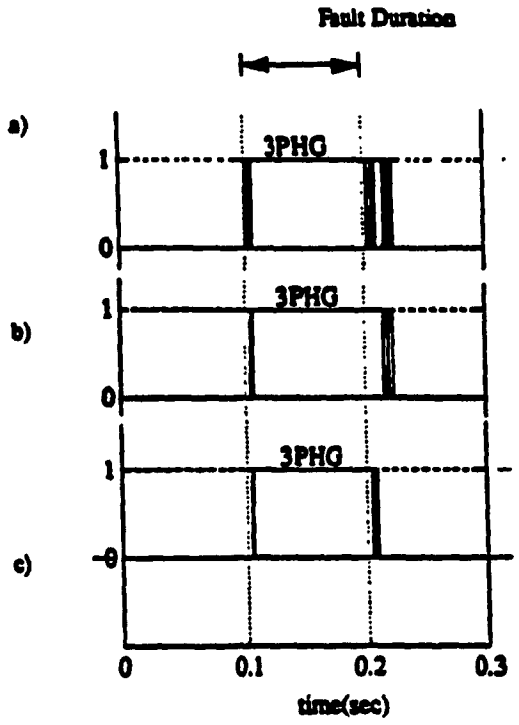

Figure 4.11 Case of Three Phase to Ground fault (3PHG)
a) Method 1, b) Method 2, c) Method 3.

Table 4.5 The relative training time required by each of the three methods indicated by the number of iterations.

Method 1:		5821
Method 2:	main network	5601
	phase detector network	3991
Methods 3:	main network	5601
	phase detector network	8521

Part 2

CHAPTER 5

NEURAL NETWORK BASED CURRENT REGULATOR FOR HVDC SYSTEMS

The transient performance of HVDC power transmission systems depends heavily on the regulators of the converter control systems. In chapter two, the equivalent circuit of the dc system and the control characteristics of a rectifier and inverter were introduced. In this chapter, after describing a typical HVDC system model, these control characteristics are further developed. The control features of the traditional PI controller are discussed. Then, a Backpropagation neural network based controller is used to replace this PI regulator. Three different approaches of the NN based controller are studied. Finally, a comparison between the traditional PI controller and the NN based controller is made.

5.1 HVDC System Model

The HVDC system, modeled using the EMTDC package (see Appendix A) is based on one pole of the two-pole 1000 MW Chateauguay (Hydro-Quebec) back-to-back tie. Although the actual tie is a 12-pulse system, the model simulated here is an equivalent 6-pulse system. The ac filters are, therefore, appropriately modified to account for the 5^{th} and 7^{th} harmonics. Data for the model is available in Appendix C. The system modeled (Figure 5.1) is divided into three subsystems:

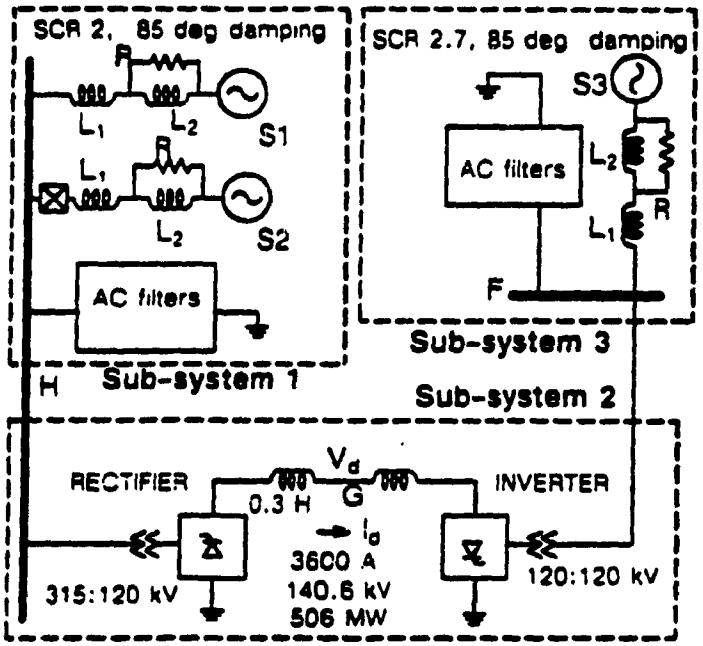

Figure 5.1 HVDC system model

Sub-system 1 : The rectifier ac system (the sending end) consists of two constant voltage, constant frequency sources S1 and S2 behind equivalent impedances (comprised of 2L-R networks) to represent simplified systems. AC filters for the 5^{th}, 7^{th}, 11^{th}, and 13^{th} harmonics are provided. The reactive power demand of the converter is supplied by a shunt capacitor bank. The system parameters are selected to model a weak ac system with a Short Circuit Ratio (SCR) of 2. The ac busbar H rating is 315 kV.

Sub-system 2 : The rectifier is connected to the inverter via two 0.3 H smoothing reactors. There is no dc line in the case of a back-to-back tie. The nominal value of the dc line voltage V_d (bus G) is 140.6 kV. The dc current I_d of the tie is 3600 A, giving a nominal dc power transmission capability of 506 MW.

Sub-system 3 : The inverter ac system consists of one constant voltage, constant frequency source S3 behind an equivalent impedance to represent a simplified weak system with a Short Circuit Ratio (SCR) of 2.7. AC filters for the 5^{th}, 7^{th}, 11^{th}, and 13^{th} harmonics are provided. The remaining reactive power demand of the converter is supplied by a shunt capacitor bank.

5.2 Control of HVDC Systems

Compared to AC systems, the control of power flow in HVDC transmission system is quite different and is intimately linked to the proper functioning of the terminal converters. DC transmission has certain features which can provide flexibility and fast control.

In general, two types of control action are required: a fairly slow, high gain control system for the fulfillment of the steady state power flow and a fast low gain control system for transients and protective purposes initiated by suitable protective equipment.

Control of Power Flow between Two Converters

A two terminal HVDC transmission system is a non-linear plant control system and poses a difficult control problem because of the following reasons:

- Presence of non-linear power system components such as power transformers, converters, and surge arrestors,
- Variable nature and topology of the power system,
- Insufficient data about the system,

- Presence of ac/dc filters which can often form resonant circuits with the power system,
- Generation of harmonics by the converters which can interact with the controllers, and
- Many operational modes are available in the control strategy employed due to system protection reasons.

In chapter two, Figure 2.10 shows the basic DC transmission circuit. This representation holds for the steady-state study of power transfer. From this circuit, the current I_d flowing in the line is determined by :

$$I_d = \frac{V_{d1} - V_{d2}}{R_L} \qquad (5.2.1)$$

Substituting the appropriate expressions for V_{d1} and V_{d2}, we get

$$I_d = \frac{V_{do1}\ \mathrm{Cos}(\alpha) - V_{do2}\ \mathrm{Cos}(\beta)}{R_{c1} + R_L + R_{c2}} \qquad (5.2.2)$$

A change of current, and therefore of power transfer, can be achieved by altering any one of four possible parameters:

(a) The control angle of the rectifier α.

(b) The control angle of the inverter β.

(c) The rectifier transformer valve winding voltage

(d) The inverter transformer valve winding voltage

Cases (c) and (d) involve tap changing of the converter transformers or change of AC source voltage. These are slow acting.

Rectifier Control

Assuming negligible commutating reactance, it can be shown that the displacement angle ϕ representing the phase-shift between the fundamental component of the current waveform and the corresponding phase voltage is equal to the firing angle α of the rectifier i.e. for $\mu = 0^{\circ}$, $\phi = \alpha$. It may be concluded then that α must be kept as near to zero as possible for minimum VAR demand. In fact, even at $\alpha = 0^{\circ}$, there is a displacement angle present due to the finite value of the commutating reactance. Any long-term control of the rectifier voltage must be made by tap-changing, allowing α to provide any required fast change of V_{dr}. In practice and under normal conditions α is kept near 15° for two reasons. First, to ensure that all valves of a bridge will be ignited at the same instant in time, and second to allow a small voltage margin for an immediate small power change if it is dictated by the rectifier grid control regulator.

Inverter control

Similar to rectifier operation the minimum inverter VAR demand will take place with $\beta = 0^{\circ}$. For $\beta > 0$ the current leads the voltage and the inverter consumes lagging VAR's. But here, it is important to realize that the range over which the inversion can be achieved is limited by β_{min} as explained in chapter two. Then the angle ϕ between the voltage and the current cannot be made zero.

An extinction angle γ must be introduced at least equal to γ_o the angle of de-ionisation of the valve. Angle γ occupies the relatively small interval during which the cathode-anode voltage is negative. An extinction angle smaller than γ_o will result in commutation failure. If it is larger than γ_o, this will result in unnecessary VAR demand. It means then that the most desirable inverter operating condition involves constant extinction angle (CAE) control.

However, if the rectifier AC voltage drops (Figure 5.2), the rectifier constant α characteristic will be displaced downwards resulting in no intersection with the inverter constant γ characteristic. Then the system will run down as $V_{doi}\ \cos(\gamma) > V_{dor}\ \cos(\alpha)$. To avoid this, a current regulator in the inverter station must be introduced. Such a regulator will increase β beyond the value required for the

constant γ and will reduce the inverter back-voltage thus tending to sustain the current.

Therefore, the inverter needs both, a constant current regulator and a constant γ controller. When the inverter characteristic is higher than the rectifier characteristic, the inverter works at constant current regulation and the rectifier works with minimum delay angle α_{min} and natural voltage regulation. When the rectifier characteristic is higher, the rectifier works on constant current with the inverter on constant γ control. The difference between the current regulator settings of the two stations is called the "current margin" and must be sufficient to give some difference between the tap voltages, thus avoiding the simultaneous operation of the current regulators, which could lead to instability.

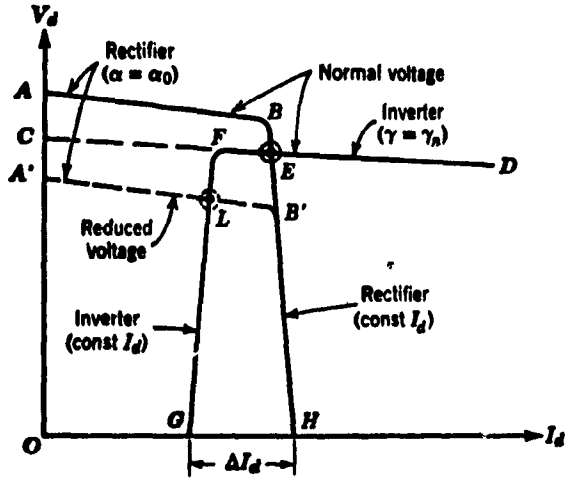

Figure 5.2 Actual control characteristics

5.3 The PI Controller in the HVDC System

As discussed in the last section, for a typical two-terminal HVDC system and under normal conditions, the rectifier may be in constant current control whilst the inverter may be in constant voltage (gamma) control. Both ends of the system have traditionally relied on PI regulators to provide fast, robust controllers. Figures 4.3-a and 4.3-b show a typical current and gamma regulators where I_{ref} is the current order, I_d is the measured current, α is the firing angle at the rectifier, γ_{ref} is the reference of the extinction angle (γ), γ_d is the measured value of this extinction angle, and β is the firing angle at the inverter. G_P and G_I are the proportional and integral gains. The time constant T is generally not set to zero because in practice the regulator is provided with an unfiltered value of I_d containing harmonics. Typically, T would be between 1 and 20 ms.

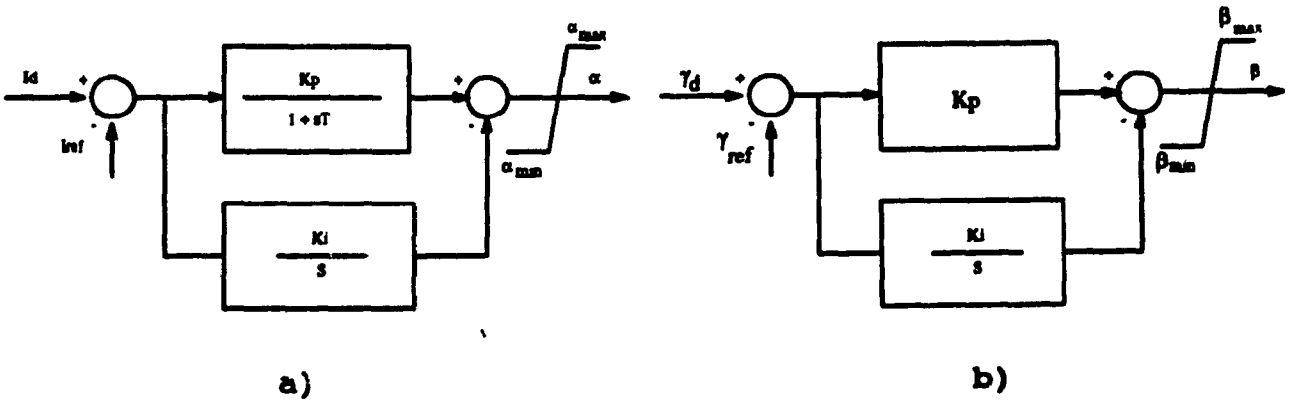

Figure 5.3 Typical PI (Current and Gamma) regulators

The dc link transient performance depends heavily on the parameters of the rectifier current regulator. The dynamic response of this current regulator is affected by the short circuit level at the commutation buses, or equivalently by the converter transformers commutation reactance and by the AC network Thevinin impedance at the commutation buses. Therefore, the tuning of the regulator parameters (G_P and G_I) is a function of all the net converter commutation resistances. These resistances vary with the network operating conditions and are affected by AC system contingencies. As a result PI regulators suffer from some disadvantages. First, their parameters are optimum over a limited range of operation. Second, prior knowledge of the system dynamics is required to optimize these parameters. In addition, PI regulators have no capability to learn from previous experience.

Figures 4.4-1 to 4.4-7 show the behavior of the system using a PI controller in the cases of deblocking the system, step changes in I_{ref} (10%, 20%, 40%), single line to ground fault, three phase to ground fault, and a dc line fault.

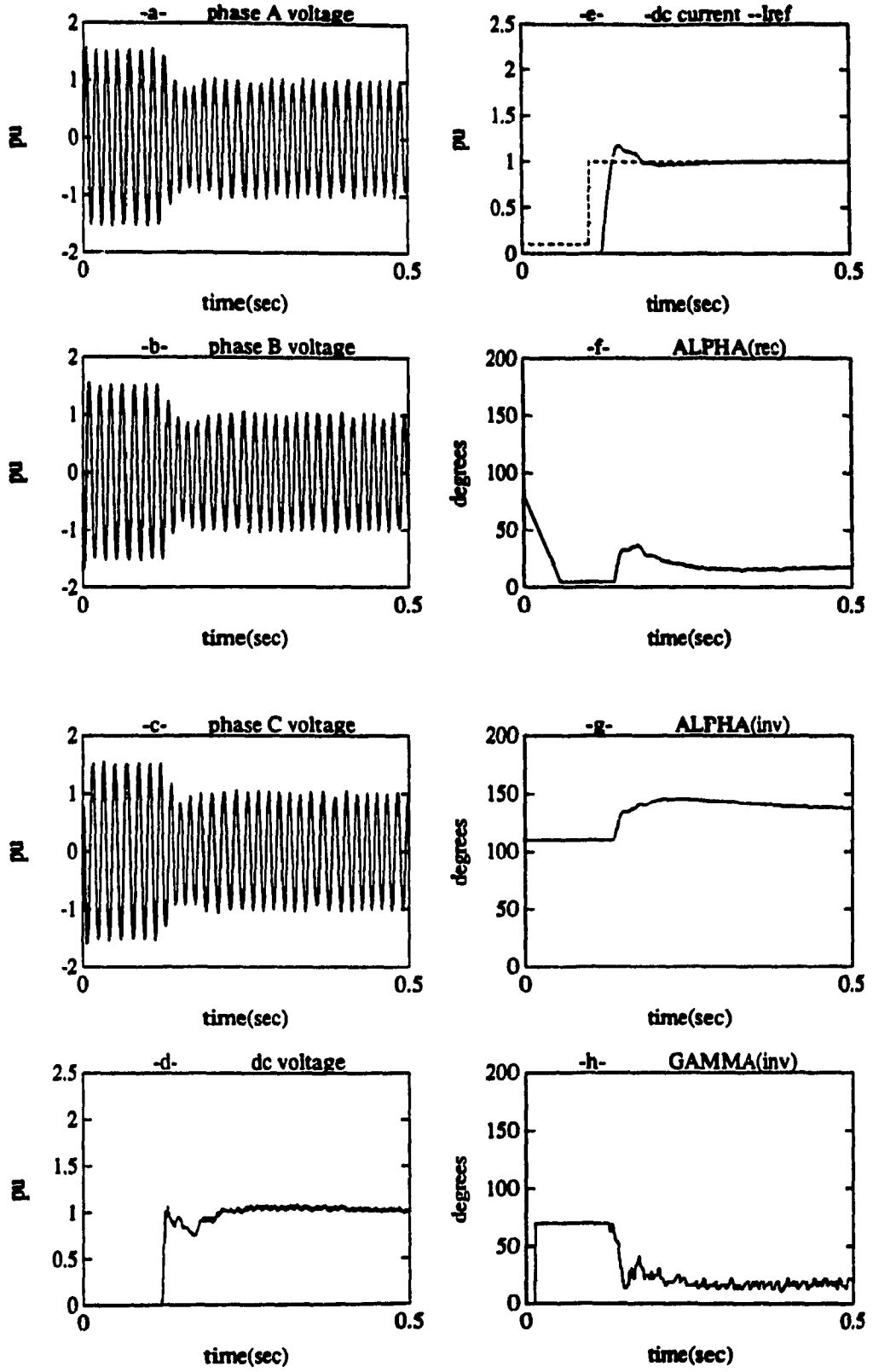

Figure 5.4-1 Deblocking the System (PI Controller)

a,b,c) AC Voltages at Rectifier Bus
d) DC Voltage at Rectifier Side
e) -DC Current --Current Reference
f) Firing Angle at Rectifier (αr)
g) Firing Angle at Inverter (αi)
h) Extinction Angle at Inverter (γ)

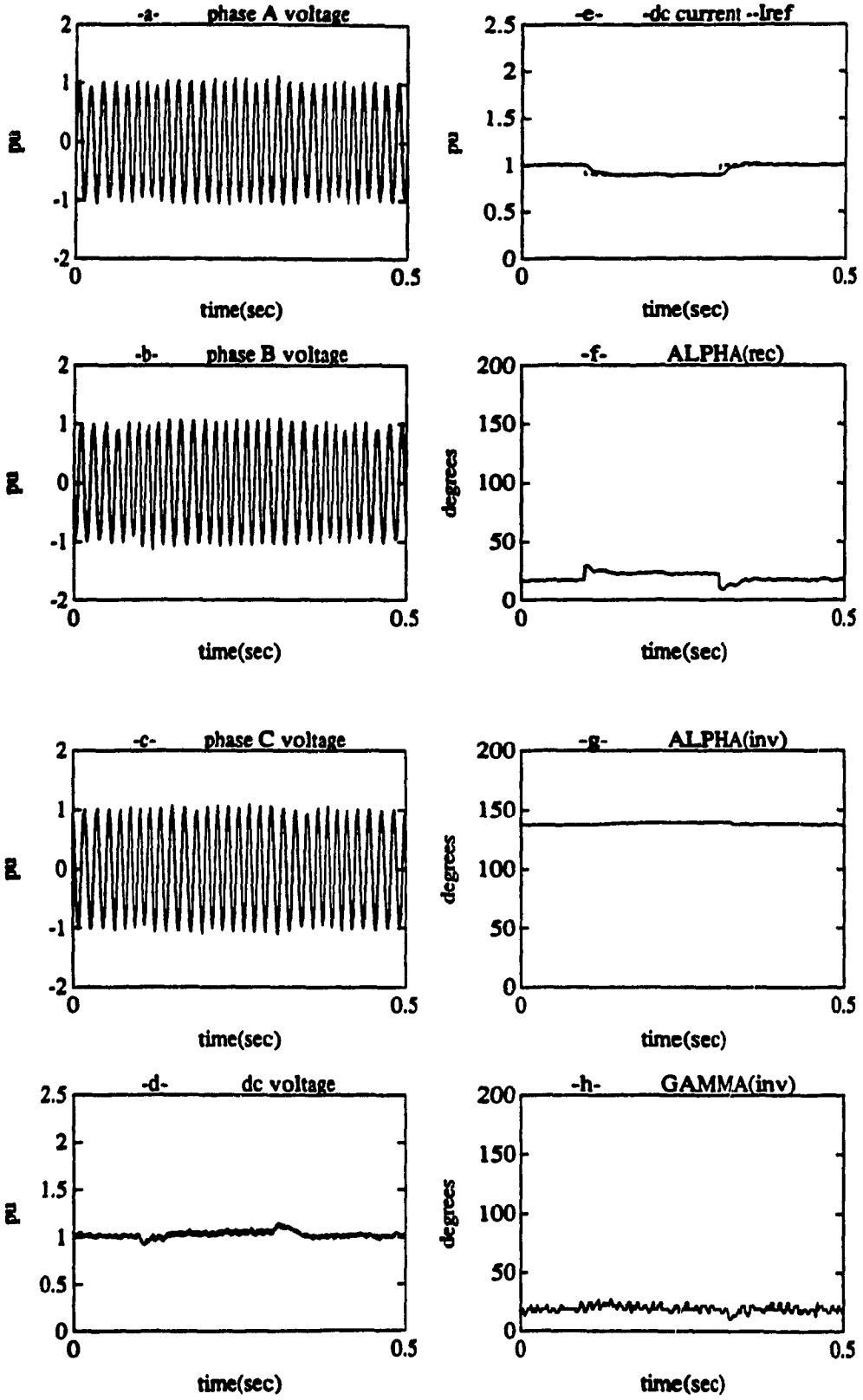

Figure 5.4-2 10% Step Change in I_{ref} (PI Controller)

a,b,c) AC Voltages at Rectifier Bus
d) DC Voltage at Rectifier Side
e) -DC Current --Current Reference
f) Firing Angle at Rectifier (αr)
g) Firing Angle at Inverter (αi)
h) Extinction Angle at Inverter (γ)

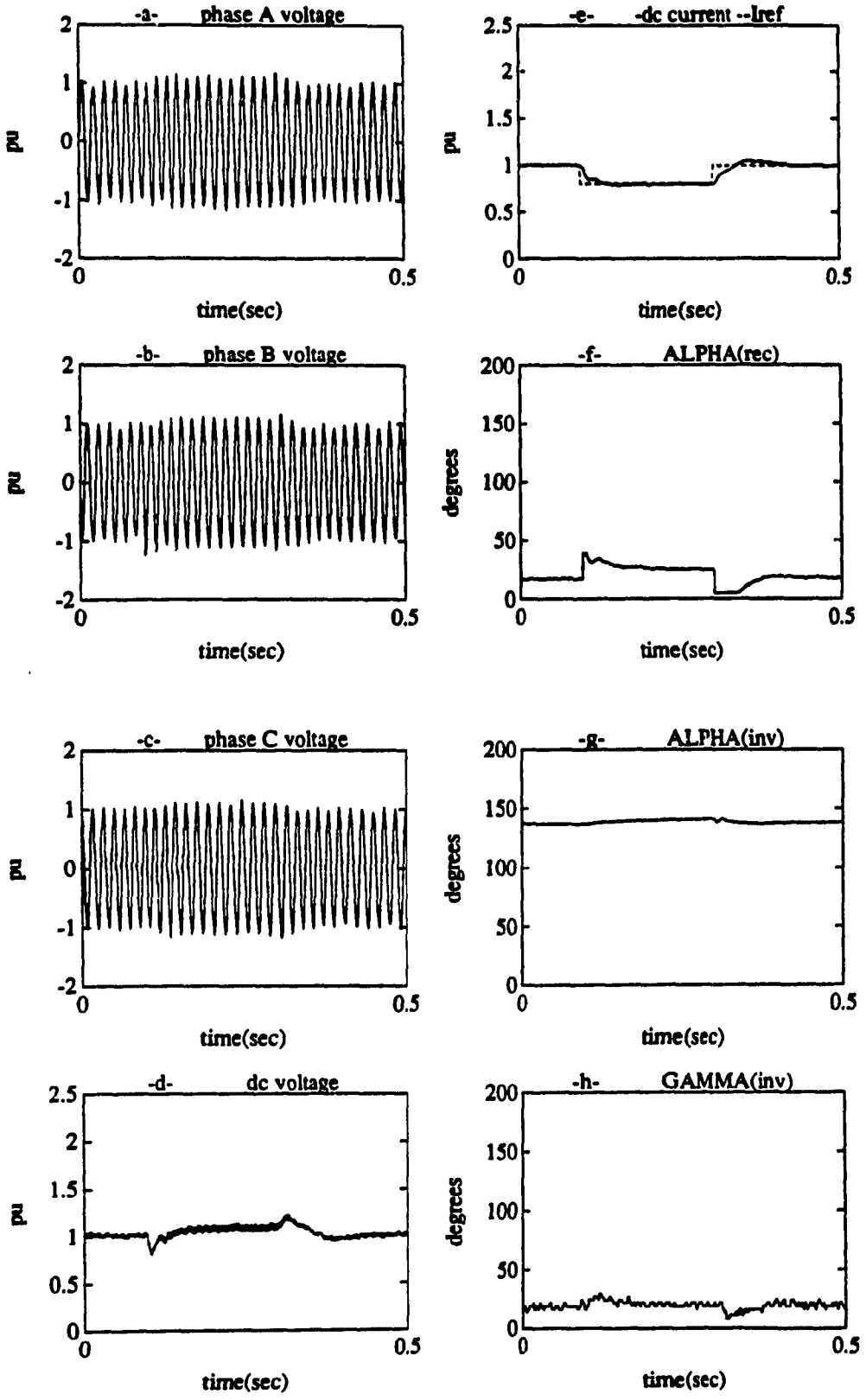

Figure 5.4-3 20% Step Change in I_{ref} (PI Controller)

a,b,c) AC Voltages at Rectifier Bus
d) DC Voltage at Rectifier Side
e) -DC Current --Current Reference
f) Firing Angle at Rectifier (αr)
g) Firing Angle at Inverter (αi)
h) Extinction Angle at Inverter (γ)

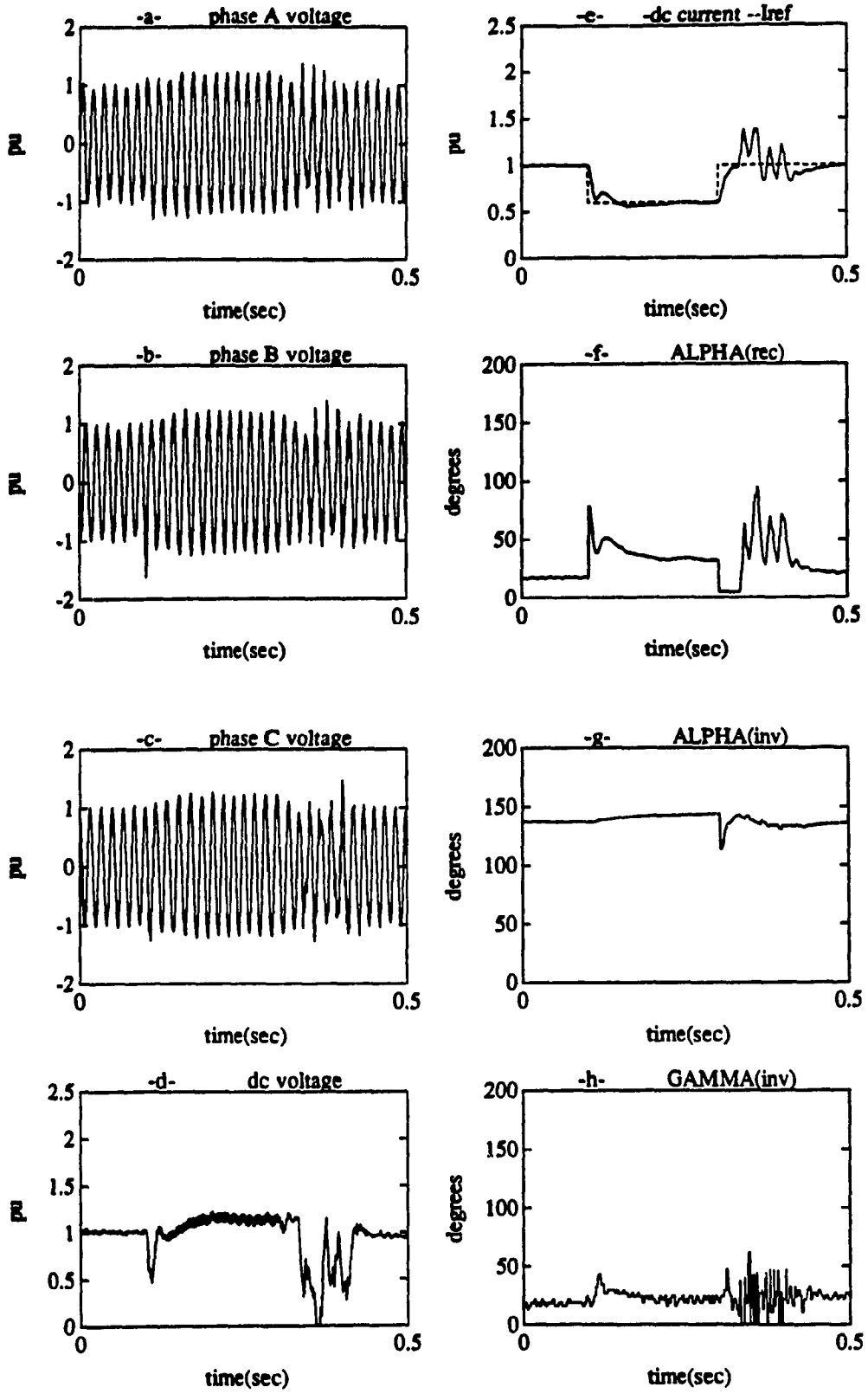

Figure 5.4-4 40% Step Change in I_{ref} (PI Controller)

a,b,c) AC Voltages at Rectifier Bus
d) DC Voltage at Rectifier Side
e) -DC Current --Current Reference
f) Firing Angle at Rectifier (αr)
g) Firing Angle at Inverter (αi)
h) Extinction Angle at Inverter (γ)

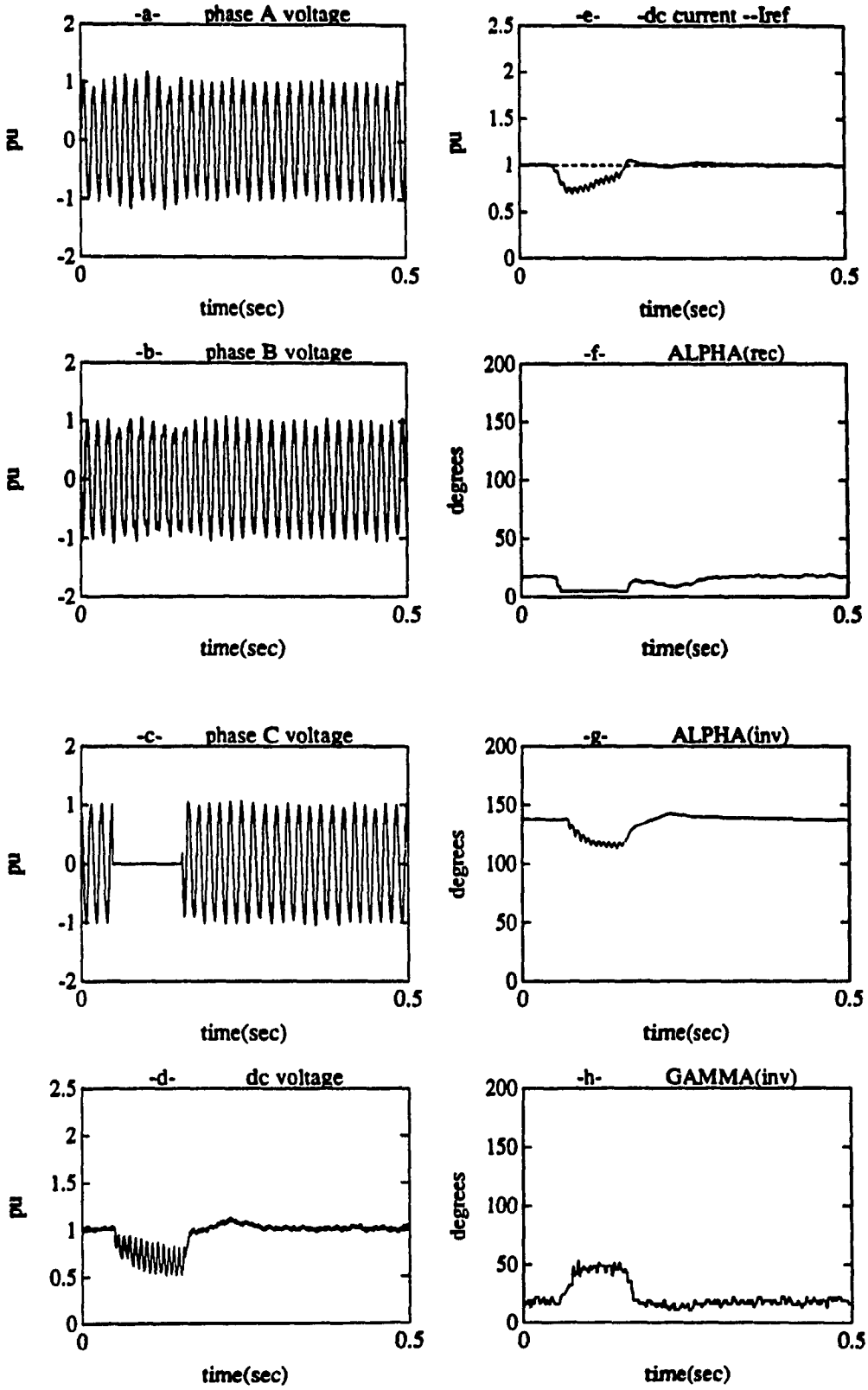

Figure 5.4-5 Single Line to Ground Fault (PI Controller)

a,b,c) AC Voltages at Rectifier Bus
d) DC Voltage at Rectifier Side
e) -DC Current --Current Reference
f) Firing Angle at Rectifier (αr)
g) Firing Angle at Inverter (αi)
h) Extinction Angle at Inverter (γ)

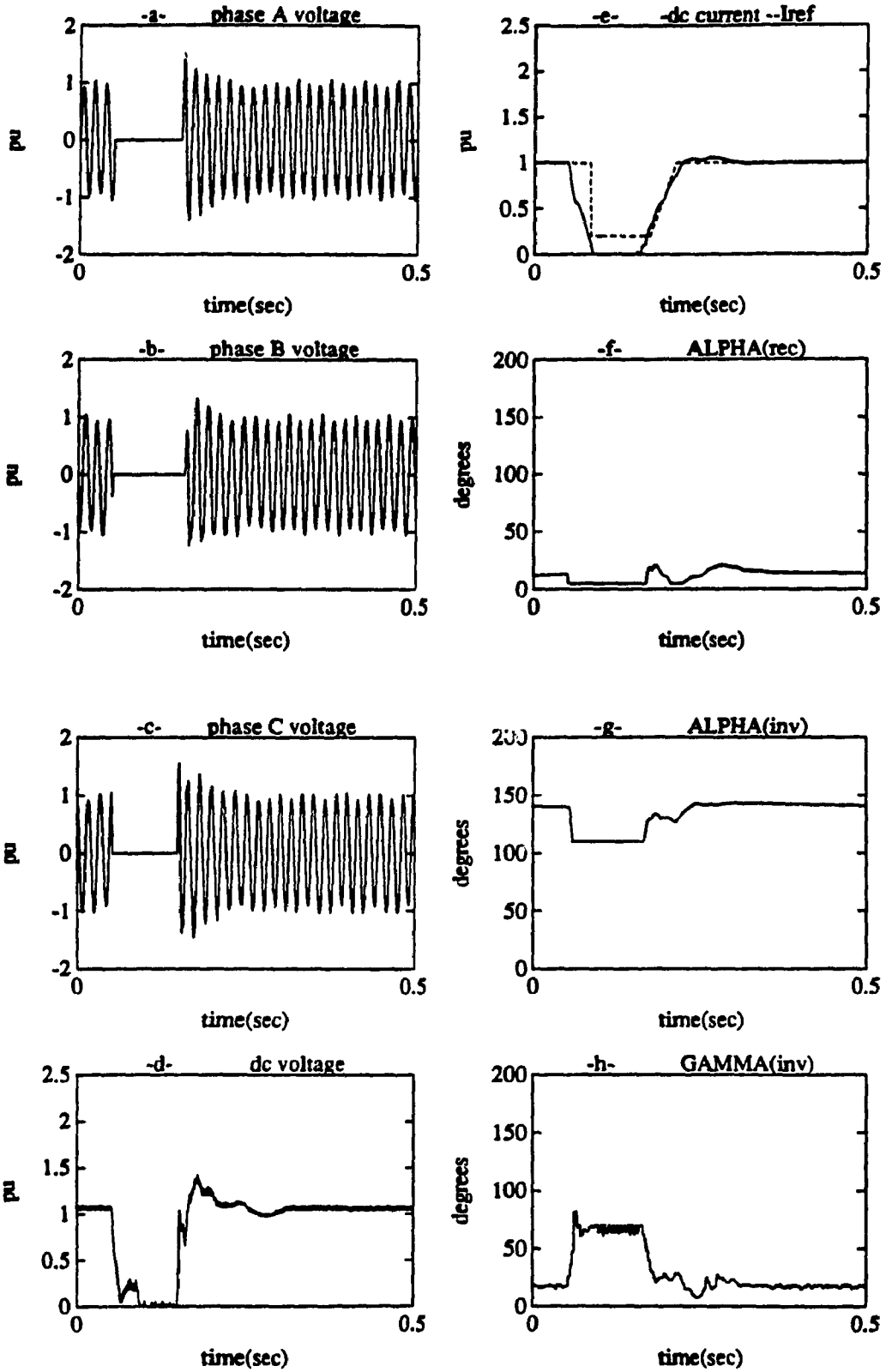

Figure 5.4-6 Three Phase to Ground Fault (PI Controller)

a,b,c) AC Voltages at Rectifier Bus
d) DC Voltage at Rectifier Side
e) -DC Current --Current Reference
f) Firing Angle at Rectifier (αr)
g) Firing Angle at Inverter (αi)
h) Extinction Angle at Inverter (γ)

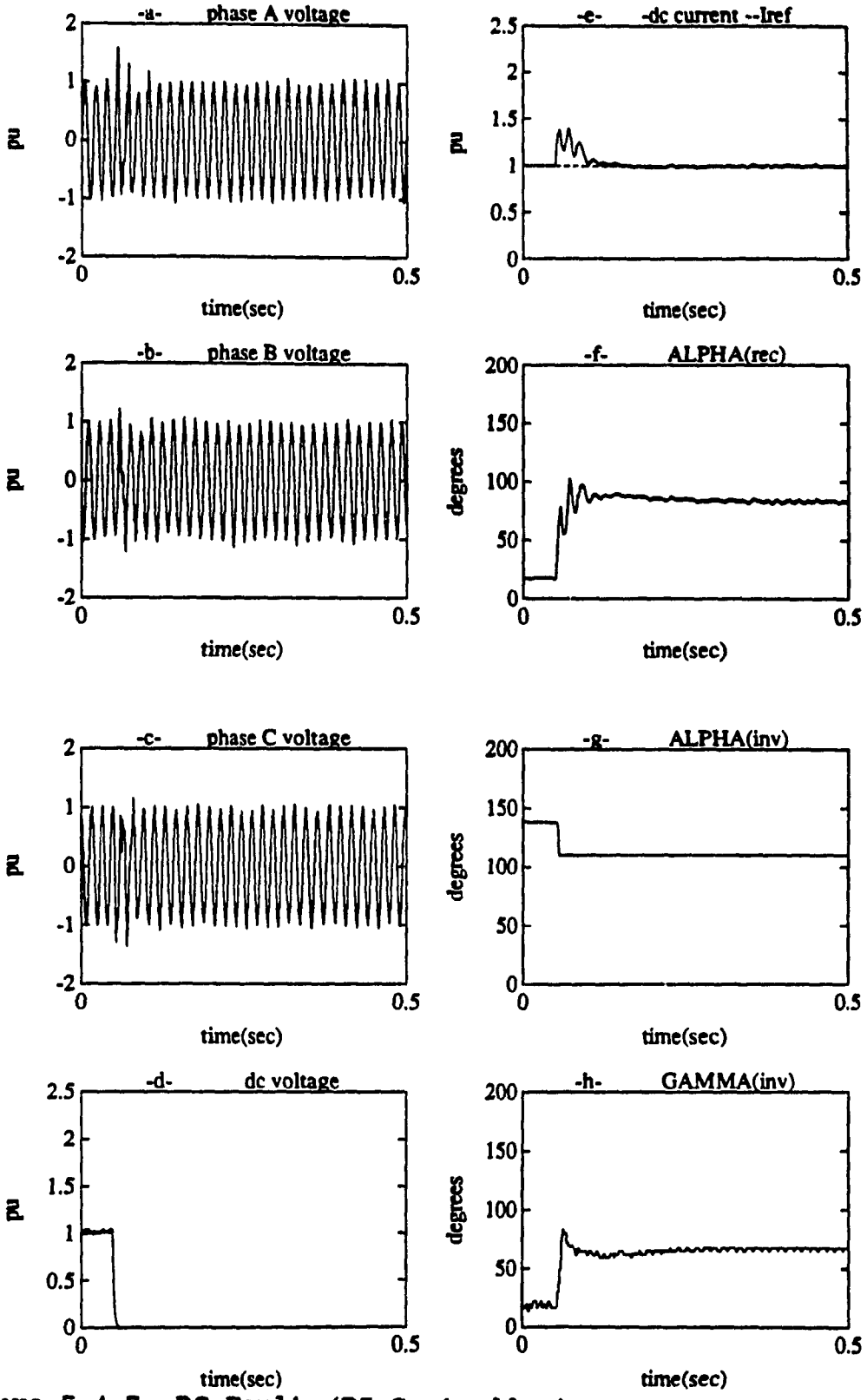

Figure 5.4-7 DC Fault (PI Controller)

a,b,c) AC Voltages at Rectifier Bus
d) DC Voltage at Rectifier Side
e) -DC Current --Current Reference
f) Firing Angle at Rectifier (αr)
g) Firing Angle at Inverter (αi)
h) Extinction Angle at Inverter (γ)

5.4 Neural Network Based Regulators

Due to their adaptability and ability to learn as well as their massive parallelism, neural networks may provide fast, robust and adaptive controllers. In addition, neural networks do not need prior knowledge of the system dynamics. Therefore they have advantages over PI controllers. In this section, the possibility of using a Backpropagation neural network as a current regulator at the rectifier in HVDC systems is explored. Three approaches have been considered. In the first approach, the neural network was trained off-line giving a fast regulator but not an adaptive one. In the second approach, the neural network adjusts its weights on-line, according to the error between the desired and measured values of the dc current. This is an adaptive controller but a slow one. The third approach is a combination of the first two resulting in both, a fast and adaptive regulator.

5.4.1 First Approach (On-Line Trained NN Based Controller)

The input to the proposed NN controller (Figure 5.5) is the current I_{ref} and its output is the firing angle α. The

error between the measured dc current I_d and the I_{ref} is used to adjust the weights of the NN according to the Delta Rule [7] (explained later). The speed of response of the controller and the system stability will depend on the learning rate η and the momentum μ used in adjusting the weights of the NN. These parameters are defined later.

Network Structure

The proposed on-line trained NN controller consists of three layers (Figure 5.5):

The Input Layer: In this layer there are only two neurons; one neuron is fed by I_{ref} . The input to the other neuron is a constant input bias B. This layer acts simply as a fan-out layer and hence the outputs of the neurons are I_{ref} and Bias.

The Hidden Layer: In this layer there are two neurons (n=2). These are connected to the outputs of the Input Layer by weights V_i and B_i, where i = 1,...,n. The outputs of these neurons are acted upon by a non-linear function, the Sigmoid function. The n outputs of the neurons in the Hidden Layer, OUT_i, are fed to the Output Layer through the weights W_i.

The Output Layer: In this layer, there is only one neuron. The inputs to this neuron are the outputs OUT_i from the hidden layer and the constant Bias B. The weights associated with these inputs are W_i and B respectively.

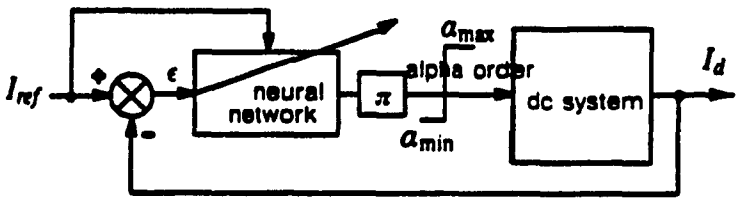

Figure 5.5 The first approach (On line trained NN)

Training the Neural Network

The neural network is trained on-line (Figure 5.6) according to the Error $\epsilon = I_{ref} - I_d$ and by using the well known Delta learning algorithm. The NN learns by adjusting its weights on-line. In this particular approach, the same error ϵ is used to adjust the weights in the Hidden and Output layers, unlike the BackPropagation (BP) method where the error is propagated back from the Output Layer to the Hidden Layer through the weights. However, not using BP

algorithm raises a system stability question. This is discussed later, in the end of this section.

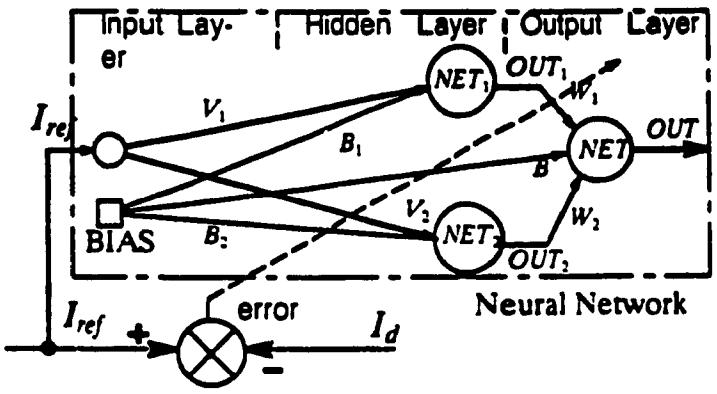

Figure 5.6 Training the Neural Network On-line

Adjusting the Weights in the Hidden Layer: The outputs in the hidden layer are given by the sigmoid function

$$OUT_1 = \frac{1}{(1 + e^{-NET_1})} \qquad (5.4.1)$$

$$OUT_2 = \frac{1}{(1 + e^{-NET_2})} \qquad (5.4.2)$$

where

$$NET_1 = V_1 \cdot I_{ref} + B_1 \cdot Bias \qquad (5.4.3)$$

$$NET_2 = V_2 \cdot I_{ref} + B_2 \cdot Bias \qquad (5.4.4)$$

Now, using the delta rule [19],

$$\delta_1 = \frac{d\ OUT_1}{d\ NET_1}(-\varepsilon) \qquad (5.4.5)$$

$$\delta_2 = \frac{d\ OUT_2}{d\ NET_2}(-\varepsilon) \qquad (5.4.6)$$

Then, the modifications in the weights are given by

$$\Delta V_1(t+1) = \eta \cdot \delta_1 \cdot I_{ref} + \mu \cdot \Delta V_1(t) \qquad (5.4.7)$$

$$\Delta V_2(t+1) = \eta \cdot \delta_2 \cdot I_{ref} + \mu \cdot \Delta V_2(t) \qquad (5.4.8)$$

$$\Delta B_1(t+1) = \eta \cdot \delta_1 \cdot BIAS + \mu \cdot \Delta B_1(t) \qquad (5.4.9)$$

$$\Delta B_2(t+1) = \eta \cdot \delta_2 \cdot BIAS + \mu \cdot \Delta B_2(t) \qquad (5.4.10)$$

where η and μ are the learning rate and momentum respectively, and have values between 0 and 1.

Therefore, updated values of the weights V_1, V_2, B_1, and B_2 are

$$V_1(t+1) = V_1(t) + \Delta V_1(t+1) \qquad (5.4.11)$$

$$V_2(t+1) = V_2(t) + \Delta V_2(t+1) \qquad (5.4.12)$$

$$B_1(t+1) = B_1(t) + \Delta B_1(t+1) \qquad (5.4.13)$$

$$B_2(t+1) = B_2(t) + \Delta B_2(t+1) \qquad (5.4.14)$$

Adjusting the Weights in the Output Layer: The output of the neuron in the Output Layer is given by the sigmoid function

$$OUT = \frac{1}{(1 + e^{-NET})} \tag{5.4.15}$$

$$NET = W_1 \cdot OUT_1 + W_2 \cdot OUT_2 + B \cdot Bias \tag{5.4.16}$$

Now, using the delta rule,

$$\delta = \frac{d\ OUT}{d\ NET}(-\varepsilon) \tag{5.4.17}$$

Then, the modifications in the weights are given by

$$\Delta W_1(t+1) = \eta \cdot \delta \cdot OUT_1 + \mu \cdot \Delta W_1(t) \tag{5.4.18}$$

$$\Delta W_2(t+1) = \eta \cdot \delta \cdot OUT_2 + \mu \cdot \Delta W_2(t) \tag{5.4.19}$$

$$\Delta B(t+1) = \eta \cdot \delta \cdot BIAS + \mu \cdot \Delta B(t) \tag{5.4.20}$$

Therefore, updated values of the weights W_1, W_2, and B are

$$W_1(t+1) = W_1(t) + \Delta W_1(t+1) \tag{5.4.21}$$

$$W_2(t+1) = W_2(t) + \Delta W_2(t+1) \tag{5.4.22}$$

$$B(t+1) = B(t) + \Delta B(t+1) \tag{5.4.23}$$

Choice of Parameters of the On-Line NN Controller: Selection of the learning rate η and momentum μ of the NN controller was made by applying 10% step changes in I_{ref} and observing

the responses. In Figure 5.7-1 is shown the effect of changing the learning rate η (with a fixed value of momentum μ) with η = a) 0.05, b) 0.2, and c) 0.5. The test case is a step change in Iref of 40%. The response in (a) is very slow, whilst in (b) it is close to an optimum value, and in (c) it is too fast and will cause instability problems. Many other values of η were tried, and it was found that the most suitable value for η is 0.2.

The effect of the momentum is shown in Figure 5.7-2 with μ = a) 0.001, b) 0.1, and c) 0.7. The test case is also a step change in Iref of 40% . Different values of μ were tried and a suitable value (0.1) was selected.

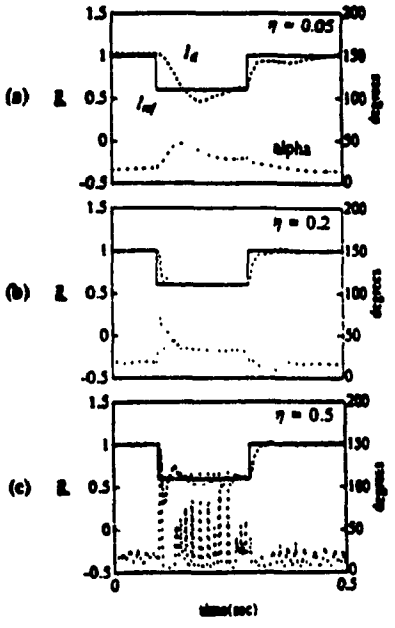

Figure 5.7-1 Effect of η

μ = 0.1

a) η = 0.05
b) η = 0.2
c) η = 0.5

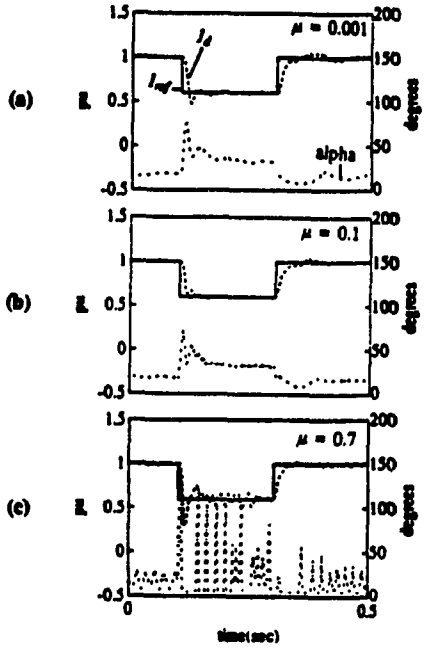

Figure 5.7-2 Effect of μ

η = 0.2

a) μ = 0.001
b) μ = 0.1
c) μ = 0.7

In Figure 5.8 is shown the impact of three different values of the learning rate i.e. η = a) 0.06, b) 0.2, and c) 0.3 on the system performance in the case of a dc line fault (without any influence from the protection circuits i.e no change in I_{ref}). The momentum is fixed at 0.1. With η = 0.06, the controller is slow and a peak dc current of 2.2 pu is observed; the settling time to bring the dc current to 1 pu is about 130 ms. With η = 0.2, the controller is faster and a peak dc current of 2.1 is observed; the settling time to bring the dc current to 1 pu is about 80 ms. However, with higher value, η = 0.3, the controller is much faster and a peak dc current of 1.5 pu is observed; the settling time to bring the current to 1 pu is reduced to about 60 ms.

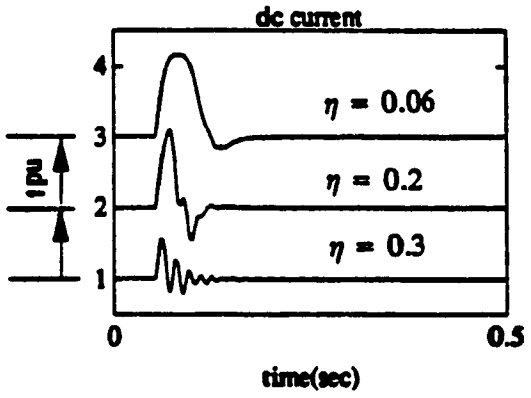

Figure 5.8 Impact of learning rate in the case of dc fault

The NN takes time to optimize its weights, although its learning rate has a strong influence on this. In Figure 5.9 is shown the case of a step change in I_{ref} of 40% for

multiple steps with two different learning rates η : a) 0.08 and b) 0.2. In both cases, it can be seen that the NN is still adapting its weights even after the 5th step. In order to obtain quickly the optimal settings of the weights, a high learning rate is preferred but there is the risk of causing instability.

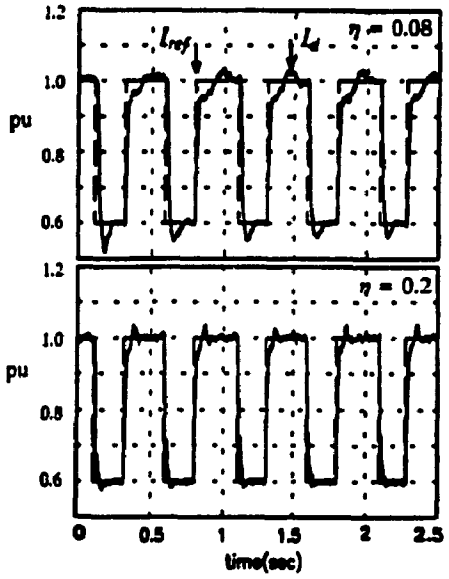

Figure 5.9 Multiple steps in Iref (2 different values Of η)

System Stability

In this particular approach, the same error ε is used to adjust the weights in the Hidden and Output layers, unlike in the Back Propagation (BP) method where the error is propagated back from the Output Layer to the Hidden Layer through the weights.

To use the conventional BP network requires the system error to be back propagated through the system for adjusting the Output and Hidden layer weights. Back propagating through the system is not feasible if we assume no "a priori" knowledge regarding the system (plant) dynamics. To see this, denote the performance index to be minimized as

$$E = 0.5 \cdot (I_{ref} - I_d)^2 \qquad (5.4.24)$$

According to the Back Propagation (BP) theory, which uses the Steepest Descent method in minimizing the error, The weight adjustment is proportional to the negative of the gradient of this error, denoted by

$$\delta = - \frac{dE}{dNET} = - \frac{dE}{dOUT} \cdot \frac{dOUT}{dNET} \qquad (5.4.25)$$

where NET is the weighted sum of the neuron inputs.
Since E is not a function of OUT explicitly we write

$$\frac{dE}{dOUT} = \frac{dE}{dI_d} \cdot \frac{dI_d}{dOUT} \qquad (5.4.26)$$

Hence

$$\delta = (I_{ref} - I_d) \cdot \frac{dOUT}{dNET} \cdot \frac{dI_d}{dNET} \qquad (5.4.27)$$

Since OUT is the input to the dc system after being scaled by the factor π, $\alpha = \pi \cdot OUT$, and therefore

$$\delta = \pi \cdot (I_{ref} - I_d) \cdot \frac{dOUT}{dNET} \cdot \frac{dI_d}{d\alpha} \qquad (5.4.28)$$

From eq. (5.2) it follows that

$$\frac{dI_d}{d\alpha} = - V_{dor} \cdot \frac{Sin(\alpha)}{R_{c1} + R_1 + R_{c2}} \qquad (5.4.29)$$

which verifies that adjusting the weights using BP requires a prior knowledge of the system.

With Back Propagation, ΔE is always negative and therefore the system is stable. However, since BP is not used here, a question about the stability of the system is raised. Results from this approach (Figures 5.10-1 ... 5.10-7) show that weight adjustments are always in the direction of minimizing the error; even though, analytical analysis is still needed to determine under what conditions this stability is guaranteed.

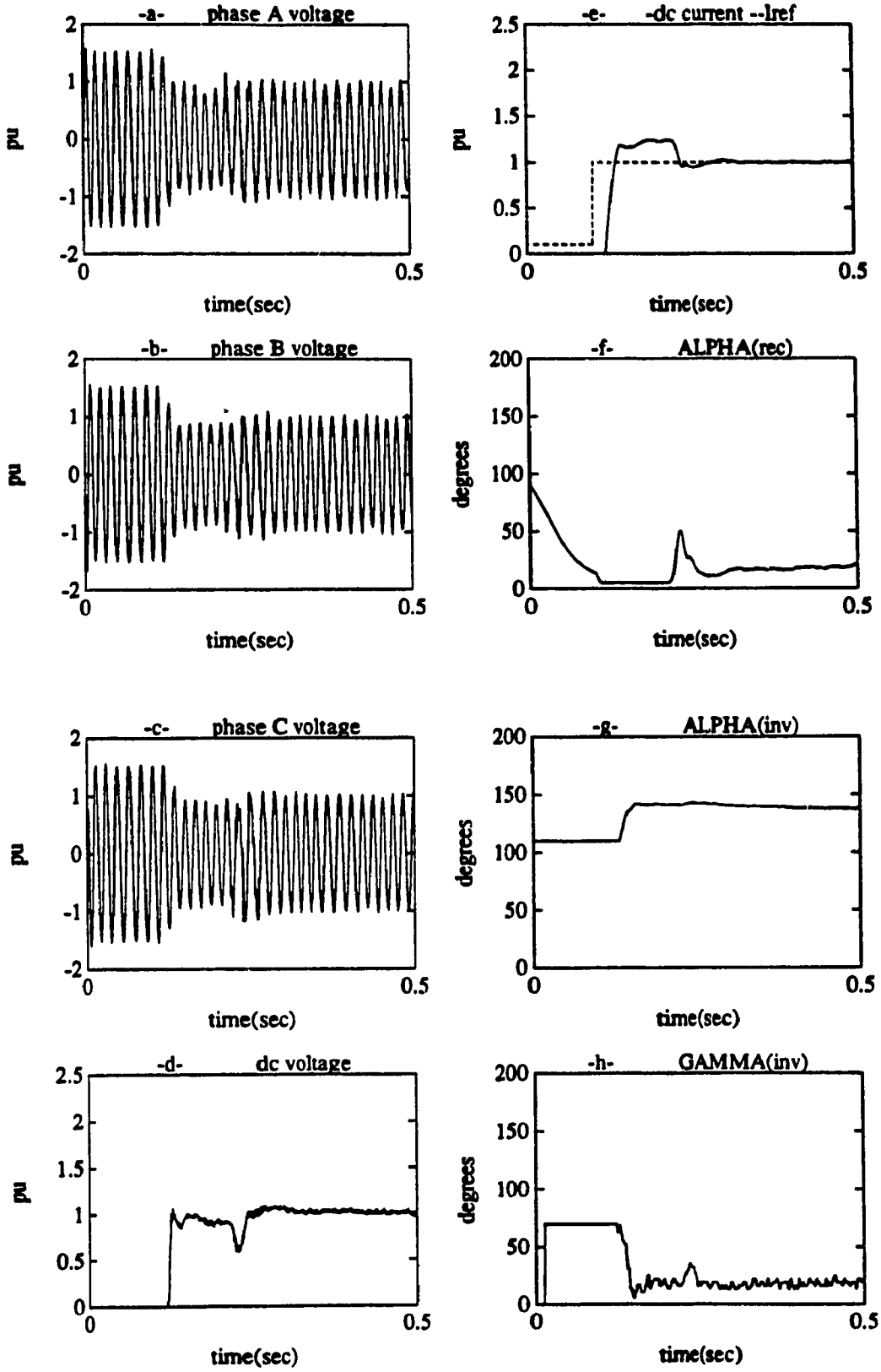

Figure 5.10-1 Deblocking the System (On-Line Trained NN)

a,b,c) AC Voltages at Rectifier Bus
d) DC Voltage at Rectifier Side
e) -DC Current --Current Reference
f) Firing Angle at Rectifier (αr)
g) Firing Angle at Inverter (αi)
h) Extinction Angle at Inverter (γ)

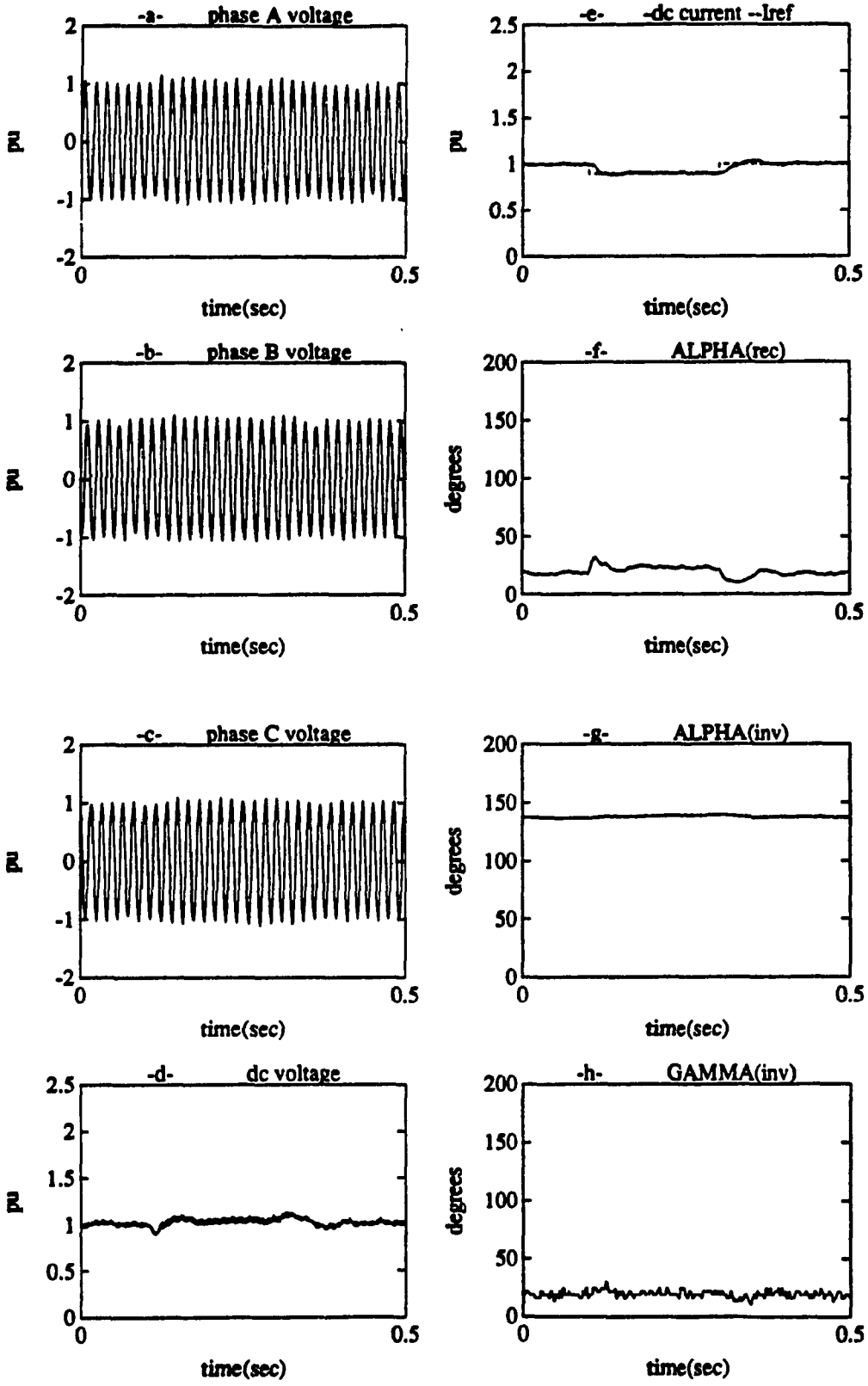

Figure 5.10-2 10% Step Change in I_{ref} (On-Line Trained NN)

a,b,c) AC Voltages at Rectifier Bus
d) DC Voltage at Rectifier Side
e) -DC Current --Current Reference
f) Firing Angle at Rectifier (αr)
g) Firing Angle at Inverter (αi)
h) Extinction Angle at Inverter (γ)

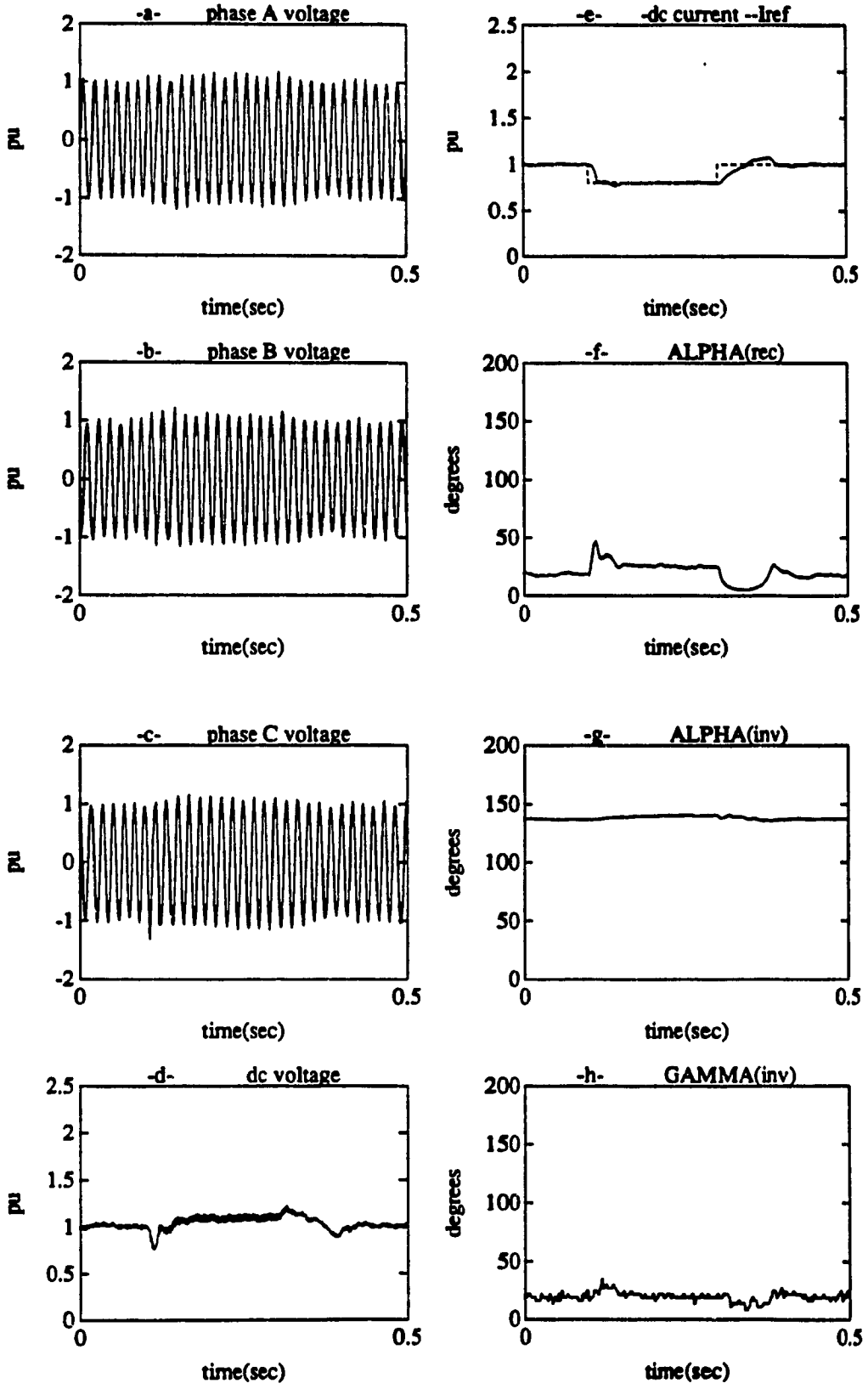

Figure 5.10-3 20% Step Change in I_{ref} (On-Line Trained NN)

a,b,c) AC Voltages at Rectifier Bus
d) DC Voltage at Rectifier Side
e) -DC Current --Current Reference
f) Firing Angle at Rectifier (αr)
g) Firing Angle at Inverter (αi)
h) Extinction Angle at Inverter (γ)

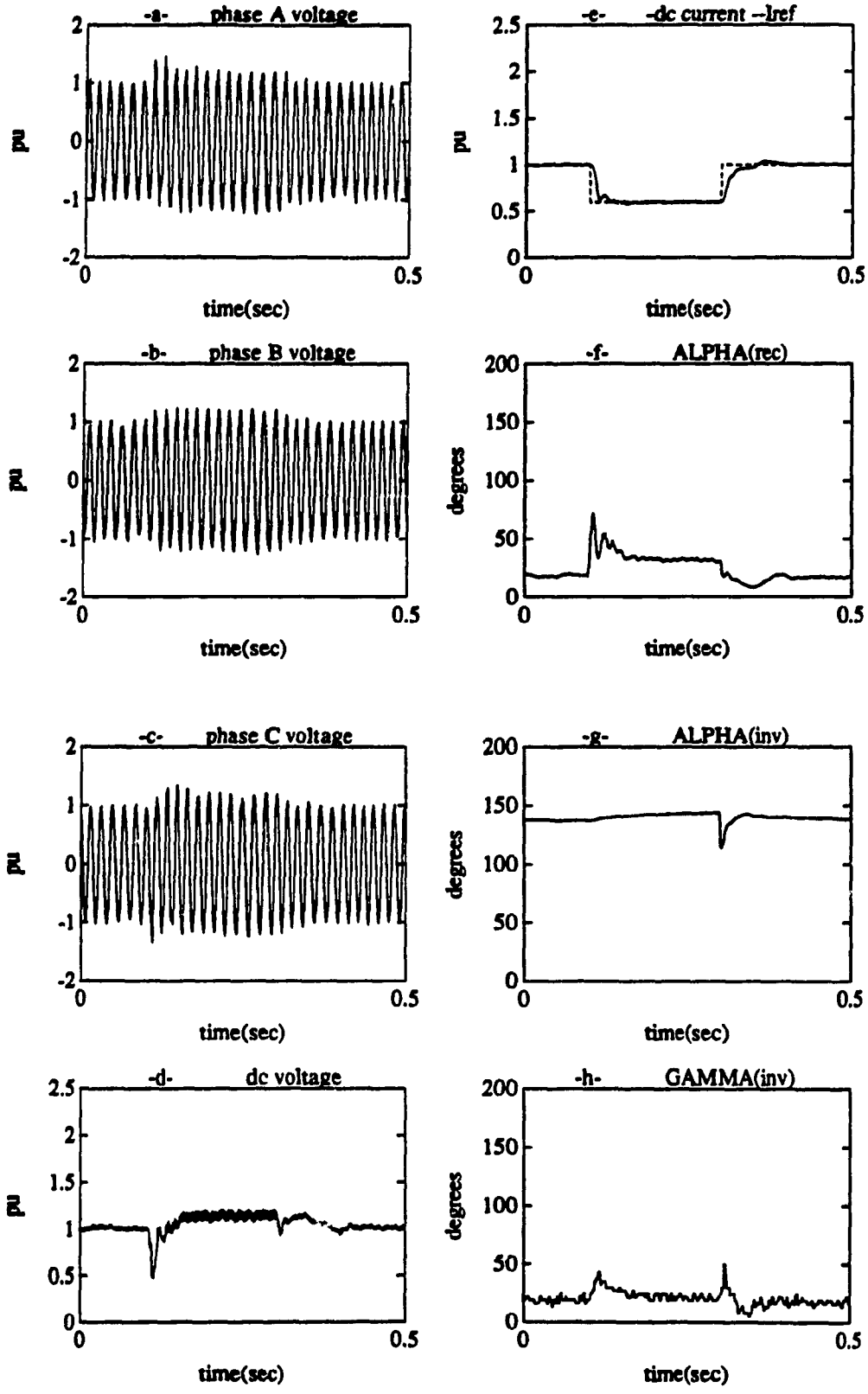

Figure 5.10-4 40% Step Change in I_{ref} (On-Line Trained NN)

a,b,c) AC Voltages at Rectifier Bus
d) DC Voltage at Rectifier Side
e) -DC Current --Current Reference
f) Firing Angle at Rectifier (αr)
g) Firing Angle at Inverter (αi)
h) Extinction Angle at Inverter (γ)

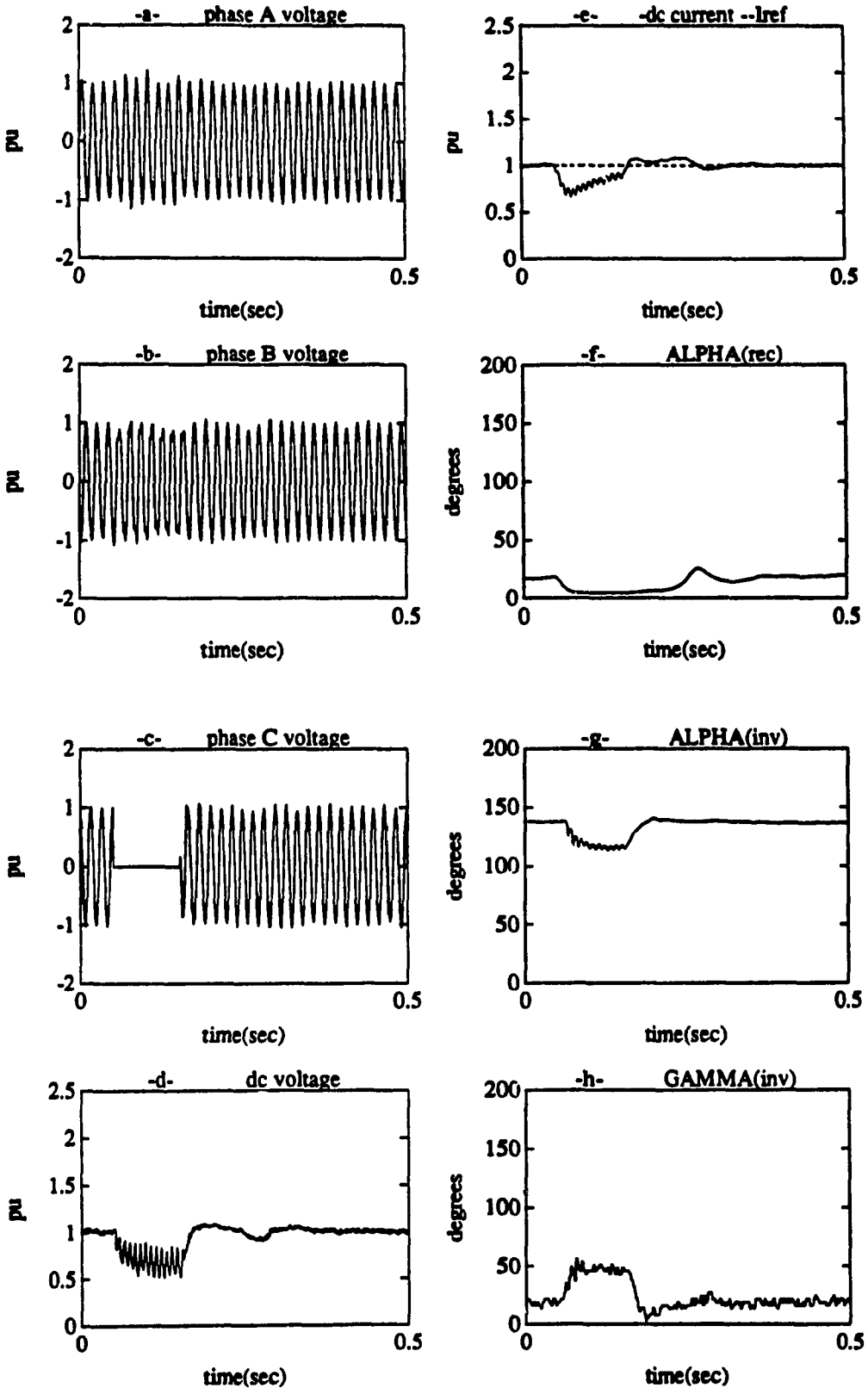

Figure 5.10-5 Single Line to Ground Fault (On-Line Trained NN)

a,b,c) AC Voltages at Rectifier Bus
d) DC Voltage at Rectifier Side
e) -DC Current --Current Reference
f) Firing Angle at Rectifier (αr)
g) Firing Angle at Inverter (αi)
h) Extinction Angle at Inverter (γ)

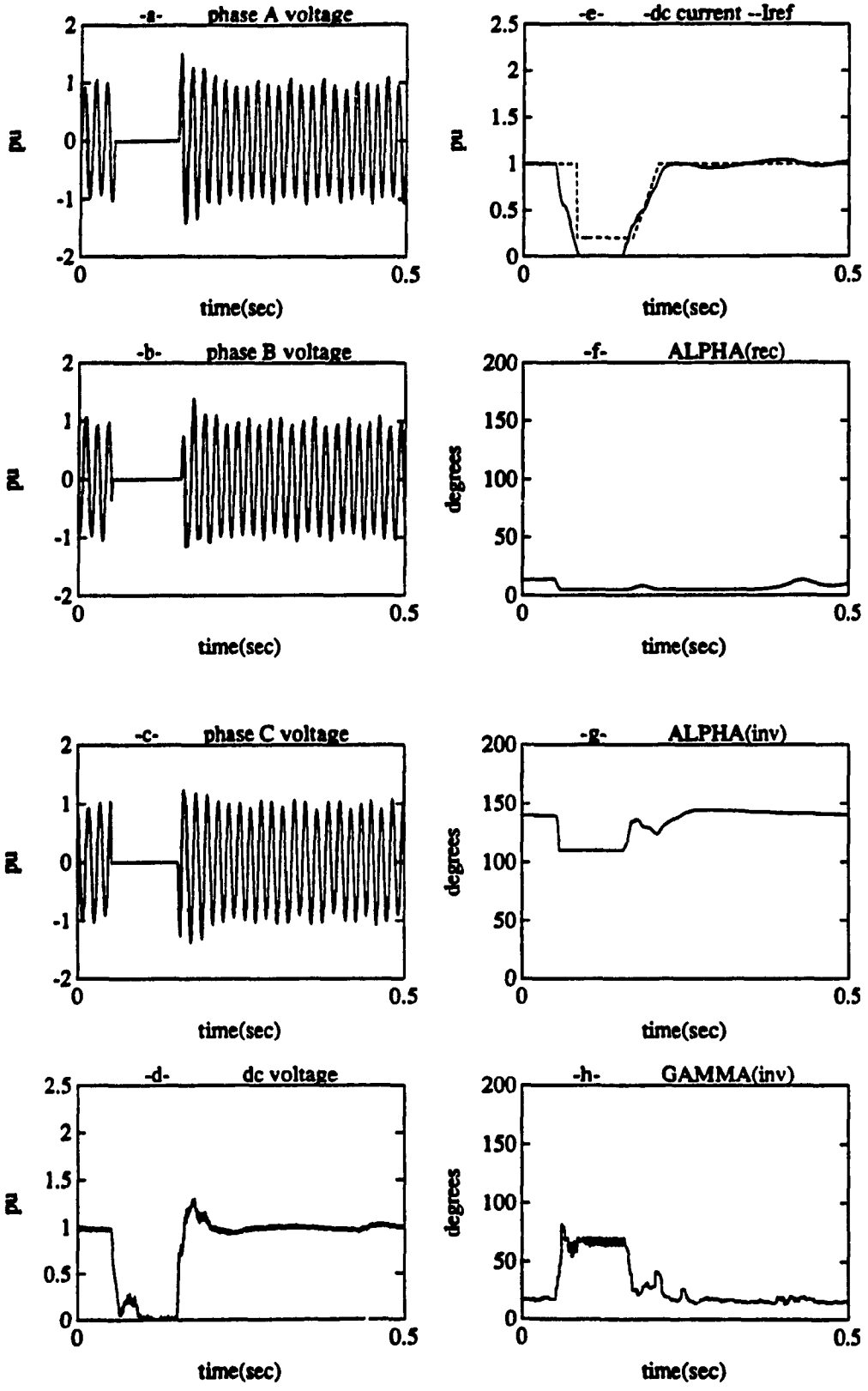

Figure 5.10-6 Three Phase to Ground Fault (On-Line Trained NN)

a,b,c) AC Voltages at Rectifier Bus
d) DC Voltage at Rectifier Side
e) -DC Current --Current Reference
f) Firing Angle at Rectifier (αr)
g) Firing Angle at Inverter (αi)
h) Extinction Angle at Inverter (γ)

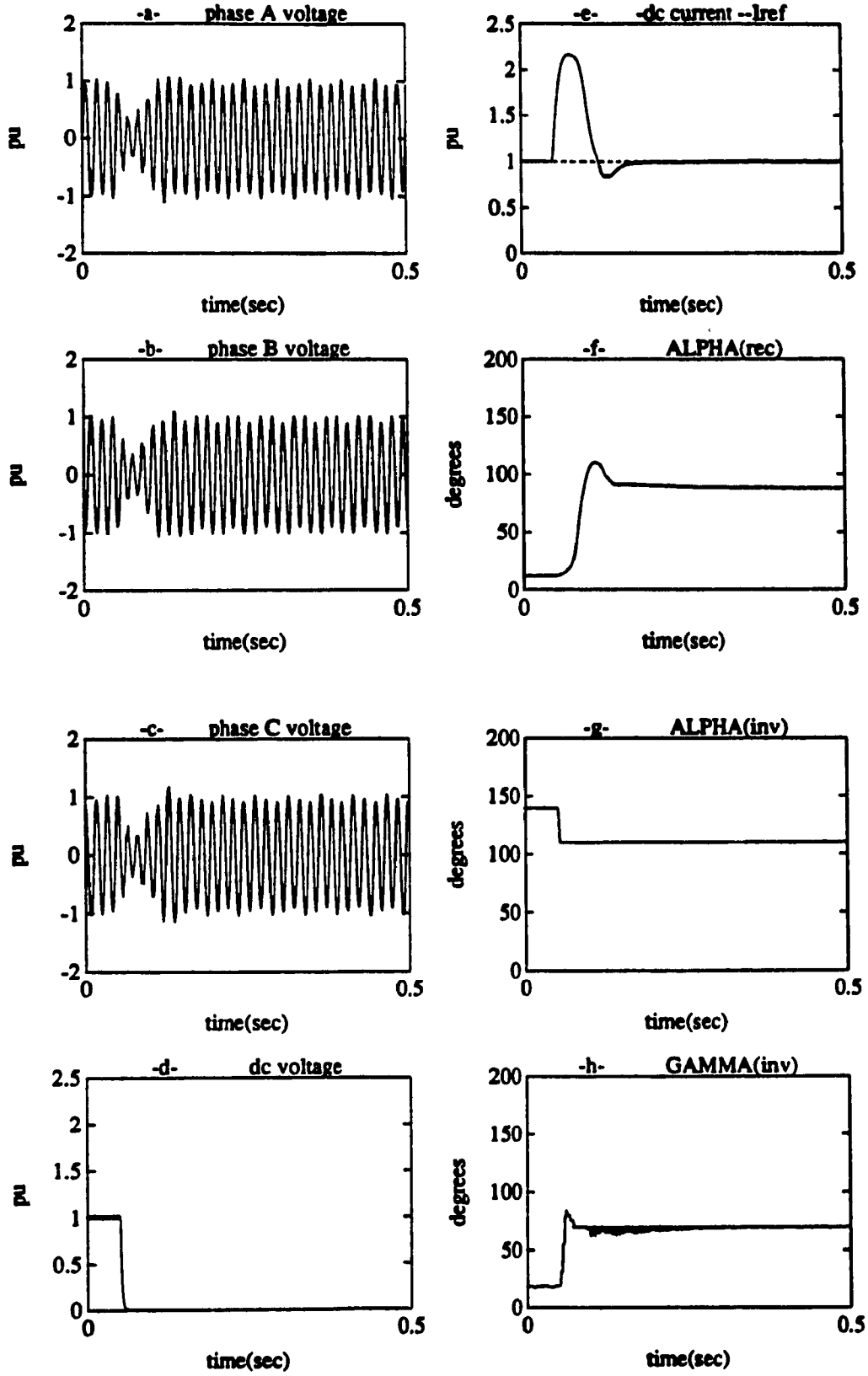

Figure 5.10-7 DC Fault (On-Line Trained NN)

a,b,c) AC Voltages at Rectifier Bus
d) DC Voltage at Rectifier Side
e) -DC Current --Current Reference
f) Firing Angle at Rectifier (αr)
g) Firing Angle at Inverter (αi)
h) Extinction Angle at Inverter (γ)

5.4.2 Second Approach (Off-Line Trained NN based Controller)

In this approach (Figure 5.11) the BackPropagation NN was trained off-line. The input to the NN, ε, is the error between the current reference, I_{ref}, and the measured current, I_d. The output of the NN (after being scaled by π) is the firing angle α.

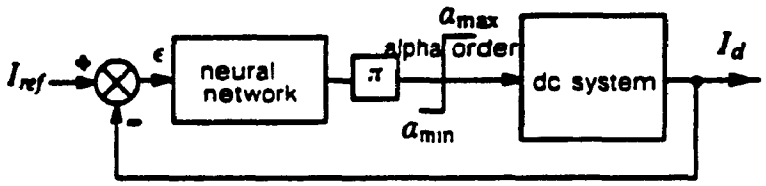

Figure 5.11 The second approach (Off-Line trained NN)

Network Structure

The NN is comprised of three layers (Figure 5.12).

The Input Layer: In this layer there are only two neurons, one of which is fed with a constant input BIAS2. The input

to the other neuron is ε. This layer acts simply as a fun-out layer and hence the outputs of the neurons are BIAS2 and ε.

The Hidden Layer: In this layer there are N neurons, where N=5. These are connected to the outputs of the Input Layer by weights X_n and BB_n, where n = 1, ..., N. The outputs of these neurons are acted upon by the sigmoid function. The outputs from this layer are fed to the Output Layer through the weights Y_n.

The Output Layer: This layer consists of one neuron only. The inputs to this neuron are the outputs O_n from the Hidden Layer and BIAS2 from the Input Layer. The weights associated with these inputs are Y_n and BB respectively. The output of this layer is OUT2 which is fed to a scaling factor π.

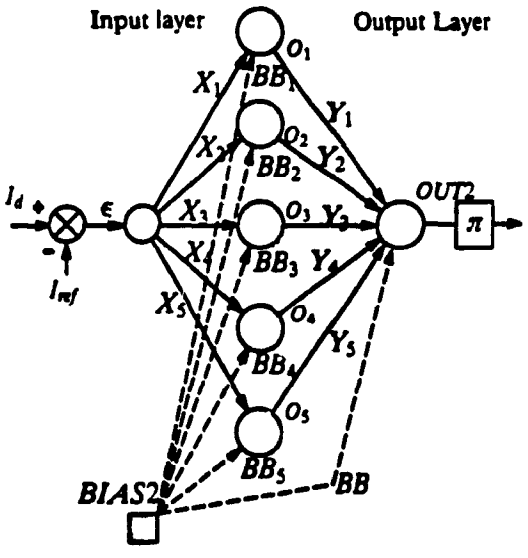

Figure 5.12 Neural network structure (second approach)

Training the Neural Network Off-Line

Figure 5.13 explains how the PI controller was used to train this NN. During the training, the output of the neural network (OUT2) is compared with the target (T), obtained from the PI controller, generating an error α_e. This error is used to adjust the weights of the Output Layer Y_n. Then according to the BackPropagation theory, the error is back propagated through the weights Y_n to the Hidden Layer to adjust its weights, X_n.

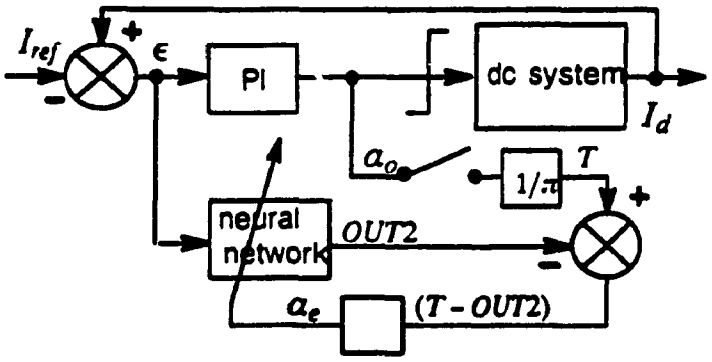

Figure 5.13 Training the neural network Off-Line

Adjusting the Weights of the Output Layer:

Using the Delta Rule at the output, δ is defined as

$$\delta = \frac{\partial OU2T}{\partial NET2} \text{ (T-OUT2)} \qquad (5.4.30)$$

where T is the target from the PI controller, α_o, after being scaled by $(1/\pi)$. That is

$$T = \alpha_o/\pi$$

and OUT2 is the output of the neural network given by

$$OUT2 = F(NET2) \qquad (5.4.31)$$

F is the Sigmoid Function giving

$$OUT2 = \frac{1}{(1 + e^{-NET2})} \qquad (5.4.32)$$

and its derivative

$$\frac{\partial F}{\partial NET2} = \frac{\partial OUT2}{\partial NET2} = OUT2 \cdot (1 - OUT2) \qquad (5.4.33)$$

NET2 is the summation of the weighted inputs to this neuron

$$NET2 = \sum_{n=1}^{N} (Y_n \cdot O_n) + BB \cdot BIAS2 \qquad (5.4.34)$$

Y_n's are the weights in the output layer

O_n's are the outputs of the neurons in the hidden layer

hence δ can be written as

$$\delta = OUT2 \cdot (1 - OUT2) \cdot (T - OUT2) \qquad (5.4.35)$$

After determining δ, the weights in the output layer are adjusted by

$$\Delta Y_n(t+1) = \eta \cdot \delta \cdot O_n + \mu \cdot \Delta Y_n(t) \qquad (5.4.36)$$

$$\Delta BB(t+1) = \eta \cdot \delta \cdot BIAS2 + \mu \cdot \Delta BB(t) \qquad (5.4.37)$$

giving updated value of the weights

$$Y_n(t+1) = Y_n(t) + \Delta Y_n(t+1) \qquad (5.4.38)$$

$$BB(t+1) = BB(t) + \Delta BB(t+1) \qquad (5.4.39)$$

where η and μ are two constants representing the learning rate and the momentum respectively of the NN. Here, because the training is done OFF-Line, the values of these constants are not very critical and do not cause a stability problem in the system. However, high values will cause oscillations and no learning while low values will lead to smooth but slow training.

Adjusting the Weights of the Hidden layer:

To adjust the weights in the hidden layer, the main mechanism in the backpropagation network is to propagate the error (α_e) back through the network from the output layer to the input layer, and then the same procedure is applied. That means δ_n which is used to adjust the weights of the hidden layer is δ weighted by the weights of the output layer

$$\delta_n = \delta \cdot Y_n \cdot \frac{\partial O_n}{\partial net_n} = \delta \cdot Y_n \cdot O_n \cdot (1-O_n) \qquad (5.4.40)$$

where O_n is the output of the n^{th} neuron in the hidden layer given by

$$O_n = F(net_n) = \frac{1}{(1 + e^{-net_n})} \qquad (5.4.41)$$

F is the Sigmoid function and net_n is the summation of the weighted inputs to this neuron.

$$net_n = X_n \cdot \varepsilon + BB_n \cdot BIAS2 \qquad (5.4.42)$$

Then the modification in the weights are

$$\Delta X_n(t+1) = \eta \cdot \delta_n \cdot \varepsilon + \mu \cdot \Delta X_n(t) \quad (5.4.43)$$

$$\Delta BB_n(t+1) = \eta \cdot \delta_n \cdot BIAS2 + \mu \cdot \Delta BB_n(t) \quad (5.4.44)$$

Hence, the updated values of the weights X_n and BB_n are

$$X_n(t+1) = X_n(t) + \Delta X_n(t+1) \quad (5.4.45)$$

$$BB_n(t+1) = BB_n(t) + \Delta BB_n(t+1) \quad (5.4.46)$$

and the training process will continue until the error α_e becomes zero or at least minimized to a very small value.

To obtain the training set from the PI controller, as it is shown in Figure 5.13, many step changes in I_{ref} with different magnitudes were taken. Also, some faults were applied to let the NN learn how to respond when such faults have occurred. The difficulty here was not the training itself but obtaining a good training set. The PI controller is not an ideal one. In addition, it is not easy to obtain a training set which contains all step changes, faults, harmonics, noise, and changes in the system. It is therefore, not a trivial problem to find a good training set. Once it is found, training the NN is simple since it is a single-input single-output network.

So, the problem with Off-Line training is the uncertainty

of the parameters of the ac/dc system, which are only approximately known (at best). Moreover, these parameters vary from time to time. This means that the parameters pre-set for either the traditional PI or the Off-Line trained NN may not be optimal for all times and operating conditions. Ideally an On-Line adaptive controller is required to overcome this problem. However, the advantage of the Off-Line trained controller (once it has been trained) is its capacity to generalize and its superior speed of response.

After it was trained off-line, this NN was used as a current regulator, replacing the PI controller. To test these NN regulators, step changes in the current order and faults were applied. Figures 5.14-1 ... 5.14-7 show the results of this approach. These results show that the off-line trained trained NN provides a fast controller. Some of the results are almost perfect (deblocking the system, Figure 5.14-1), but some of them show that more training is needed. For example, in the 40% step change in the current order (Figure 5.14-4), the off-line trained NN could not reduce the dc current to exactly 0.6 pu, as the PI and the on-line trained NN in first approach did. Also, when the dc fault is applied and not cleared, the off-line trained NN was not able to bring the current down to its reference value of 1 pu (Figure 5.14-7). Here, the answer is simply

more training and a better training set is needed. But for the time being, these two cases are used to show the effect and the advantage of the adaptive part in the third approach.

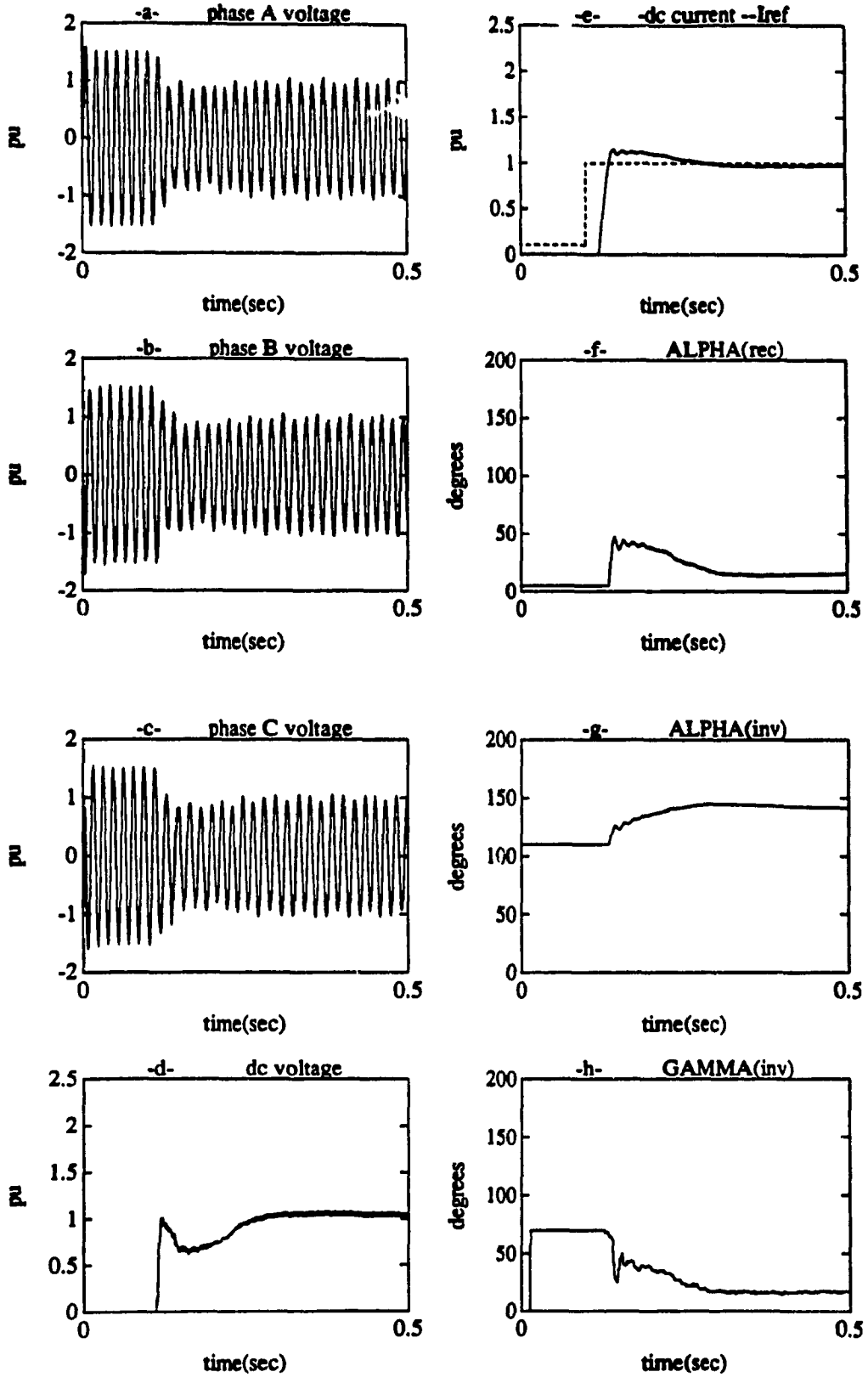

Figure 5.14-1 Deblocking the System (Off-Line Trained NN)

a,b,c) AC Voltages at Rectifier Bus
d) DC Voltage at Rectifier Side
e) -DC Current --Current Reference
f) Firing Angle at Rectifier (αr)
g) Firing Angle at Inverter (αi)
h) Extinction Angle at Inverter (γ)

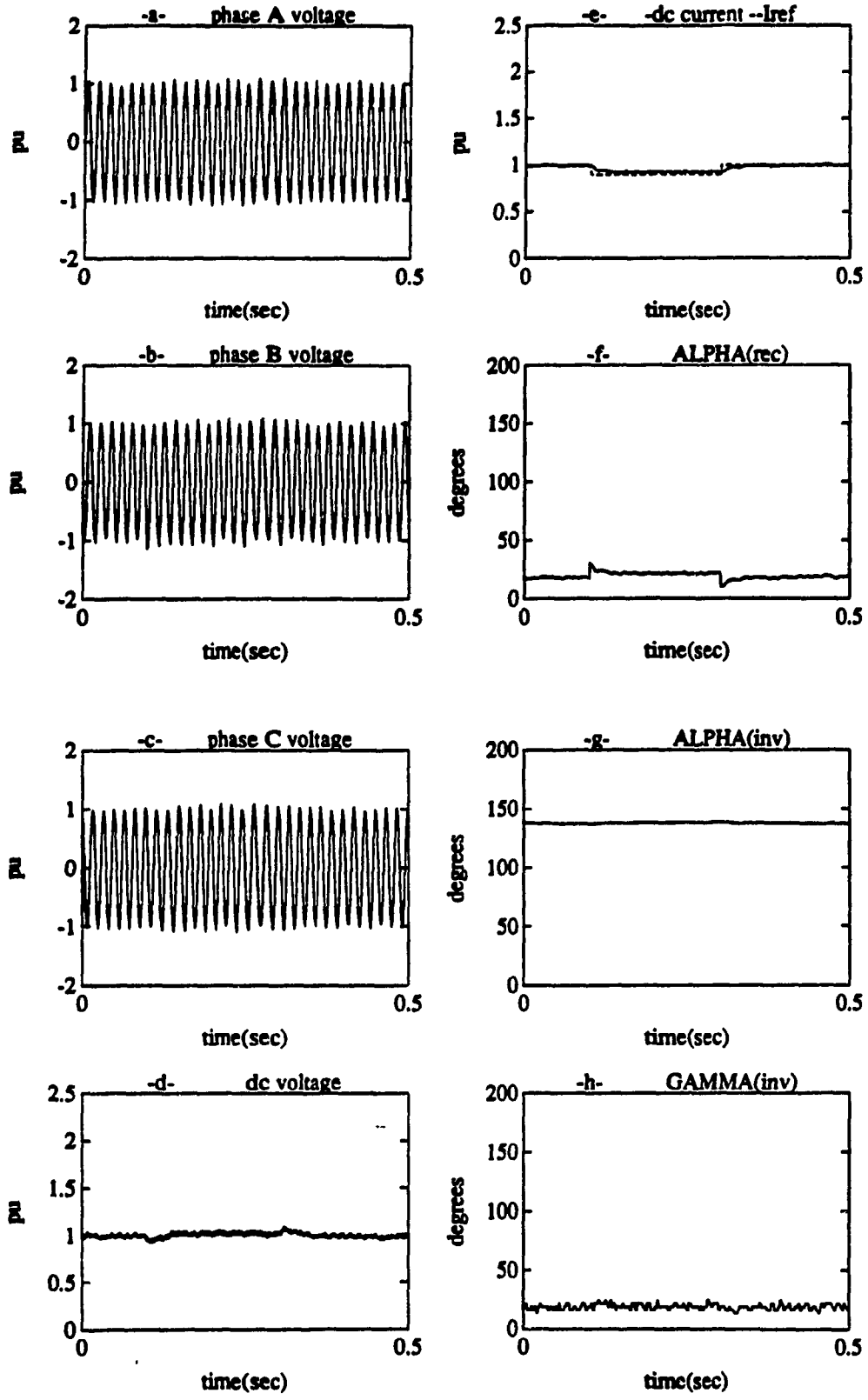

Figure 5.14-2 10% Step Change in I_{ref} (Off-Line Trained NN)

a,b,c) AC Voltages at Rectifier Bus
d) DC Voltage at Rectifier Side
e) -DC Current --Current Reference
f) Firing Angle at Rectifier (αr)
g) Firing Angle at Inverter (αi)
h) Extinction Angle at Inverter (γ)

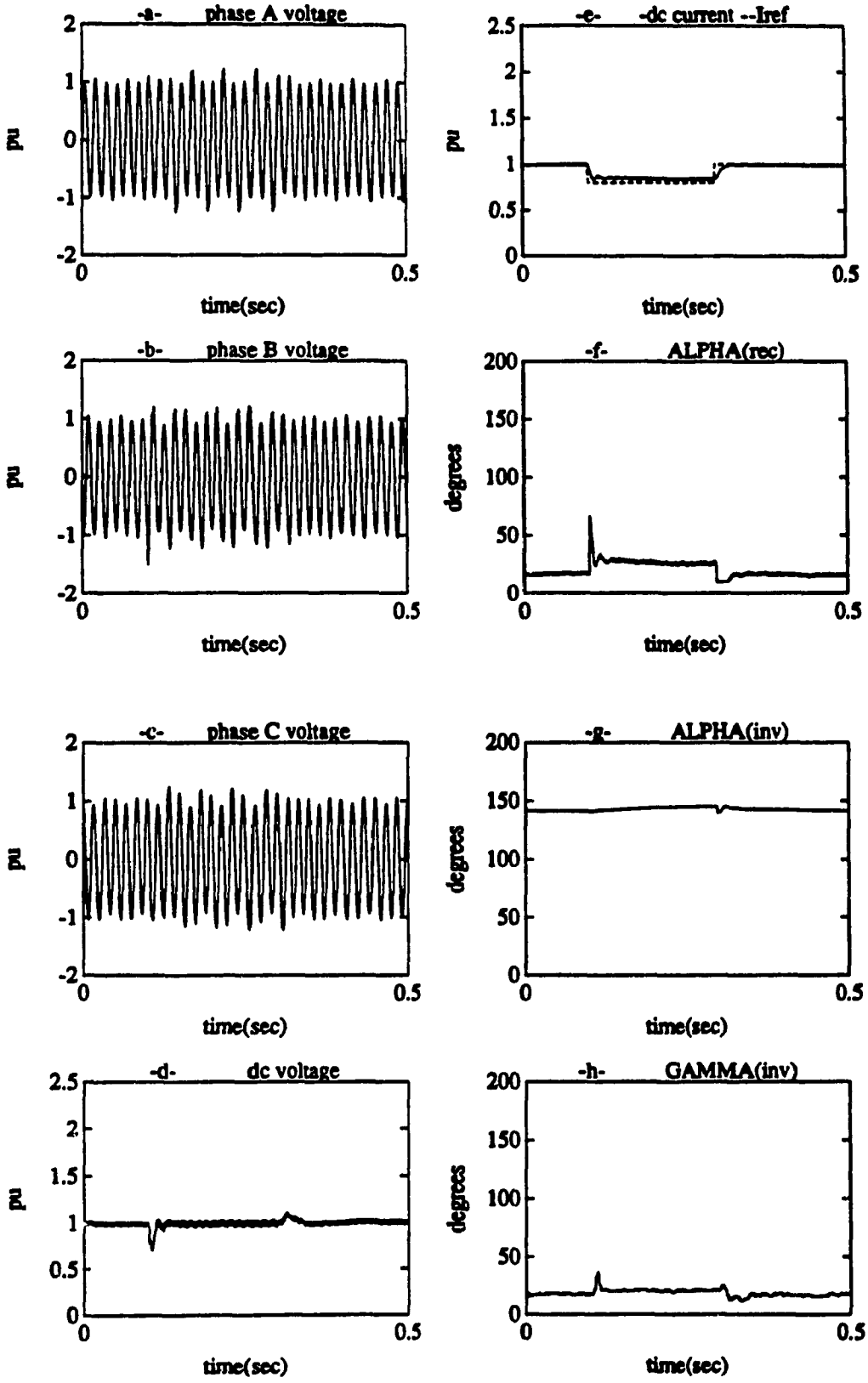

Figure 5.14-3 20% Step Change in I_{ref} (Off-Line Trained NN)

a,b,c) AC Voltages at Rectifier Bus
d) DC Voltage at Rectifier Side
e) -DC Current --Current Reference
f) Firing Angle at Rectifier (αr)
g) Firing Angle at Inverter (αi)
h) Extinction Angle at Inverter (γ)

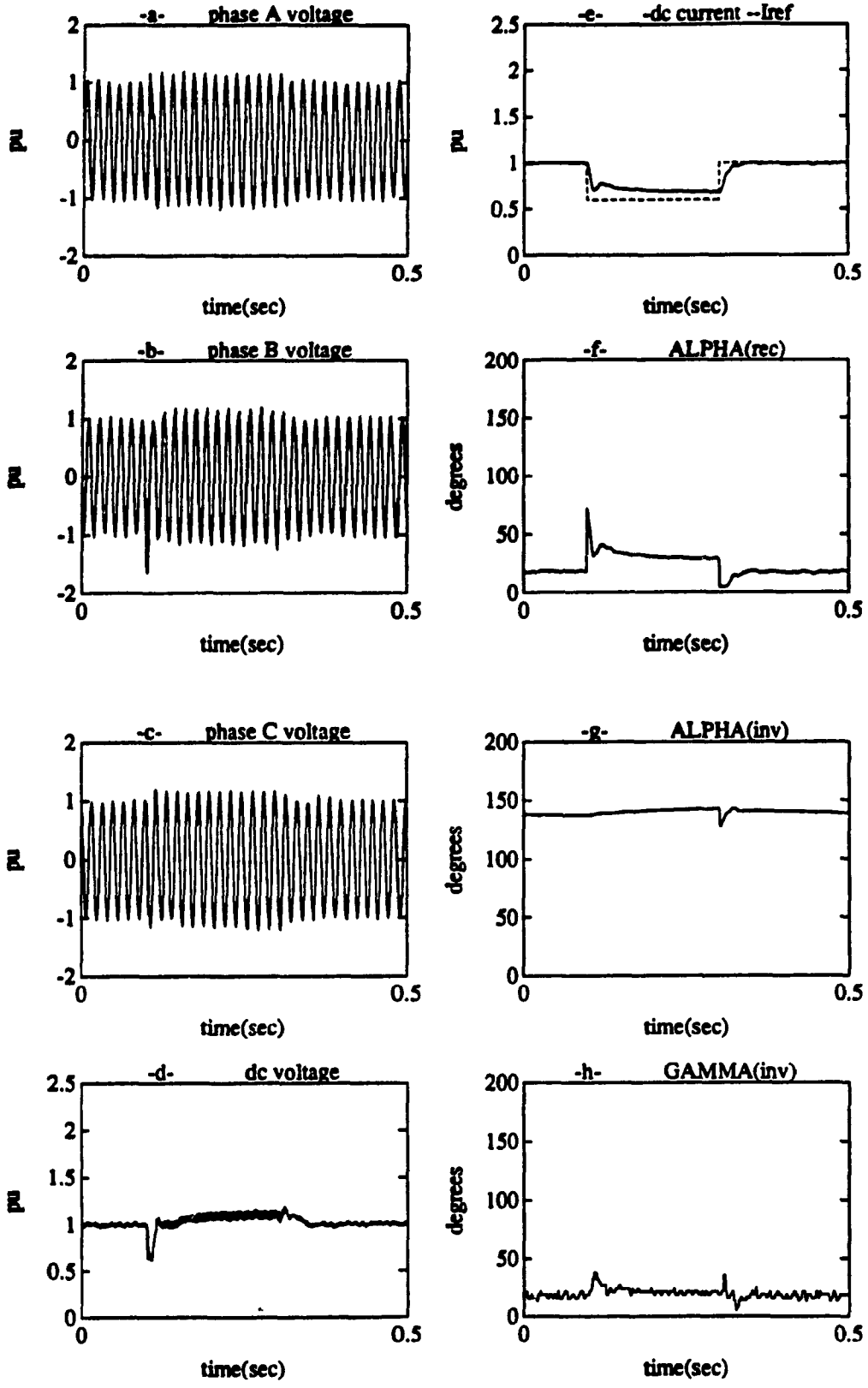

Figure 5.14-4 40% Step Change in I_{ref} (Off-Line Trained NN)

a,b,c) AC Voltages at Rectifier Bus
d) DC Voltage at Rectifier Side
e) -DC Current --Current Reference
f) Firing Angle at Rectifier (αr)
g) Firing Angle at Inverter (αi)
h) Extinction Angle at Inverter (γ)

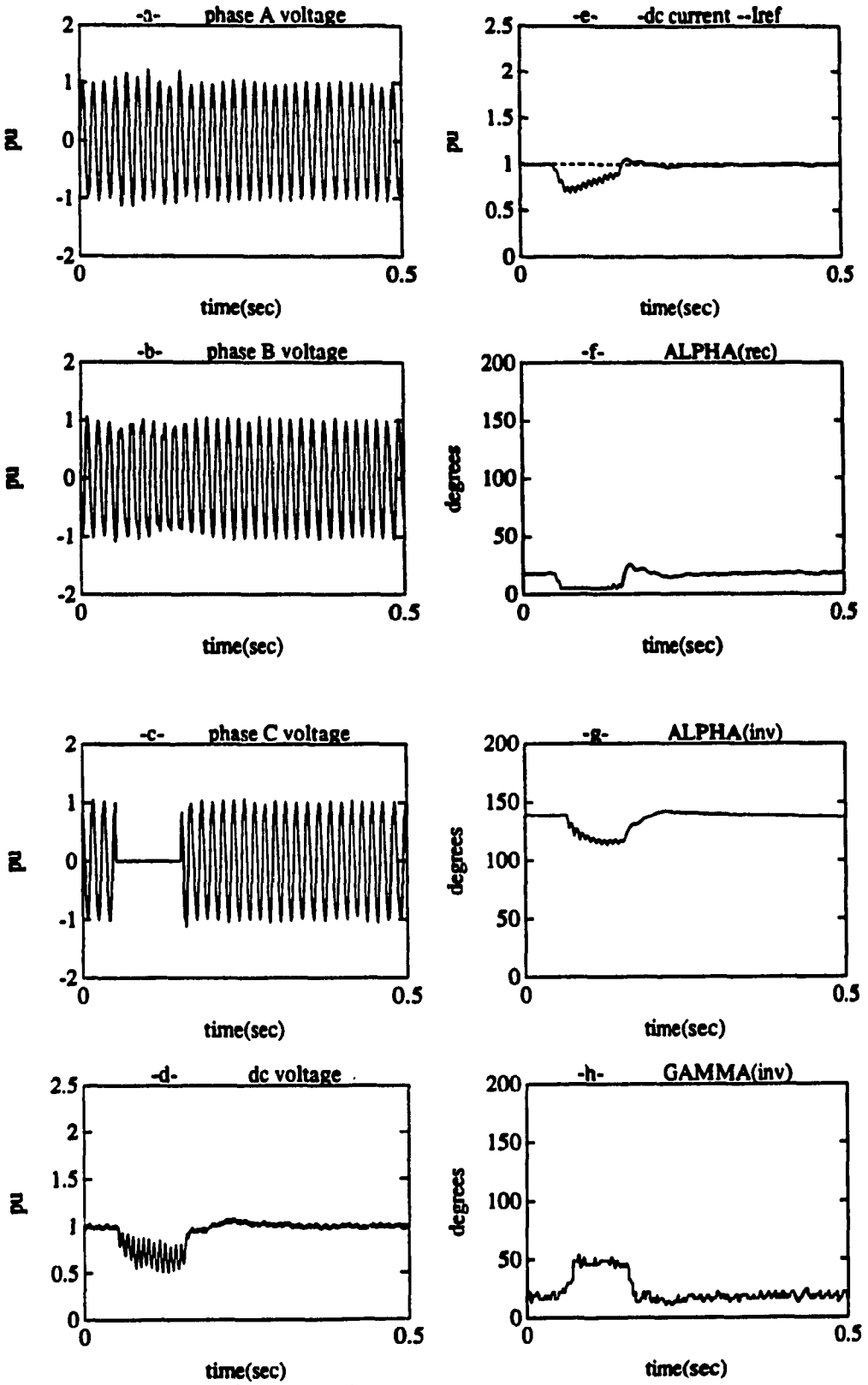

Figure 5.14-5 Single Line to Ground Fault (Off-Line Trained NN)

a,b,c) AC Voltages at Rectifier Bus
d) DC Voltage at Rectifier Side
e) -DC Current --Current Reference
f) Firing Angle at Rectifier (αr)
g) Firing Angle at Inverter (αi)
h) Extinction Angle at Inverter (γ)

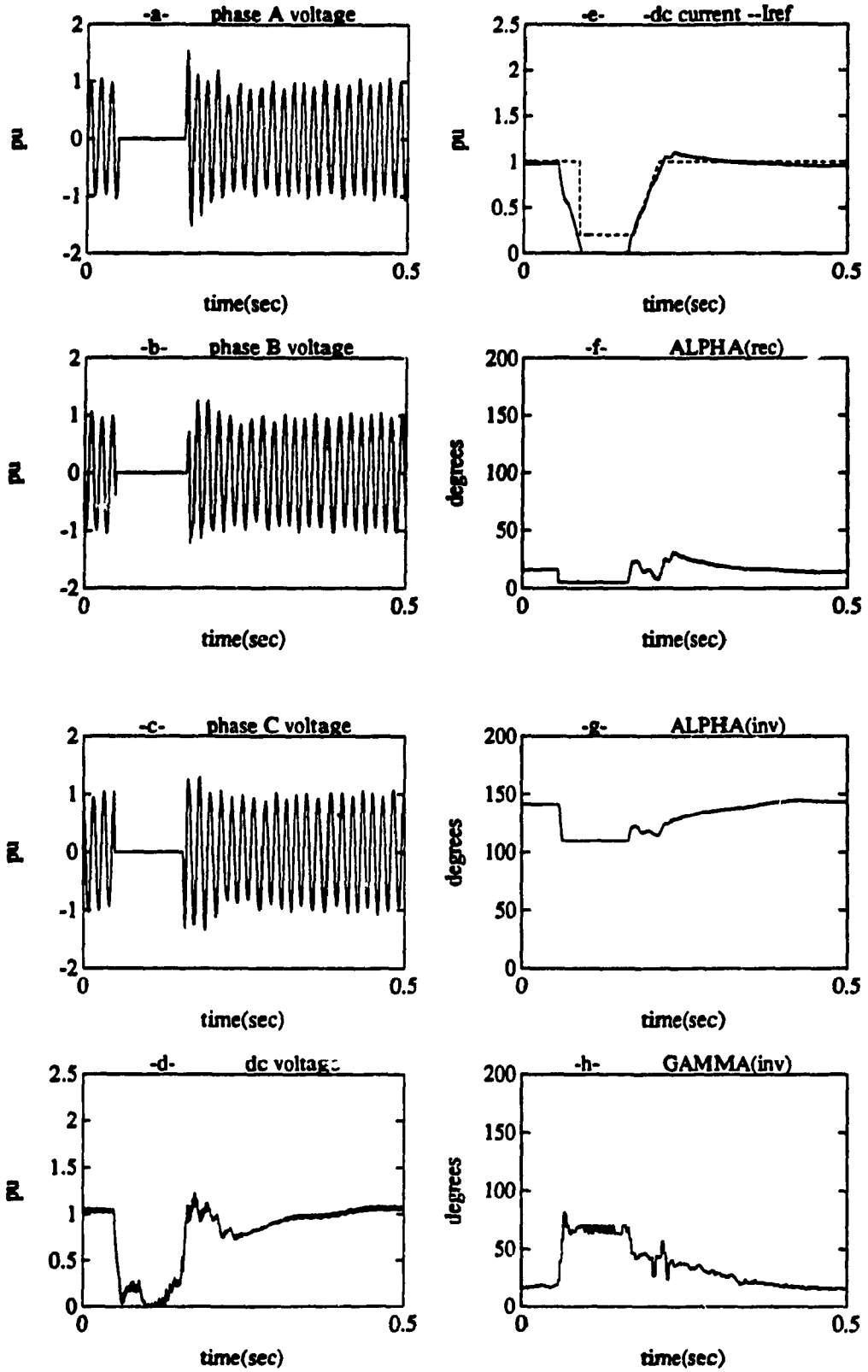

Figure 5.14-6 Three Phase to Ground Fault (Off-Line Trained NN)

a,b,c) AC Voltages at Rectifier Bus
d) DC Voltage at Rectifier Side
e) -DC Current --Current Reference
f) Firing Angle at Rectifier (αr)
g) Firing Angle at Inverter (αi)
h) Extinction Angle at Inverter (γ)

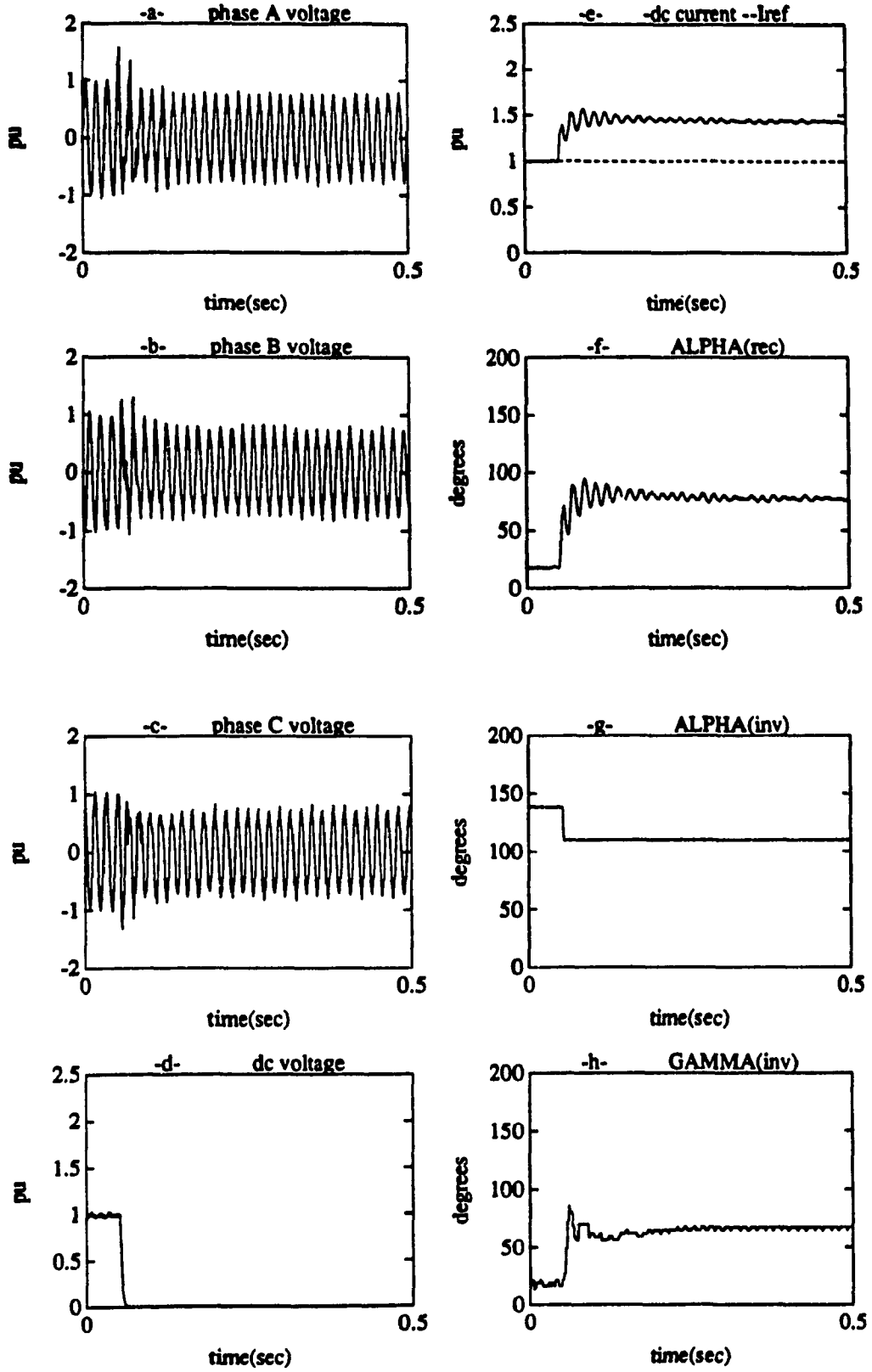

Figure 5.14-7 DC Fault (Off-Line Trained NN)

a,b,c) AC Voltages at Rectifier Bus
d) DC Voltage at Rectifier Side
e) -DC Current --Current Reference
f) Firing Angle at Rectifier (αr)
g) Firing Angle at Inverter (αi)
h) Extinction Angle at Inverter (γ)

5.4.3 The Third Approach (Parallel, On and Off-Line Trained, NN Based Controllers)

In the first approach, the NN adjusts its weights On-Line when an error exists between the reference and the measured value of the system's output. This on-line learning gives an adaptive regulator but relatively a slow one. In the second approach, all the training is done Off-Line. The result is a fast controller but not an adaptive one. Any changes in the ac or dc system will result in inoptimal weights.

For a single NN, adjusting the weights on-line may destroy the off-line training. Understanding human memorization presents serious problem; new memories are stored in such a fashion that existing ones are not forgotten or modified. But in artificial NNs, too often, learning a new pattern erases or modifies previous training. Here in Backpropagation network, the training vectors are applied sequentially until the network has learned the entire set. If, however, a fully trained network must learn a new training vector, it may disrupt the weights so badly that complete retraining ma be required.

Therefore, in this approach, and to utilize the speed and steady-state stability of the Off-Line trained controller,

and the adaptive features of the On-Line trained controller, a new configuration is derived using the two previously discussed NN controllers in parallel. The networks of the first two approaches are combined (in parallel) to have both advantages, fast and adaptive regulator.

Figure 5.15 shows the configuration of this approach. The outputs from the two networks are simply summed, but the On-Line trained part was slowed down (low values of learning rate η and momentum μ) to give a chance to the Off-Line trained NN to act first. Results of this approach are shown in Figures 5.16-1 ... 5.16-7.

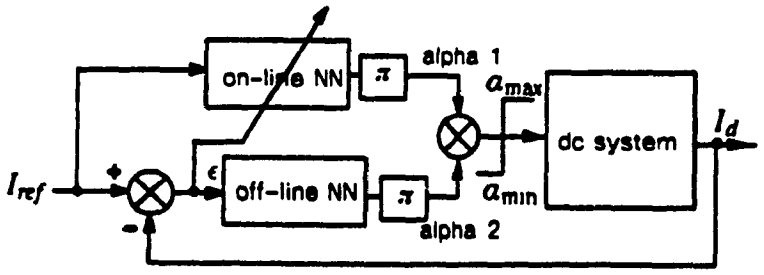

Figure 5.15 The Third Approach (Parallel, On and Off-Line, Trained NN Based Controllers)

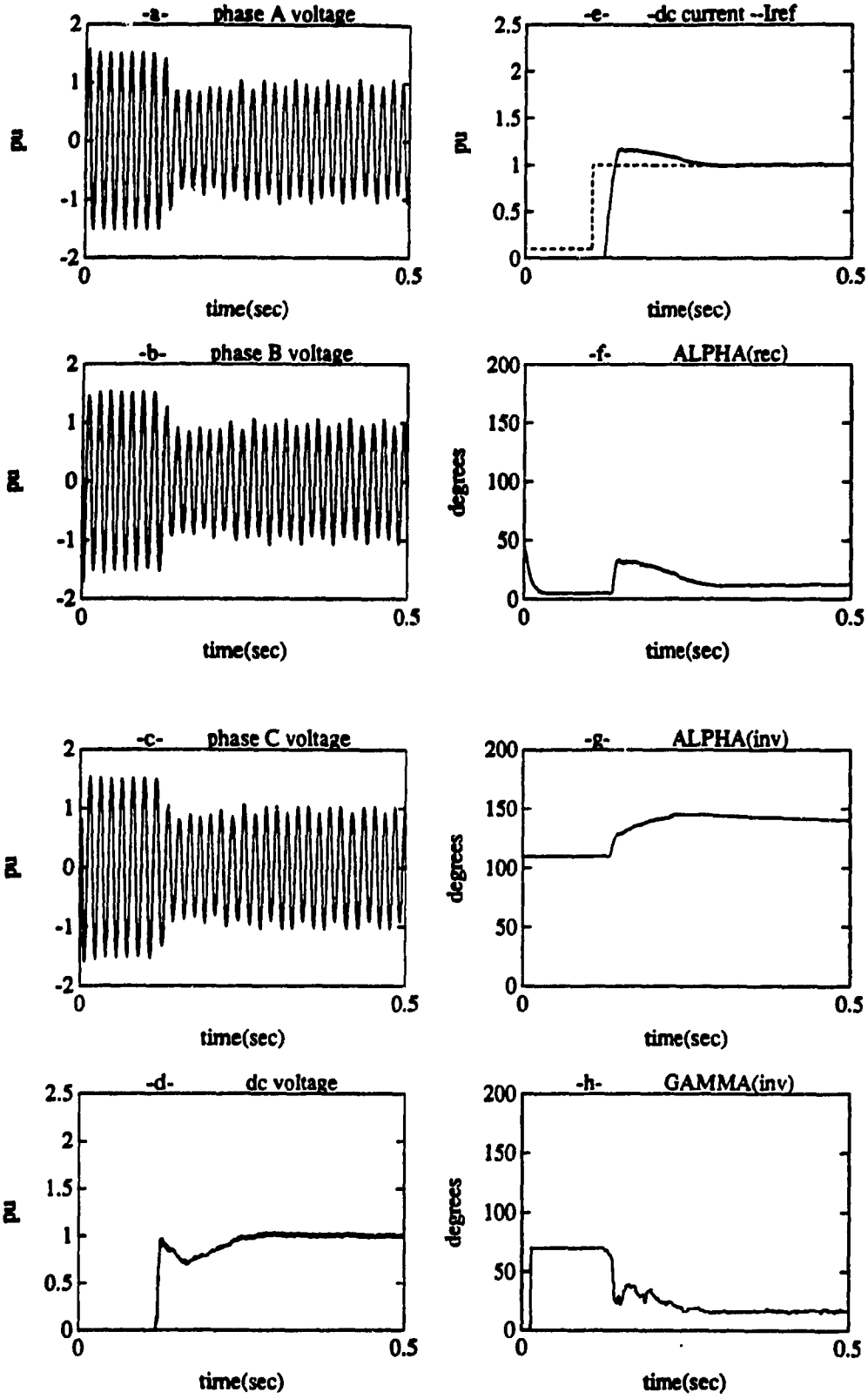

Figure 5.16-1 Deblocking the System (On and Off-Line Trained NN)

a,b,c) AC Voltages at Rectifier Bus
d) DC Voltage at Rectifier Side
e) -DC Current --Current Reference
f) Firing Angle at Rectifier (αr)
g) Firing Angle at Inverter (αi)
h) Extinction Angle at Inverter (γ)

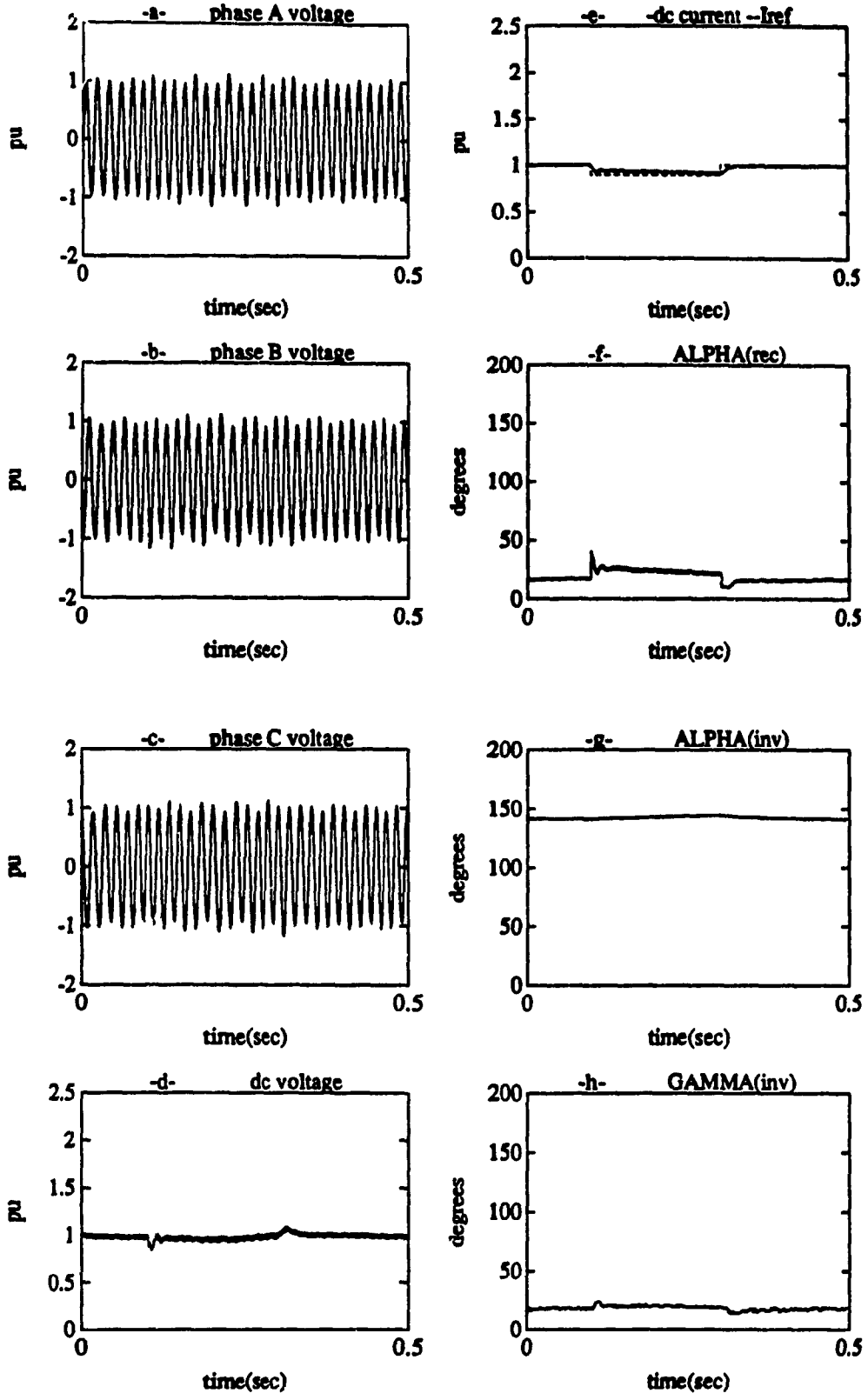

Figure 5.16-2 10% Step Change in Iref (On and Off-Line Trained NN)

a,b,c) AC Voltages at Rectifier Bus
d) DC Voltage at Rectifier Side
e) -DC Current --Current Reference
f) Firing Angle at Rectifier (αr)
g) Firing Angle at Inverter (αi)
h) Extinction Angle at Inverter (γ)

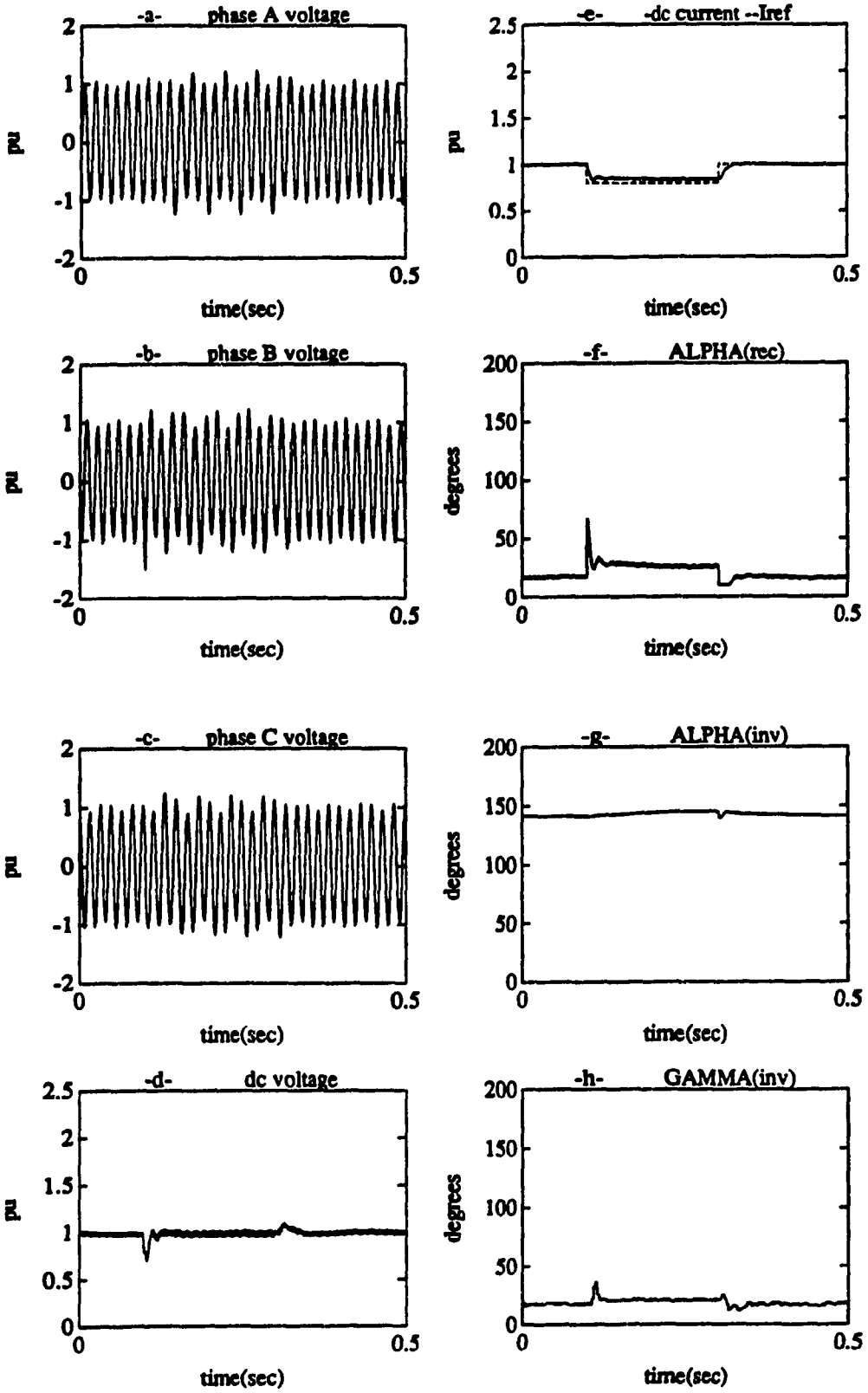

Figure 5.16-3 20% Step Change in Iref (On and Off-Line Trained NN)

a,b,c) AC Voltages at Rectifier Bus
d) DC Voltage at Rectifier Side
e) -DC Current --Current Reference
f) Firing Angle at Rectifier (αr)
g) Firing Angle at Inverter (αi)
h) Extinction Angle at Inverter (γ)

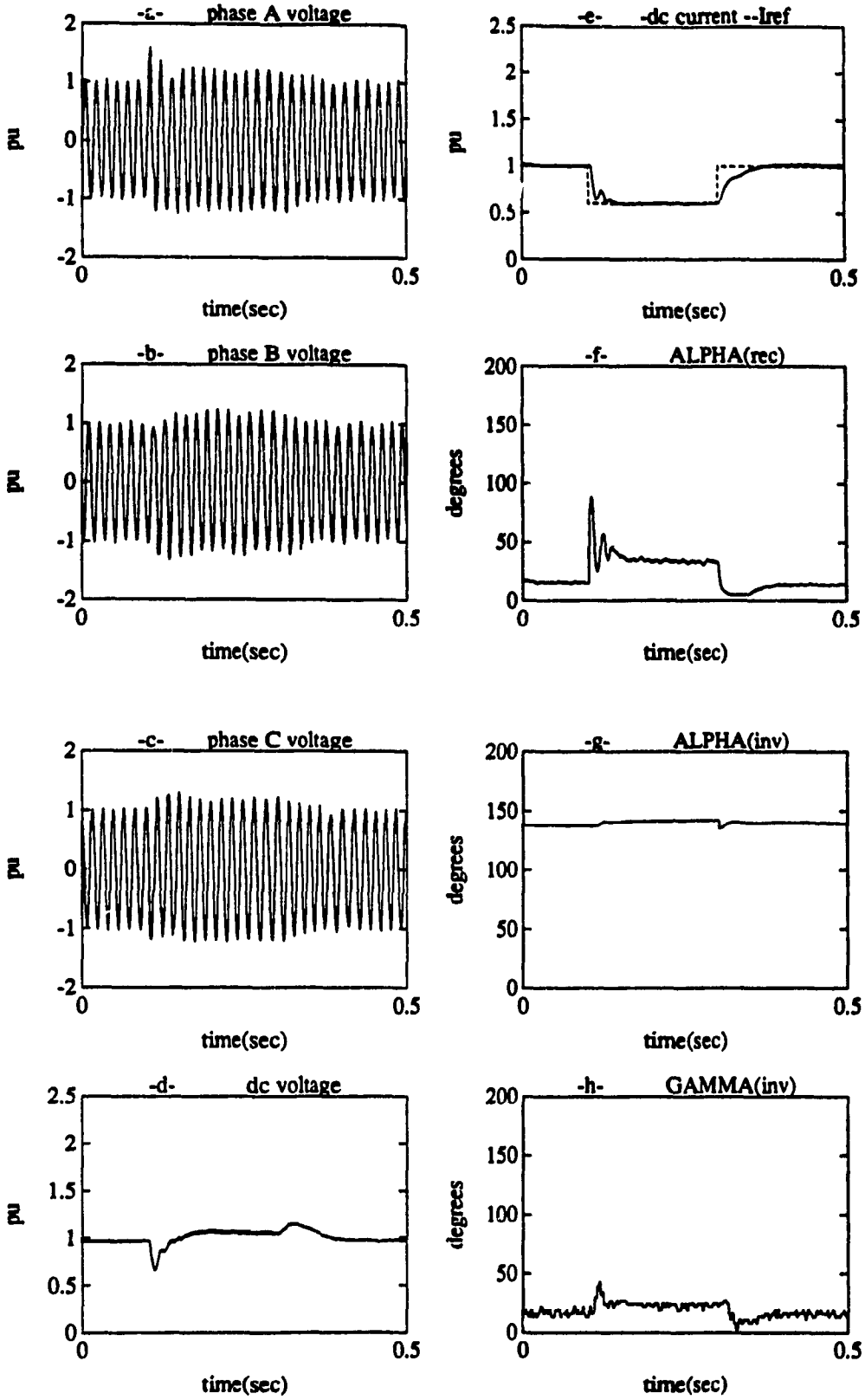

Figure 5.16-4 40% Step Change in Iref (On and Off-Line Trained NN)

a,b,c) AC Voltages at Rectifier Bus
d) DC Voltage at Rectifier Side
e) -DC Current --Current Reference
f) Firing Angle at Rectifier (αr)
g) Firing Angle at Inverter (αi)
h) Extinction Angle at Inverter (γ)

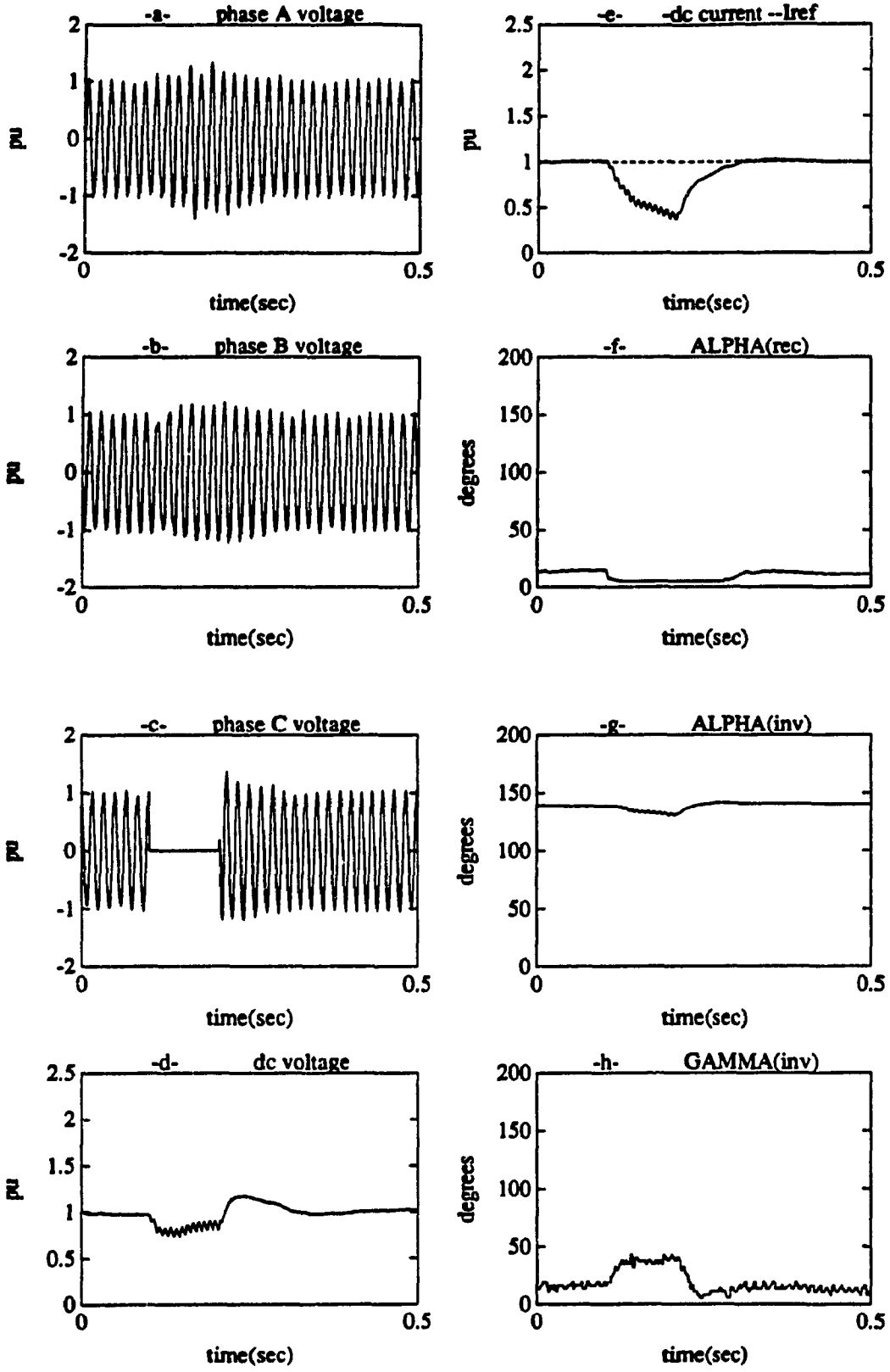

Figure 5.16-5 Line to Ground Fault (On and Off-Line Trained NN)

a,b,c) AC Voltages at Rectifier Bus
d) DC Voltage at Rectifier Side
e) -DC Current --Current Reference
f) Firing Angle at Rectifier (αr)
g) Firing Angle at Inverter (αi)
h) Extinction Angle at Inverter (γ)

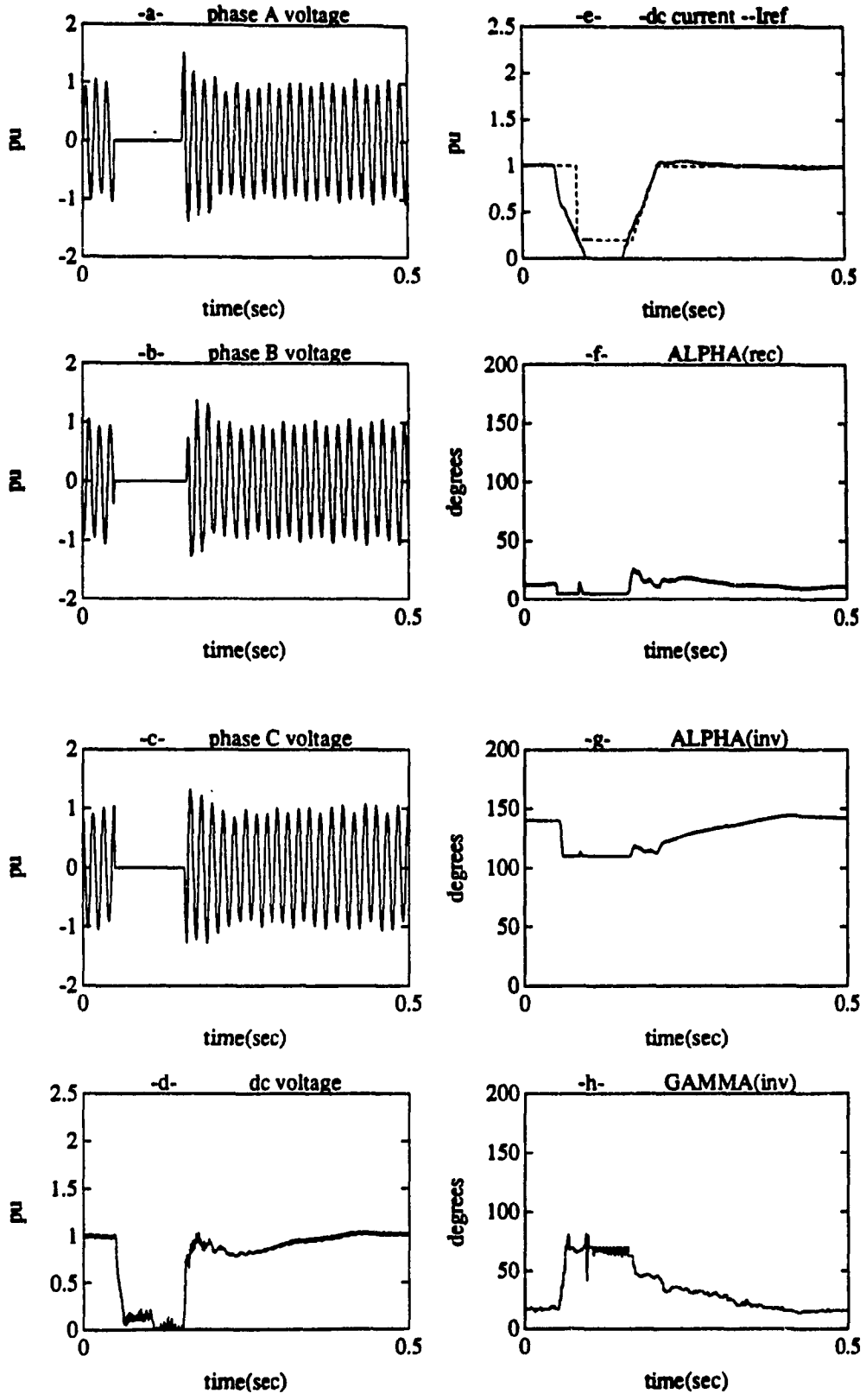

Figure 5.16-6 3PH to Ground Fault (On and Off-Line Trained NN)

a,b,c) AC Voltages at Rectifier Bus
d) DC Voltage at Rectifier Side
e) -DC Current --Current Reference
f) Firing Angle at Rectifier (αr)
g) Firing Angle at Inverter (αi)
h) Extinction Angle at Inverter (γ)

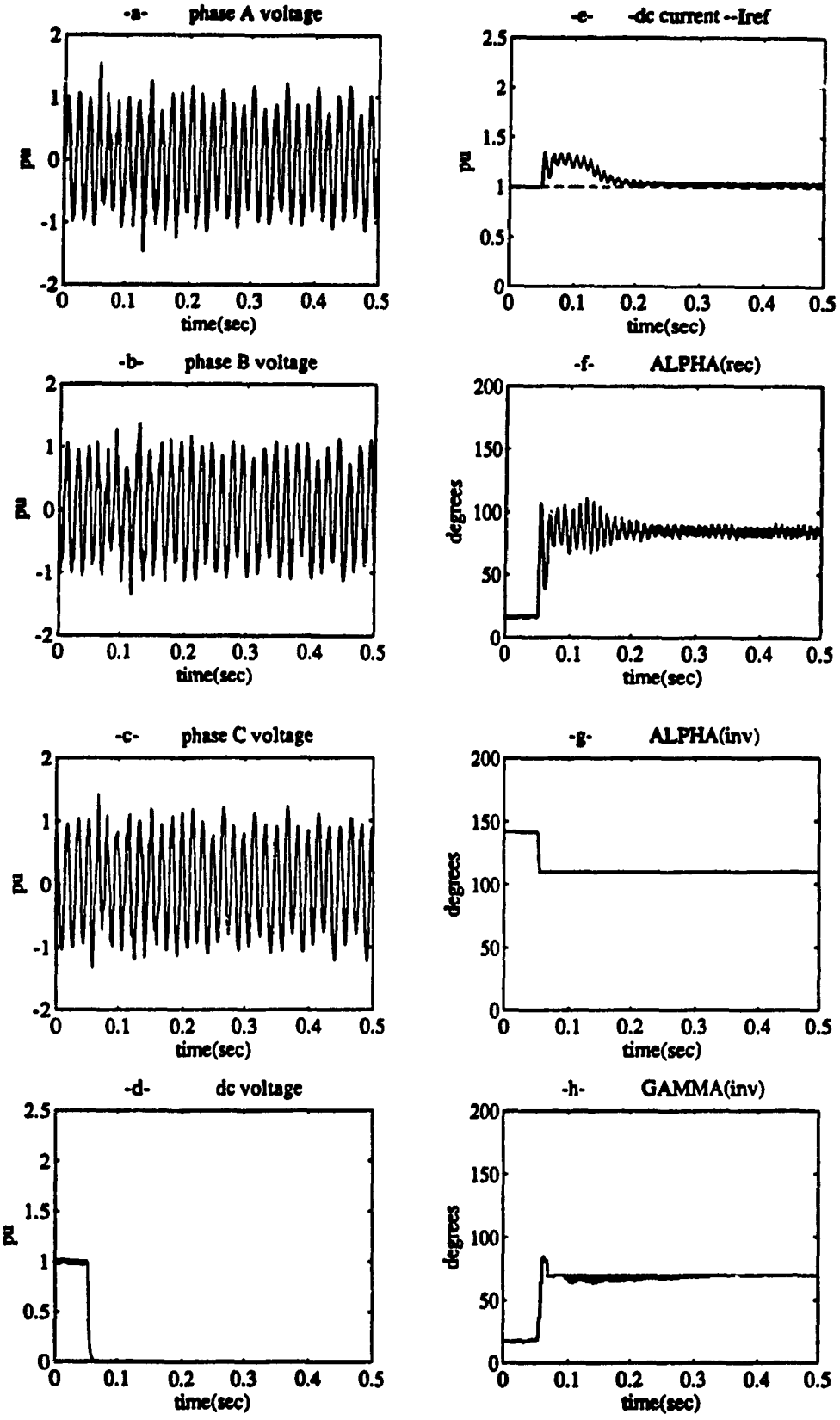

Figure 5.16-7 DC Fault (On and Off-Line Trained NN)

a,b,c) AC Voltages at Rectifier Bus
d) DC Voltage at Rectifier Side
e) -DC Current --Current Reference
f) Firing Angle at Rectifier (αr)
g) Firing Angle at Inverter (αi)
h) Extinction Angle at Inverter (γ)

5.5 Comparison

The behavior of the controllers in controlling the desired current for a full range of typical system disturbances was studied, and results have been shown. Here, some of these results are compared.

Step Changes in Current Order

The response of the four current controllers to a relatively large step change of 40% to the current order I_{ref} are shown in Figure 5.17. Signals shown are the current order I_{ref} and the current response I_d (left-hand scales), and the firing angle α of the rectifier (right-hand scales).

The PI controller has acceptable performance (Figures 5.4-2 and 5.4-3) for smaller (10% and 20%) step changes in I_{ref}. However, for 40% step change, the perturbation was enough to cause the controller to hit its α_{min} limit of 5 degrees on recovery (Figure 5.17-a). Following this the controller was unable to regain control quickly enough and this resulted in multiple commutation failures at the inverter end.

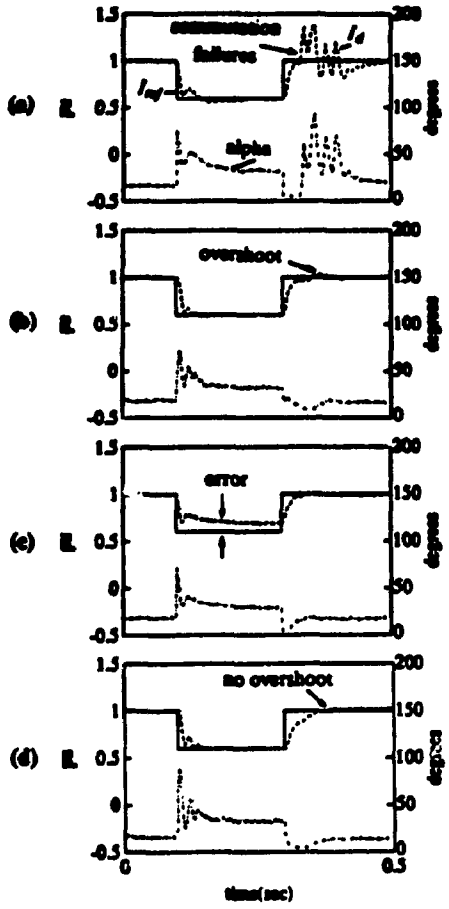

Figure 5.17 40% Step change in current order

The on-line trained NN controller (Figure 5.17-b) needs to have relatively fast dynamic characteristics to be able to control the current. However, on the recovery step, the controller was unable to avoid an overshoot of the current even though no commutation failures at the inverter end resulted. This is due to the fast dynamic characteristic of the NN controller provided by high values of the learning rate and momentum.

Although the off-line NN trained controller (Figure 5.17-c) has a fast response, it is unable to match completely the current order descent to 60% within the time period of 200 ms. This is a result of the limited training set utilized; actually, it is very difficult to train the off-line NN for all operating conditions. On the recovery step, the controller touched the α_{min} limit but was able to recover more rapidly to control the current to its ordered value.

As can be expected, the parallel combination of the off-line and on-line trained NN controllers (Figure 5.17-d) resulted in an acceptable performance on the descent and recovery steps. Here, the adaptive part was able to take the current down to 60% while the other part (off-line trained NN) was unable to do so alone. This is also clear in the case of a dc fault (to be discussed later).

Three Phase Fault at rectifier end

The response of the four current controllers to a three phase ac fault at the rectifier bus are shown in Figure 5.18. Loss of the dc voltage, which results from loss of ac voltage at the rectifier, triggers the application of a

protection circuit called the Voltage Dependent Current Limit (VDCL) after a delay of about 25 ms. The application of the VDCL causes I_{ref} to be reduced to 0.2 pu. On recovery of the dc voltage, the I_{ref} is ramped up to 1.0 pu in 50 ms, after a delay of about 20 ms. Signals shown in Figure 5.18 are the current order I_{ref} and current response I_d (left-hand scales), and the firing α of the rectifier (right-hand scales).

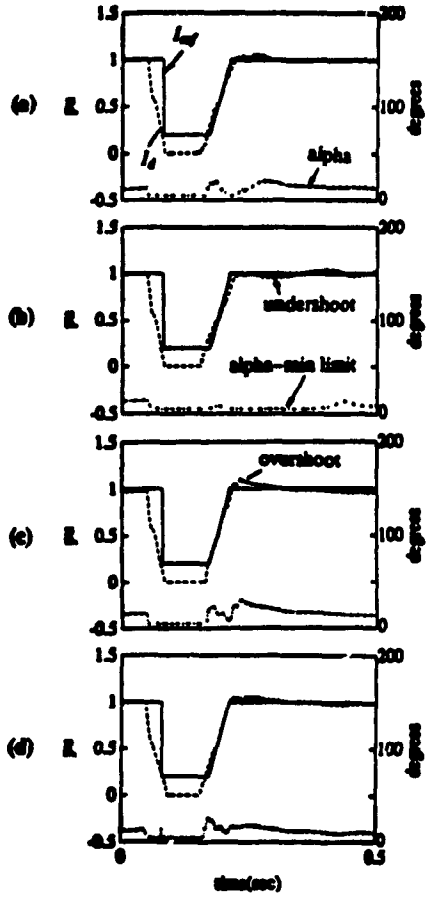

Figure 5.18 Three phase fault

The PI controller (Figure 5.18-a) was able to follow the VDCL ramp only till about 0.6 pu I_d when the controller hit

its α_{min} limit of 5 degs. Subsequently, the current Id increased as a function of the dc voltage (which indirectly is a function of the dc voltage). The controller was eventually able to regain control of the current at about 0.3 seconds.

With the on-line trained NN controller (Figure 5.18-b), the response was somewhat similar, but the controller was forced to its α_{min} of 5 degs for a much longer duration. The controller was eventually able to regain control of the current at about 0.5 sec. During the period, 0.3 to 0.5, the dynamic response was oscillatory at a low frequency. Better selection of the learning rate and momentum of the NN controller would have achieved better responses.

In the case of the off-line trained NN controller (Figure 5.18-c), the response was more stable. However, there is a considerable overshoot of the current, followed by a period of undershoot. The controller did not achieve the desired value of the current until much after 0.5 sec.

In the case of the parallel on and off-line trained NN controller (Figure 5.18-d), the response has a mix of the characteristics of the individual controllers discussed above.

DC Side Fault

In Figures 5.4-7, 5.10-7, 5.14-7, and 5.16-7 are shown the responses of the four current controllers in the case of a dc side fault. This is a serve test to study the dynamic response of the controllers to a large disturbance. Usually protection circuits would come into play for this test, but it was decided to disable all protection circuits and hence the current order is maintained at 1.0 pu after the fault is applied.

The PI controller is (Figure 5.4-7) fast and controlled, and quickly reduces the current error to zero. The controller alpha indicates the converter is rapidly phased back to an α of over 80 degs to reduce the current to 1 pu. The α is finally maintained at close to 85 degs, just enough to maintain the fault current at 1 pu. The speed of response of the optimized controller was able to limit the peak fault current to about 1.4 pu.

In the case of the on-line trained NN controller (Figure 5.10-7), this peak was closer to 1.8 pu due to a slow response. However, the settling time was similar to that of the PI controller. This test showed clearly that the on-line trained NN controller is slow in response, due to

non-optimal settings of the learning rate and momentum. In Figure 5.8 it was shown clearly the impact of the learning rate in case of dc fault where for high value of η (0.3) the controller was much faster and a peak value of 1.5 pu was observed, and the settling time to bring the dc current to 1 pu was also reduced.

For the off-line trained controller (Figure 5.14-7), it transiently phases back its α to 80 degs, but the large current error takes an infinity long time to reduce the current to 1 pu. It is clear here that more training is needed. Indeed, it is non-trivial task to generate a suitable training set to handle all contingencies.

In the third approach, Figure 5.16-7 shows the effect of the adaptive part (when it is in parallel with the off-lone trained NN) in bringing the current down to 1 pu while the off-line trained part was not able to do this alone.

Block/Deblock of Rectifier

When a dc system is first energized, the current order is typically ramped up to 1 pu within 75 ms. However, to subject the controller to much more severe condition, the current order is stepped up instantaneously in this test.

As shown in Figures 4.4-1, 4.10-1, 4.14-1, and 4.16-1, the PI and all NN controllers were able to survive the steep increase in current although this is a function of the capacity of the supporting ac system. After an over shoot (relatively small), these controllers were able to maintain the current at the desired value of 1 pu.

CHAPTER 6

CONCLUSIONS

NNs may be used to distinguish typical faults that can occur in an ac-dc system. Three types of NN models have been studied. These can sense ac bus voltages either as rms values (with or without phase angle information) or as sampled instantaneous values of sine waves. Depending in which method is used, some confusion can occur in distinguishing a line to line fault from a remote ac fault. A delay of 1-2 cycles in detection of faults when using rms values is expected due to the algorithm required for determining the rms value. This may not be too critical in practice. However, where this delay is unacceptable, instantaneous values may be used.

Also, In this study, the possibility of replacing a PI controller with a NN based controller for the rectifier terminal of an HVDC li[illegible] was explored. This NN controller has a part which is trained off-line and a part which is

trained on-line. The off-line trained NN has the non-variable characteristics of the system used for the training inherently trained into it, whilst the on-line trained NN is better able to adapt its parameters to suit the variable characteristics of the system. It is shown that the combined NN controller can adapt its weights on-line to provide improved or similar performance, when compared to traditional PI controllers, for small and large-signal disturbances. The response of this simple (having only 5 neurons in the hidden layer in the off-line part and 2 neurons in the on-line part) NN controller is somewhat slower for very fast transients due to inadequate training (lack of determining a very good training set for the off-line part, and non-optimum learning rate for the on-line part).

Further Work

Some work remains to be done before a neural network controller can be considered as a suitable replacement of the existing PI controller for the HVDC converter applications.

Another configuration for the on-line trained NN controller is needed such that the error used to adjust the

weights is located directly at the output of the neural network, i.e E is a function of OUT explicitly. If that is the case, Back Propagation can be used without backpropagating the error through the system, and then knowledge of the system and its parameters is not needed.

Further analytical work is necessary to determine an optimum learning rate η which has a very important effect on the speed of response and the system stability. In addition, some advanced optimization techniques (second order methods) may be used instead of using the Steepest Descent (first order method) in minimizing the error.

APPENDIX A

THE EMTDC ELECTROMAGNETIC TRANSIENTS PROGRAM

EMTDC is a simulation tool which can be used for simulation studies on power systems. The need for EMTDC first arose when early versions of BPA's EMTP were distributed in the early 70.s. It was recognized that if transfer functions such as were used in the Continuous System Modeling Program (CSMP) could interface to the electric circuit network solution of EMTP, then the usefulness of EMTP could be increased. As a result, a project was started at Manitoba Hydro to prepare a computer program which combined Dr. Dommels electromagnetic transients circuit solution method [45] with an interface to continuous system modeling functions. This early program was functioning before TACS was introduced to EMTP.

Over the years, building blocks in the form of subroutines and functions have been developed so that today, models for most power system elements are available in modular form for EMTDC. The libraries of building blocks are so extensive that any conceived power system can be constructed. The strength of EMTDC is with this ability to assemble conceivable system from available building blocks or from

building blocks developed by the user. Electric circuits including network elements, transmission lines, cables and transformers are entered as data file similar to EMTP except in free format. Here the similarity ends. Starting from a subroutine skeleton, the user assembles his dynamic models, controls, switches, generators etc. using FORTRAN statements with calls to various EMTDC library models or user constructed subroutines and function building blocks similar to the way a CSMP model is developed. This dynamic build subroutine is compiled and loaded with the main line program and libraries. Electric circuit quantities such as voltage, currents, power, and reactive power can be read directly or through metering functions, processed by the dynamic model and returned to the electric circuit in the form controlled voltage or current sources, switches etc.

EMTDC is a very powerful study tool which does everything that EMTP can do, and when it comes to dc transmission simulation, can do it better. Its modular structure minimizes set-up time and maximizes size of the model. For a simple two terminal dc transmission link, EMTDC ran five times faster per time step calculation than for the same model on EMTP on the same computer at a fraction of set-up time [47]. Having its dc models tested against actual system performance, EMTDC is well proven and is the most powerful dc simulator in existence today [46],[47].

APPENDIX B

Rectifier End The data for the ac filters at the rectifier end (315 kV) is:

n	5th	7th	11th	13th	Capacitor
R (ohms)	4.96	3.54	2.26	1.91	
L (H)	0.274	0.137	0.0548	0.039	
C (μF)	1.0265	1.047	1.060	1.063	2.4
Q (MVA)	40	40	40	40	80

The rectifier end ac system (Effective Short Ratio = 16) is comprised of two sources with equivalent impedances in parallel. Each impedance network is comprised of
R = 26.2 ohms, L_1 = 0.0444 H, L_2 = 0.0199 H.

Inverter End The data for the ac filters at the inverter end (120 kV) is:

n	5th	7th	11th	13th	Capacitor
R (ohms)	0.75	0.514	0.326	0.276	
L (H)	0.039	0.02	0.008	0.0057	
C (μF)	7.074	7.217	7.3	7.32	16.58
Q (MVA)	40	40	40	40	80

The inverter end source data (ESR = 2.7) is:
R = 8.13 ohms, L_1 = 0.0079 H, L_2 = 0.0159 H.

DC Subsystem L_d = 0.1 H, R_d = 0.1 ohms
U_d = 140.6 kV, I_d = 3600 A, P_d = 506 MW.

APPENDIX C

Rectifier End The data for the ac filters at the rectifier end (315 kV) is:

n	5th	7th	11th	13th	Capacitor
R (ohms)	4.96	3.54	2.26	1.91	
L (H)	0.274	0.137	0.0548	0.039	
C (μF)	1.0265	1.047	1.060	1.063	2.4
Q (MVA)	40	40	40	40	80

The rectifier end ac system (Effective Short Ratio = 2) is comprised of two sources with equivalent impedances in parallel. Each impedance network is comprised of
R = 104.8 ohms, L_1 = 0.1776 H, L_2 = 0.0796 H.

Inverter End The data for the ac filters at the inverter end (120 kV) is:

n	5th	7th	11th	13th	Capacitor
R (ohms)	0.75	0.514	0.326	0.276	
L (H)	0.039	0.02	0.008	0.0057	
C (μF)	7.074	7.217	7.3	7.32	16.58
Q (MVA)	40	40	40	40	80

The inverter end source data (ESR = 2.7) is:
R = 8.13 ohms, L_1 = 0.0079 H, L_2 = 0.0159 H.

DC Subsystem L_d = 0.1 H, R_d = 0.1 ohms
U_d = 140.6 kV, I_d = 3600 A, P_d = 506 MW.

PUBLICATIONS RESULTED FROM THIS STUDY

[1] N. Kandil, V.K. Sood, K. Khorasani, and R.V. Patel, " Fault Identification in an AC-DC Transmission System Using Neural Networks ", IEEE Trans. on Power Systems, Vol.7, No.2, pp 812 - 819, May 1992.

[2] V.K Sood, N. Kandil, R.V. Patel, and K. Khorasani, " Neural Network Based Current Controller for HVDC Transmission Systems ", IEE Second International Conference on Artificial Neural Networks Pub. No.349, 18-20 Nov. 1991, Bournemouth, England. pp 373 - 378.

[3] V.K Sood, N. Kandil, R.V. Patel, and K. Khorasani, " Comparative Evaluation of Neural Network Based Current Controllers for HVDC Transmission ", Power Electronics Specialists Conference,PESC'92, June 29 - July 3, 1992, Toledo, Spain.

[4] N. Kandil, V.K. Sood, R.V. Patel, and K. Khorasani, " Evaluation of an Off-Line Neural Network Based Current Regulator for HVDC Transmission Systems ", Canadian Conference on Electrical and Computer Engineering, CCECE'92, 14-16 September, 1992, Toronto, Ontario, Canada.

REFERENCES

[1] A. Ekstrom, "*High Power Electronics, HVDC and SVC*", EKC-Electric Power Research Center, Stockholm, 1989.

[2] C. A. Gross, "*Power System Analysis*", Wiley, New York, 1986.

[3] E. W. Kimbark, "*Direct Current Transmission*", Wiley, New York, 1971.

[4] Manitoba HVDC Research Center, "*EMTDC User's Manual*", Winnipeg, Manitoba, Canada, 1988.

[5] NeuralWare Inc, "*Neuralworks, revision 2.00*", Neuralware, Inc. Sewickley, PA, 1988.

[6] B. Soucek and M. Soucek, "*Neural and Massively Parallel Computers, The Sixth Generation*", Wiley, New York, 1988 .

[7] P. D. Wasserman, "*Neural Computing, Theory and Practice*", Van Nostrand Reinhold, New York, 1989.

[8] A. Ekstrom and G. Liss, "*A Refined HVDC Control System*", IEEE Trans. on Power Apparatus and Systems, Vol. PAS-89, No.536, May/June 1970.

[9] M. Kawato, Y. Uno, M. Isobe and R. Susuki, "*A hierarchical Model for Voluntary Movement and its Applications to Robotics*", Proc. IEEE International Conference on Neural Networks, Vol. IV, 1987, pp. 573-582.

[10] D. Psaltis, A. Sideris and A Yamamura, "*A Multi-Layerd NN Controller*", IEEE Control Systems Magazine, Vol.8, 1988, N0.2, pp. 17-12.

[11] T. Yabuta and T. Yamada, "*Possibility of Neural Networks Controller for Robot Manipulator*", Proc. IEEE International Conference on Robotics and Automations, Cincinnati, Ohio USA, May 13 - 18, pp. 1686-1691.

[12] Y. Ito, T. Furuhashi, S. Okuma, and Y. Uchikawa, "*A Digital Current Controller for a PWM Inverter Using a Neural Network and its Stability*", 21 st Annual IEEE PESC 1990 Record, San Antonio, Texas, pp. 219-224.

[13] V. K. Sood, N. Kandil, R. Patel, and K. Khorasani, "*Neural Network Based Current Controller for HVDC Transmission System*", Second IEE International Conference on Neural Networks, Bournemouth, U.K., 18-20 Nov 1991.

[14] K. S. Narendra and K. Parathasarathy, "*Identification and Control of Dynamical Systems Using Neural Networks*", IEEE Trans. on Neural Networks, Vol. 1, No. 1, March 1990.

[15] W. T. Miller, R. S. Sutton, and P. Werbos, "*Neural Networks for Control*", MIT Press, Cambridge, MA, 1991.

[16] B. Widrow and F. W. Smith, "*Pattern Recognizing Control Systems*", Proc. Computational and Informational Sciences (COIVS), 1964, Washington D.C., Spartan.

[17] E. Bernard, "*Optimization for Training Neural Networks*", IEEE Trans. on Neural Networks, Vol.3, No.2, pp. 232-240, March 1992.

[18] B. Muller and J. Reinhardt, "*Neural Networks, an Introduction*", Springer-Verlag, Berlin, 1990.

[19] Y-H. Poa, "*Adaptive Pattern Recognition and Neural Networks*", Addison-Wesley, Reading, MA, 1989.

[20] F. F. Soulie and J.Herault, "*Neurocomputing: Algorithms, Architectures and Applications*", Springer-Verlag, Berlin, 1990.

[21] M. M. Nelson and W. T. Illingworth, "*A Practical Guide to Neural Nets*", Addison-wesley, Reading, MA, 1991.

[22] P. R. Adby and M. A. H. Dempster, "*Introduction to Optimization Methods*", Chapman and Hall, London, 1974.

[23] R. Fletcher, "*Practical Methods of Optimization*", John Wiley & Sons, New York, 1987.

[24] D. G. Luenberger, "*Linear and Non Linear Programing*", Second Edition, Addison-Wesley, Reading, MA, 1984.

[25] K. S. Narendra and K. Parthasarathy, "*Identification and Control of Dynamical Systems Using Neural Networks*", IEEE Trans. on Neural Networks, Vol. 1,

No. 1, March 1990, pp. 4-27.

[26] D. Psaltis, A. Sideris, and A. Yamamura, "*Neural Controllers*", Proc. of First International Conference on Neural Networks, Vol. 4, San Diego, CA, 1987, pp. 551-558.

[27] Y. Ichikawa and T. Sawa, "*Neural Network Application for Direct Feedback Controllers*", IEEE Trans. on Neural Networks, Vol. 3, No. 2, March 1992, pp. 224-231.

[28] S. Weerasooriya and M. A. El-Sharkawi, "*Laboratory Implementation of a Neural Network Trajectory Controller for DC Motor*", IEEE PES 1992 Winter Meeting, New York, January 26-30, 1992.

[29] M. A. Johnson and M. B. Leahy Jr, " *Adaptive Model-Based Neural Network Control: Validation and Analysis*", IEEE ISIC 1990, Vol. 1, pp. 486-491, Philadelphia, PA, September 5-7, 1990.

[30] Y. Zhang, G. P. Chen, O. P. Malik, and G. S. Hope, "*An Artificial Neural Network Based Adaptive Power System Stabilizer*", IEEE/PES 1992 Winter Meeting, New York, January 26-30, 1992.

[31] D.H. Nguyen and B.Widrow, "*Neural Networks for Self-Learning Control Systems*", IEEE Control Systems Magazine, Vol. 10, No. 3, pp. 18-23, April, 1990.

[32] A. Guez, J. L. Elibert, and M. Kam, "*Neural Network Architecture for Control*", IEEE International Conference on Neural Networks, San Diego, CA, June 21-24, 1987.

[33] R. J. Thomas and E. Sakk, "*Dynamical Implications of Using Neural Networks as Controllers*", Proceedings of the First International Forum on Applications of Neural Networks to Power Systems, Cat.No. 91TH0374-9, PP. 134-138.

[34] D.J. Sobajic and Y-H. Pao, "*Artificial Neural Net Based Dynamic Security Assessment for Electric Power Systems*", IEEE Trans. on Power Systems, Vol.4, No.1, pp 220 - 228, Feb 1989.

[35] S. Ebron, D.L. Lubkeman and M. White, "*A Neural Network Approach to the Detection of Incipient Faults Power Distribution Feeders*", IEEE Transmission and Distribution Conference, April 2 - 7, 1989, New Orleans, LA, Paper No. 89 TD 377-3 PWRD.

[36] N.I. Santoso and O.T. Tan, "*Neural Net Based Real Time Control of Capacitors Installed on Distribution Systems*", IEEE PES Summer Meeting, July 9 - 14, 1989, Long Beach, California, Paper No. 89. SM 768-3 PWRD.

[37] R.K. Hartana and G.G. Richards, "*Harmonic Source Monitoring and Identification Using Neural Networks*", Paper No. 90 WM 238-6 PWRS presented at IEEE PES Winter Meeting, Atlanta, Georgia, Feb 4 - 6 1990.

[38] Y. Ito, T. Furuhashi, S. Okuma, and Y. Uchikawa, "*A Digital Current Controller for a PWM Inverter Using Neural Network and its Stability*", 21st Annual IEEE PESC 1990 Record, San Antonio, Texas, pp 219 - 224.

[39] M-Y. Chow, R. J. Thomas, "*Neural Network Synchronous Machine Modeling*", Proceedings of 1989 IEEE International Symposium on Circuit and Systems, Vol. 1, pp. 495-498, Portland, OR, May 8-11, 1989.

[40] R. K. Hartana and G.G. Richards, "*Harmonic Source Monitoring and Identification Using Neural Networks*", IEEE Transactions on Power Systems, Vol. 5, No. 4, PP. 1098-1104, November 1990.

[41] D. Neibure and J. Germond, "*Power System Static Security Assessment Using the Kohonen Neural Network Classifier*", IEEE Transactions on Power Systems, Vol. 7, No. 2, PP. 865-872, May 1992.

[42] Y-Y. Hsu and C-R. Chen, "*Tuning of Power System Stabilizer Using an Artificial Neural Network*", IEEE/PES 1991 Winter Meeting, New York, February 3-7, 1991.

[43] Y-H Pao, and D.J. Sobajic, "*Combined Use of Unsupervised and Supervised Learning for Dynamic Security Assessment*", IEEE Transactions on Power Systems, Vol. 7, No. 2, PP. 878-884, May 1992.

[44] M. R. Buhl and R. D. Lorenz, "*Design and Implementation of Neural Networks for Digital Current Regulation of Inverter Drives*", Conf. Record of IEEE, IAS Annual Meeting, 1991, pp. 415-421.

[45] H.W. Dommel, "*Digital Computer Solution of Electromagnetic Transients in Single and Multiphase Networks*", IEEE transaction on Power Apparatus and Systems, Vol. PAS-88, No. 4, pp 388-399, April 1969.

[46] D.A. Woodford, A.M. Gole, R.W. Menzies, "*Digital Simulation of DC Links and AC Machines*", IEEE Transactions on Power Apparatus and Systems, Vol. PAS-102, pp 1616-1623. June 1983.

[47] D.A. Wood, "*Validation of Digital Simulation of DC Links*", IEEE Transactions on Power Apparatus and Systems, Vol, PAS - 104, No. 9, Sep. 1985, p 2588.